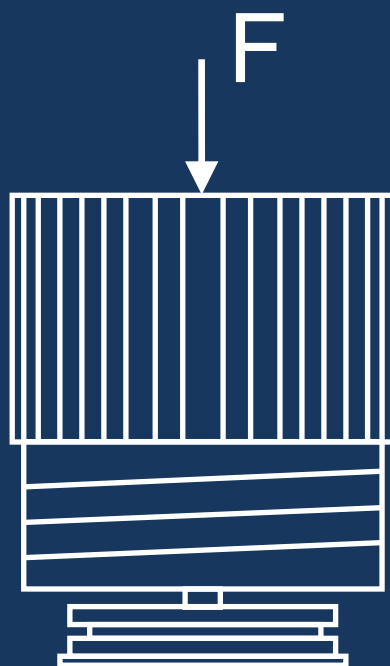


# Micro-traces on a victim's jacket

The influence of contact force on forensic trace collection efficiency when sampling textiles with adhesive tape

Graduation thesis

Selma Damsteeg - van Berkel





# The influence of contact force on forensic trace collection efficiency when sampling textiles with adhesive tape

Graduation thesis

By

S. Damsteeg - van Berkel

to obtain the degree of Master of Science  
at the Delft University of Technology,  
to be defended on Tuesday the 31<sup>st</sup> of January 2017 at 9:30 AM



Netherlands Forensic Institute  
*Ministry of Security and Justice*

Student number: 4011066  
Project supervisors: Dr. ir. Arjo J. Loeve (BioMechanical Engineering, TU Delft)  
Prof. dr. Jenny Dankelman (BioMechanical Engineering, TU Delft)



# Preface

---

This report is the result of my graduation project, which completes my Master Biomechanical Design at the Delft University of Technology. In this project I could make a contribution to the field forensic investigation, which clearly shows the versatility of mechanical engineering.

Over the past years the collaboration between the Netherlands Forensic Institute (NFI) and the department of Biomechanical Engineering at the TU Delft has grown. This project was launched at the request of the NFI. The goal of this project was to understand micro-trace collection with adhesive tape better, so that this collection can be more efficient in the future. A new method was designed to determine the efficiency of the collection of microparticles from textile with adhesive tape. This new method and the results are described in this report.

I would like to acknowledge the following people, because this project was only possible with their generous contribution.

Thanks to Arjo Loeve, for his close supervision of this project. Thank you for all your feedback, by which you learned me about the critical attitude a researcher should have.

Thanks to Jenny Dankelman. During all of our meetings you helped me to find the right direction in this graduation process.

Thanks to the employees of the Netherlands Forensic Institute: Bas de Jong, Marcel van Beest, Fleur Beemster, Paul van den Hoven, Renske van Wijk, Martine Verhoeff, Marcel de Puit and all other employees I spoke with. With your contribution I was able to grasp a bit of the practice of DNA collection, by means of interviews and by visiting the DNA lab while real evidentiary items were sampled. Besides, thank you for the provision of materials I needed in this experiment.

Thanks to the three Sanders, employees of the TU Delft, who all supported me practically. Sander Leeftang, thank you for helping me in my experiments with the tensile tester. Sander Oldenhof, thank you for learning me the basics of laboratory work, so I was able to deposit the micro-traces on my samples. Sander van Asperen, thank you for instructing me about how to use the digital microscope.

Thanks to my family and friends, for supporting me during my graduation process. A special thanks to my husband Jan-Willem, for encouraging me during my graduation project, and even willing to listen to my endless thoughts about tape and micro-traces. Also a special thanks to my fellow students who were also studying in 'the tower' of the faculty 3mE. You made this place a pleasant place for our long days of studying.

Selma Damsteeg – van Berkel  
January 2017, Delft

THANKS TO ALL OF YOU

# Index

---

Preface .....	5
Index.....	6
Abstract .....	8
Nomenclature.....	9
<b>1 Introduction to stubbing and the influence of stubbing force .....</b>	<b>10</b>
1.1 Background – The importance of trace DNA and its collection method.....	10
1.2 Problem statement and research goals – The influence of stubbing force .....	11
1.3 Research questions .....	12
1.4 Hypotheses.....	13
1.5 Report outline.....	13
<b>2 Materials and methods .....</b>	<b>14</b>
2.1 Stubs .....	14
2.1.1 Adhesive performance of tape after UV irradiation .....	15
2.2 Substrate material.....	16
2.3 Micro-traces.....	19
2.4 Sample preparation.....	19
2.5 Applied stubbing forces .....	21
2.5.1 Method of force application .....	21
2.5.2 Magnitude of stubbing forces .....	23
2.6 Measurement of external factors.....	27
2.7 Counting micro-traces .....	28
2.7.1 Microscopy.....	28
2.7.2 Image processing in Photoshop.....	30
2.7.3 Image processing in MATLAB .....	31
2.8 Data analysis .....	34
2.8.1 Collection efficiency for different stubbing forces.....	34
2.8.2 Distribution of microspheres over the height of the textile substrates before and after stubbing .....	34
<b>3 Results .....</b>	<b>35</b>
3.1 Adhesive performance of tape after UV irradiation .....	35
3.2 Collection efficiency for different stubbing forces .....	37
3.3 Distribution of microspheres over the height of the textile substrates before and after stubbing .....	39
3.4 Other measured external factors.....	40
<b>4 Discussion .....</b>	<b>41</b>
4.1 Collection efficiency for different stubbing forces .....	41
4.1.1 Number of microspheres on the substrate before stubbing vs. trace collection efficiency.....	43
4.2 Collection efficiencies at different height levels of the substrate structure .....	43

4.2.1 Inaccuracies.....	44
4.3 Recommendations to improve the used method.....	45
4.3.1 Improve particle detection .....	45
4.3.2 Improve determination of particle depth location.....	45
4.4 Future research .....	46
<b>5 Conclusion .....</b>	<b>50</b>
Bibliography .....	51
Appendices.....	52
Appendix A – Stub-tape cutting procedure.....	53
Appendix B – Technical drawings of stub-pin holders.....	55
Appendix C – List of available panty hoses at HEMA.....	56
Appendix D – Considerations for the substrate material choice.....	57
Appendix E – Procedure to produce the spools of threads.....	59
Appendix F – Calculation of the concentration of microspheres in the suspension.....	61
Appendix G – Measured diameters of the used textile threads.....	62
Appendix H – Graphs of the substrate impression versus the stubbing force.....	63
Appendix I – Photoshop editing procedure.....	64
Appendix J – MATLAB files.....	66
Appendix K – Determination of the substrate area that was fully covered by tape.....	77
Appendix L – Validation of microspheres counting by MATLAB.....	78
Appendix M – Datasheet experiment results.....	80
Appendix N – Collection efficiency at different substrate structure heights (PSS and PC) .....	81
Appendix O – Collection efficiency on glass.....	84

# Abstract

---

DNA can function as a significant part of evidence in forensic investigation, because it can link a potential perpetrator to a crime. Even by skin contact, micro-traces of DNA-containing material can be transferred. This type of DNA is called 'trace DNA'. When DNA is collected from an evidentiary item for forensic purposes, the goal is to collect as much as possible of the targeted DNA and as least as possible of other traces. The focus of this research is the collection of trace DNA from textiles. In the Netherlands Forensic Institute (NFI) this is mostly done by tape-lifting: using double-sided tape stuck to a stub, which is called 'stubbing'. This method is used for about 10 years now at the NFI. However, the evolution of stubbing for DNA collection has mainly been empirically driven and no studies are done to improve its technique, even though this would be very useful when miniscule amounts of DNA are searched. The stubbing force (the normal force applied on the stub while stubbing) is assumed to influence the trace collection efficiency when stubbing, because a higher stubbing force results in a larger actual contact area between the adhesive tape and the textile, by which traces on the textile can adhere to the tape. Though, the stubbing force is manually applied in the current stubbing procedure by which it cannot be accurately controlled. Thereby, this possibly leads to a difference in the quality of resulting samples among different forensic investigators.

This research is focussed on how the stubbing force is related to the efficiency of the collection of micro-traces, and on how the collection efficiency differs for traces from different depths in the substrate structure. This latter issue is questioned, because if trace DNA from multiple DNA sources are present on an evidentiary item, which is often true, it is assumed that DNA-containing material of the last handler is present in more superficial layers of the substrate. In that case, it would be very useful to know how traces can be collected selectively from specific depths of the substrate to obtain samples with a higher ratio between the targeted DNA and other traces.

In this research, microspheres were used as representation of trace DNA. These spheres are sized in the same order of magnitude as skin cells (25  $\mu\text{m}$ ), which are a possible component in trace DNA. Microparticles were applied to the substrates in a suspension of ethanol, to get a uniform distribution over different samples. Experiments were performed on multiple textile substrates: flat spools wrapped by three different types of polyester threads. Traces were collected by stubbing while using 5 different stubbing forces. The stub tapes, as well as the substrates (before and after sampling) were analysed by using the microscope. In MATLAB a script was designed to automatically count these particles using image recognition routines.

Results gave insight in how stubbing force increased for the used materials. To define the trace collection efficiency from specific depths in the substrate structure, the designed method was too inaccurate. Though, the measured impression of the used textiles indicated that when stubbing with 1 N, the substrates were almost impressed to its maximum impression. This indicates that when stubbing with a stubbing force of 1 N particles are potentially not only collected from the most superficial layer in the substrates but also from deeper layers. Recommendations for future research are given in the discussion.

# Nomenclature

---

Substrate	Physical surface (for example of an evidentiary item) on which a trace can be present
Actual contact area	Real contact area between two surfaces, also considering the surface roughness on microscopic scale
Apparent contact area	Apparent contact area on macroscopic scale (contact area that would exist if the contacting surfaces would be perfectly flat and perfectly aligned)
Stub	Forensic tool that is used to collect forensic traces: aluminium pin with a piece of double-sided adhesive tape on it, placed in a holder to handle it, and covered by a vial to avoid contamination
Stubbing	Tape-lifting method for which a stub with double sided adhesive tape is used
Stubbing force	Contact force between the stub and the substrate during tape application. If a substrate was sampled with a stubbing force of $xN$ , this indicates the maximum normal force that was applied on the stub during this contact.
Fibre	Thinnest filament of a thread, for example from cotton or polyester
Yarn	Fibres loosely twisted together
Thread	Two or more yarns twisted

# 1.

## 1 Introduction to stubbing and the influence of stubbing force

---

### 1.1 Background - The importance of trace DNA and its collection method

Human witnesses are often lacking at a crime scene, therefore physical evidence plays an important role in forensic investigation. DNA-containing material is important physical evidence, because it can be used for the identification of people that were in some way involved in the crime scene. DNA can be transferred from the human body to the environment in many ways. Even by skin contact, micro-traces of DNA-containing material can be transferred. This type of DNA is called 'trace DNA'. Trace DNA can be transferred via direct contact, for example by grabbing, touching, or wearing items, but even further by indirect body contact.

Imagine the following case: a victim was brutally murdered by an unidentified person. His jacket is torn, probably by a serious fight. Therefore, it is very likely that trace DNA of the killer is present on this jacket, even though these traces are not visible with the naked eye. In this example, it would be really valuable to find trace DNA on the jacket, for it may provide a possible link between the murder case and one of the suspects. For an optimal result, it is crucial to collect as much as possible DNA of the killer and as little as possible other material that may contaminate the sample. In that way the chance is at its highest that the right person is coupled to the DNA profile resulting from the analysis of the DNA sample. To achieve this, it is of particular interest to select the right collection method and to use this method optimally.

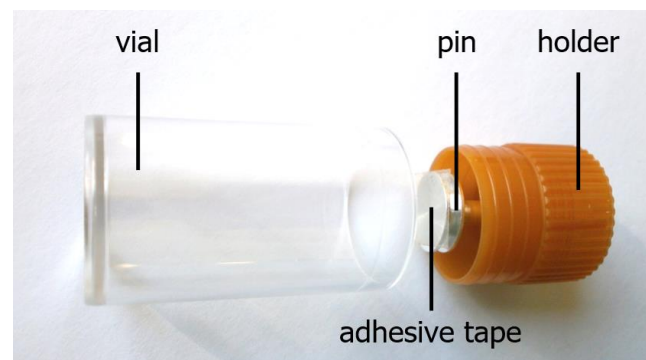


*Figure 1 Stub that is used for DNA collection, with a double-sided adhesive tape attached to its pin ( $\varnothing$  12.7 mm).*

Different methods exist for the collection of trace DNA. For traces on evidentiary items of textile, such as the jacket in the example above, forensic investigators at the Netherlands Forensic Institute (NFI) use adhesive tape to lift DNA traces from textile. The adhesive tape is double sided and is stuck to a so called 'stub', see Figure 1. This tape-lifting method, more specifically called 'stubbing', is mainly used for the collection trace DNA from cotton/polyester or cotton<sup>1</sup>. It is a well working method that has been used about 10 years at the NFI for the collection of trace DNA. Yet, only a few studies were found that investigated this stubbing method. In a prior

---

<sup>1</sup> Personal interviews, 30/09/2015 [1].

literature study [1], one study was found that investigated what tape was most suitable to use [2] and one study that investigated the relation between the number of tape-lifts and the amount of collected DNA [3].

## 1.2 Problem statement and research goals – The influence of stubbing force

To optimize the chance that the right person is coupled to a crime by using a DNA sample, the collected DNA sample should contain as much as possible of the targeted DNA and as least as possible 'noise', which can be DNA from another person, or material that inhibits the further processing of the DNA. If no noise is present on the sampled evidentiary item, the only focus during stubbing is to collect as much target DNA as possible. However, in practice this would rarely happen, because when an evidentiary item is previously touched by other people, their DNA can still be present on the item.

To get the ratio between targeted DNA and noise as high as possible, it has to be known where these different micro-traces are expected in the substrate (the surface on which the trace is present). It is assumed by forensic experts that the distribution of DNA traces from different DNA sources is mostly layered. DNA-containing material of the last occurred touch event is assumed to be present more superficially than earlier applied traces such as wearer's DNA (DNA transferred by wearing the evidentiary garment)<sup>2,3</sup>. This assumption is plausible, especially when the trace deposited by the last touch event is dry and does not easily penetrate through the substrate. However, no studies were found that support this hypothesis. So, there are multiple trace distributions possible, schematically represented in Figure 2. Note that these are simplified representations and that layered traces might not be strictly layered.

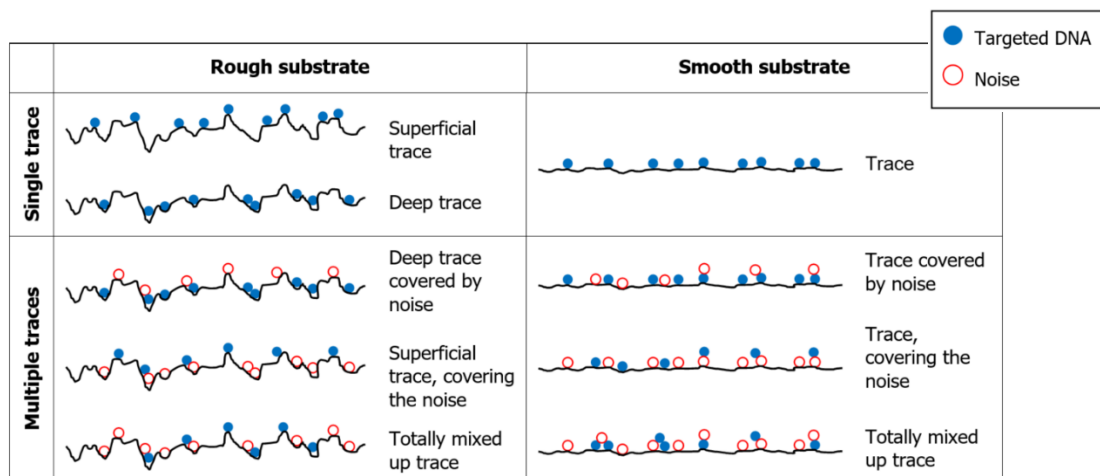


Figure 2 Targeted DNA and noise can be positioned on a substrate in various compositions, which are represented in this table. Note that on rough substrates the different traces can also be present in the same height of the structure (deep or superficial).

If the targeted DNA and the noise are fully mixed (and these traces have the same adhesive properties), it is probably impossible to influence the ratio between targeted DNA and noise with adaptations to the stubbing technique. In this case, it would mostly be favourable to collect as much as possible of the mixed traces. Therefore, it will be investigated in this research what stubbing force should be used to collect as much as possible micro-traces from a textile substrate.

When the targeted DNA and the noise are present in different depths of the substrate structure, the used stubbing technique can possibly influence the ratio between these traces in the resulting sample. To do so, a technique should be found with which it is possible to selectively collect material from certain depths of the substrate. In prior literature study [1], it

<sup>2</sup> Kramer, Gerco. Personal interview. 30/09/2015 [1].

<sup>3</sup> Verhoeff, Martine. Personal interview. 30/09/2015 [1].

turned out that this is most likely possible by adapting the force that is used during stubbing. The stubbing force influences the impression of the substrate and thereby contact between the tape and the trace present on the substrate is influenced.

Nowadays, the stubbing force is manually applied. There seems to be high variations in the used stubbing force among forensic experts and among repeating trials of individual experts. This was tested by Wendt [4], who measured the vertical force while forensic investigators stubbed on different textiles that were placed over mock-up skin. Furthermore, no experiments were found that studied the influence of stubbing force on micro-trace collection efficiency. Nevertheless, forensic investigators use a higher stubbing force to collect deeper traces<sup>4</sup>, even though there is no evidence to support this is true. Moreover, it has never been defined what a 'high' or 'low' stubbing force is. Therefore, another goal of this research is to investigate the relation between the used stubbing force during stubbing and the collection efficiency of micro-traces from different depths in the substrate structure.

To improve the ratio between targeted DNA and noise in samples, two DNA transfer steps need to be considered. Firstly, it should be investigated how traces are distributed over the substrate structure after various scenarios of DNA deposition by humans and ageing of the traces. Secondly, it should be examined if it is possible to selectively collect traces from selective layers in the substrate structure by stubbing. Together, these insights could give more information about the stubbing technique that should be used for selective collection of the targeted trace.

This research is only focussed on the second transfer step, see Figure 3. Therefore controlled trace deposition is used, so purely the influence of the stubbing technique on the trace collection efficiency can be measured without unintendedly measuring influences of variations in trace deposition on the experiment results.

Other microparticles than trace DNA were chosen as deposition material (see paragraph 2.3), because quantifying amounts of DNA was not feasible in this project. Gaining knowledge about the influence of stubbing force on the collection efficiency of these microparticles will be the first step to gain more insight in the relation between stubbing force and the efficiency of the collection of trace DNA through stubbing.

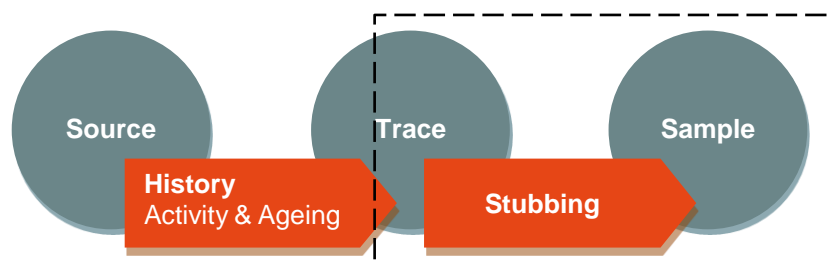


Figure 3 The ratio between the targeted DNA and noise in a sample is influenced by the deposition of a trace by the DNA source (a human) and ageing of this trace, and by how this trace is collected. This research is focused only on this second transfer step (see dashed frame).

### 1.3 Research questions

Two research questions were formulated:

#### Question 1

What is the influence of the stubbing force on the efficiency of the collection of microparticles from a substrate? And how does this effect differ for different textiles?

#### Question 2

How does the particle collection efficiency of stubbing differ for microparticles at different depths in the substrate structure?

<sup>4</sup> Verhoeff, Martine. Personal interview. 30/09/2015 [1].

## 1.4 Hypotheses

Microparticles can be tape-lifted from a textile substrate due to adhesive bonding between the adhesive tape and the microparticles. Adhesive bonding is determined by two aspects: bond strength and bond formation [5]. Because of the low weight of the microparticles, it was hypothesised that only low bond strength is needed to result in adhesive bonding by which the microparticles can be tape-lifted from the textile. Therefore, the adhesive bonding between the tape and the microparticles was thought to be mainly dependent on bond formation, which is possible when contact is made between the tape and the particles. In this hypothesis, electrostatic attraction between the tape and the microspheres over a distance is disregarded.

Contact between the tape and a microparticle will be formed under approximately the same conditions as contact between the tape and the textile that is close adjacent to that particle. Therefore, the number of collected microparticles during tape-lifting from textile is hypothesised to be approximately equal to the actual contact area between the tape and the textile  $A_{actual\ contact} [mm^2]$  times the particle coverage on the actual contact area  $\rho_{particle\ coverage} [\#/mm^2]$ , see equation 1.1. The particle coverage depends on how the microparticles are distributed over the textile.

$$n_{collected\ microparticles} [\#] \approx A_{actual\ contact} [mm^2] \cdot \rho_{particle\ coverage} [\#/mm^2] \quad Eq. 1.1$$

This theory leads to the hypotheses specific for research question 1 and 2:

### Hypothesis to research question 1:

Under a higher stubbing force, textile fibres are compressed more, by which the actual contact area between the tape and the textile increases. Therefore, it was hypothesised that stubbing an equal sample with a higher stubbing force results in a larger amount of collected microspheres. This statement is true until the actual contact area between the tape and the textile is as large as possible, and it is expected to be only valid if the surface that is not covered by the tape yet does contain microparticles.

### Hypotheses to research question 2:

The efficiency of the collection of microparticles that are located deeper in the substrate structure is lower than for particles that are located more superficially when stubbing with the same stubbing force. This difference is larger when stubbing with lower stubbing forces. It is hypothesised that it is possible to solely collect particles that are superficially present in the substrate surface when stubbing with a low stubbing force by which only contact between the tape and the superficial area of the substrate is made.

## 1.5 Report outline

In chapter 2 the materials and methods are discussed that were required to find an answer for the research questions. In chapter 3 the results of the experiments are displayed, which are discussed in chapter 4. Finally, chapter 5 provides a summarized conclusion of this research.

## 2.

## 2 Materials and methods

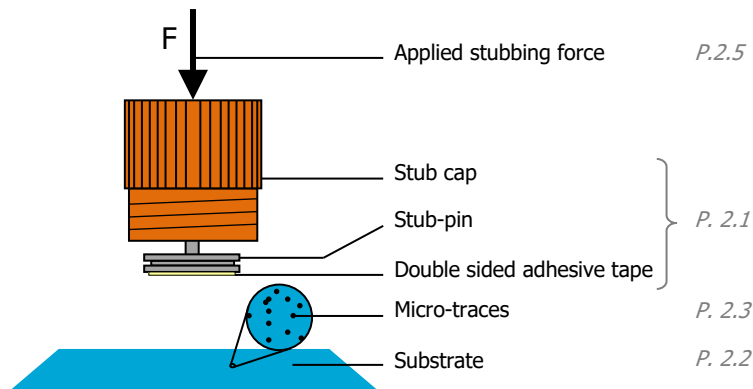


Figure 4 Schematic experiment setup.

Microparticles were deposited on three types of polyester substrates. The micro-traces were collected by stabs, using different stubbing forces. The stub-tape and the substrates were analysed using a microscope. The microparticles in the microscope images could automatically be counted in a MATLAB script based on image recognition routines. Thereby, the trace collection efficiencies could be calculated.

To perform these experiments, multiple materials had to be selected, see Figure 4. In this figure, the paragraphs are indicated in which the mentioned materials are described.

## 2.1 Stubs

The same aluminium stub-pins as those currently used at the NFI for DNA collection were used in these experiments, see Figure 5. The stub holders were not used, because it was more practical to directly clamp the stub-pins into the setup. Double sided adhesive tape (Scapa 4405, which is also used at the NFI) was stuck to the  $\text{\O}12.65$  mm surface of the stub-pin. The top surface beneath the transparent tape was painted black to improve the visibility of microparticles on the tape.

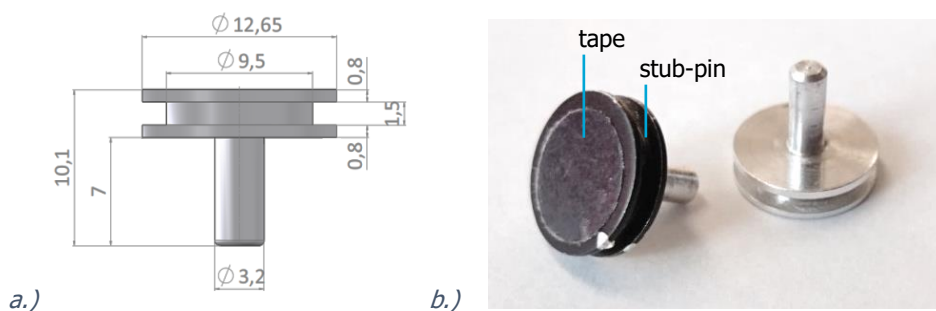


Figure 5 a.) Aluminium stub-pin (dimensions in mm). b.) Picture of stub-pins with a black painted top surface and a round tape stuck to it. This is how the stabs were used in this research.

For forensic investigation purposes, the adhesive tape that is stuck on the stub-pin is usually cut in squares, for which the exact dimensions of the tape are not really important. The corners of the tape go beyond the edges of the stub-pin, and thereby these parts of the tape are not supported by the pin during stubbing. These loose corners are practical for detaching the tape from the pin after DNA collection by using tweezers. However, for the current research purposes it was important that all used tapes were equally sized and that the whole tape was supported by the stub-pin. Therefore, the adhesive tape was punched in 10 mm diameter round pieces. Pieces of double sided tape were placed on a flat wooden plate with the silicone paper cover at the bottom side. Circles were punched out with an arc punch, using a steel hammer. Every round tape was lifted out of the arc punch using tweezers and placed with the uncovered side of the tape on a clean stub-pin. Finally, the tape was pressed gently to the stub with the rounded side of the tweezers and pressed more firmly to the stub by placing a mass on the tape (still covered by silicone paper). This silicone paper cover was removed at the moment that the tape was used for experiments. The stubs were placed in a holder, see Figure 50 in Appendix B, and stored in a closed box to protect it from contamination. The tape cutting procedure is described in more detail in Appendix A.

### **2.1.1 Adhesive performance of tape after UV irradiation**

In this research, the same stub-pin and adhesive tape were used as currently used at the NFI, so that results of this research are applicable in the current procedures. However, in the current stub preparation procedure, the adhesive tape is irradiated with UV light. This is done to avoid the presence of DNA of an innocent DNA source on the tape. The adhesive tape is not recommended for direct exposure to sunlight or UV light [6]. However, no studies were found that studied the influence of this UV irradiation process on the adhesive performance of the stub tapes. Therefore, this effect had to be examined. If a noticeable effect was measured, it would have been necessary to apply UV irradiation in the stub preparation procedure for this research. This would ensure that tape would be used with similar adhesive properties as the tape that is currently used for forensic trace collection.

The influence of the UV irradiation process on the adhesive performance of the double sided adhesive tape was examined by comparing the adhesive force between the tape and a glass slide for not UV irradiated tape and for tape that was UV irradiated. Adhesive tape was cut in 10 mm diameter circles, like it was done for the main experiments (described in Appendix A). 12 of the cut tapes were not UV irradiated. 12 tapes were UV irradiated according to the standard procedures of the NFI: both sides of the tape were exposed to UV light (2 lamps: Philips TUV TL-D 15W T8 UV-C 437 nm) in a fume cabinet for 1 hour, see Figure 6. The first side was UV irradiated before the tapes were cut. Therefore, a strip of adhesive tape was rolled out with its silicon protection paper situated at the bottom side and fastened to a clean surface. The second side of the tape was UV irradiated after the tapes were cut and stuck to the stubs and after the silicon protection paper was removed from the tape. 12 other tapes were UV irradiated according to a similar procedure, but instead of the UV light source of the NFI, a new setup was used that was developed at the TU Delft by Windemeijer et al. [7], see Figure 7. This setup was designed to enable making the adhesive tape DNA free by exposing both sides of it to UV light for only 5 minutes instead of 1 hour. The minimum UV dose measured in the fume hood at the NFI was used as minimum required UV dose in the new setup, which is 20.000 J/m<sup>2</sup> in 1 hour [7]. The setup consists of two Philips PL-L 55 W UV lamps with a length of 52 cm, and the tape could be placed with a distance of 7.5 cm under the lamps. During the UV irradiation, the environment was properly ventilated, for ozone might have been released during this procedure [7].



*Figure 6 Fume cabinet with a UV light source.  
In the fume hood, a holder is placed that  
contains stubs with tape.*



*Figure 7 UV light source prototype developed at  
the TU Delft by Windemeijer et al. [7].*

The maximum adhesive force between the tape and standard microscope glass slides (76x25mm) was measured after stubbing with 1, 3 and 9 Newton (3 trials for 1 and 3 N, and 6 trials for 9 N stubbing force). The force on the stub was applied as described in subparagraph 2.5.1. The glass slide was clamped in the substrate clamp, see Figure 18, and cleaned with a cleanroom wipe and ethanol before every trial.

The results of this experiment are displayed in paragraph 3.1. Based on these results it was chosen not to apply UV irradiation to the tape in further experiments of this research.

## 2.2 Substrate material

The following four options were considered as substrate materials to use in this research:

1. **Fabrics**  
Woven fabrics bought off-the-shelf.
2. **Spools of threads**  
Textile threads wound around a flat metal spool.
3. **Modified plastics**  
Plastic surfaces with a variation in hardness and roughness. The variation in hardness could be achieved by using different plastics. Macro roughness could be achieved by CNC face milling with an angular milling cutter. Different milling depths can be used. Micro roughness on the plastic surface could be achieved by using sand paper or sand blasting (the second option is required when macro roughness is already applied to the material).
4. **Panty hoses**  
Panty hoses made from a mixture of polyamide (a synthetic fibre) and elastane, see Appendix C.

To choose the most suitable substrate material for these experiments, the optional substrate materials were evaluated based on several requirements. Firstly, to contribute to the research questions, which are specifically focussed on stubbing from textile, the substrate material should not deviate too much from textile. Therefore modified plastic was not a suitable option.

Secondly, systematic variation between different versions of the substrate should be possible, so the influence of these variations on the relation between stubbing force and trace collection efficiency could be studied. Woven fabrics and panty hoses cannot vary systematically because more factors would vary simultaneously: the thread type, weaving type, and for panty hoses also the ratio between the different materials of which these consisted (polyamide and elastane), see Appendix C. Finally, the substrate choice was determined by practical considerations: manufacturability and availability in future research. Based on these last requirements spools with threads scored the best. The considerations above are discussed in more detail in Table 5 in Appendix D. This table shows some other considerations on which the substrate choice was based. In conclusion, spools with threads were regarded as the most suitable substrate material for these experiments.

Three different threads were selected to wrap around the spools, see Figure 8. For a good visibility of the micro-traces on the substrate, the substrate colour was chosen to be black. More specifications are displayed in Table 1.



Figure 8 Polyester substrates made of three different threads: sewing polyester, extra strong sewing polyester and crochet polyester. See Table 1 for the thread specifications.

Table 1 Specifications of the used threads.

Thread type	Material	Brand	Colour	Length	Weight/length	No/tkt**
Crochet	100% polyester	Amy, Zeeman textielSupers	black	140 m	0.36 g/m	-
Sewing	100% polyester	Sew-all thread, Güttermann, made in Germany	black	200 m	0.03 g/m*	100*
Sewing	100% polyester	M782 Extra Strong, Güttermann, made in Germany	black	100 m	0.075 g/m*	40*

\* From: [www.guetermann.com](http://www.guetermann.com)

\*\* The ticket number is a measure for the thickness of a sewing thread.

The spool base was produced from steel according to the dimensions in Figure 9. Firstly, a thread was knot through one of the holes. Then, the thread was manually wrapped around the spool base (around the long axis). Every winding had to be adjacent to the previous winding, in such a way that now 'gaps' were visible with the naked eye between neighbouring windings. Finally, the thread was knot through the second hole in the spool.

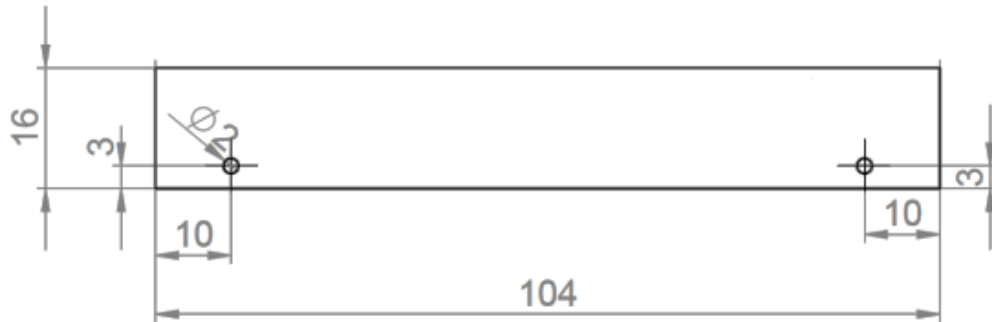


Figure 9 Dimensions of the base of the spools, made from steel with 3 mm thickness (dimensions in mm).

Before use (or reuse) of a spool with fibres it was cleaned with water. To clean a spool, all its four long edges were kept under a warm, fast running water tap for about 10 seconds each side. The spool was moved back and forth during this to make sure the water flowed over the whole surface. After cleaning, the spool was dried by rolling it into a cleanroom wipe and compressing it firmly. Then the spool was dried in the air, under room temperature for at least 12 hours, with all sides of the substrate free to dry.

The spools were labelled so these could be distinguished during the experiments. On each spool 5 sample circles were defined. These could be distinguished by a cover that contained circular gaps of 14 mm diameter, see Figure 10. This cover was placed on the spool after microtraces were deposited on the substrate (see paragraph 2.4). For a more detailed description of the preparation of the substrates, see Appendix E.

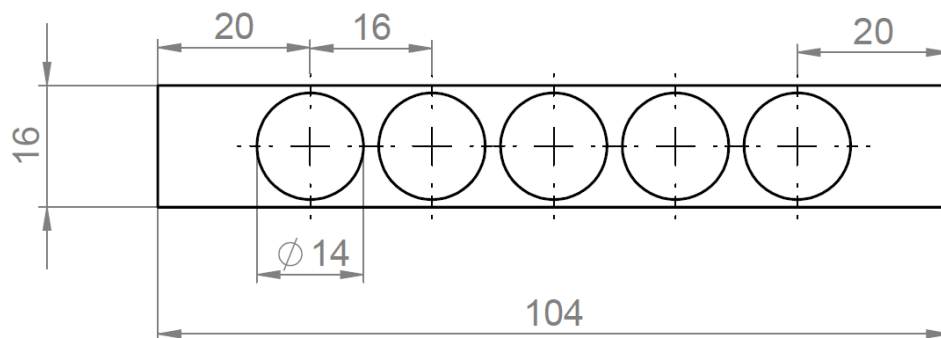


Figure 10 Sample cover made from aluminium of 0.5 mm thickness (dimensions in mm). The covers were manufactured in a laser cutter.

Standard microscope glass slides (76x25 mm) were used as fourth substrate type. The variation in height profile of the glass slides can be negligible. Therefore, this substrate was used as reference to indicate the collection efficiency when full contact between the tape and the substrate is approached. Note that even when sampling from glass, there is no completely full contact, because the tape does not have an entirely flat surface and microparticles can be overlapped, by which contact with other particles is impossible.

### 2.3 Micro-traces

In these experiments, a representing material for trace DNA was used, because using real trace DNA was impractical in terms of costs and time and because quantification of DNA is not very accurate. Furthermore, the content of trace DNA cannot be unambiguously determined. The content strongly varies per DNA source, preceding activities, etc. So, even if real DNA-containing material had been chosen as deposition material for these experiments, it could not be defined what this exactly should consist of: sweat, skin cells, saliva and/or other material.

Red fluorescent polystyrene microspheres (25  $\mu\text{m}$  diameter, 12% Coefficient of Variation, Fluoro-Max™, Thermo scientific) were chosen to use as representing micro-traces in these experiments. These particles were chosen for several reasons. Firstly, the size of these particles is in the same order of magnitude as the size of skin cells, which have a diameter of about 30  $\mu\text{m}$  [8] and which can be present in trace DNA. The microspheres have very little difference in size and shape, which is advantageous, because thereby no unintended effects of particle size on the collection efficiency could be measured. Secondly, these microspheres are visible very well under the microscope, even without a fluorescent light source. And finally, the material can remain in a suspension without dissolving, which is needed for the selected deposition method.

### 2.4 Sample preparation

The microspheres were deposited on the substrates in a suspension of ethanol, see Figure 11. This liquid spreads out well over the textile, better than water, and so it results in a uniform distribution of the particles over the whole surface of the spools.

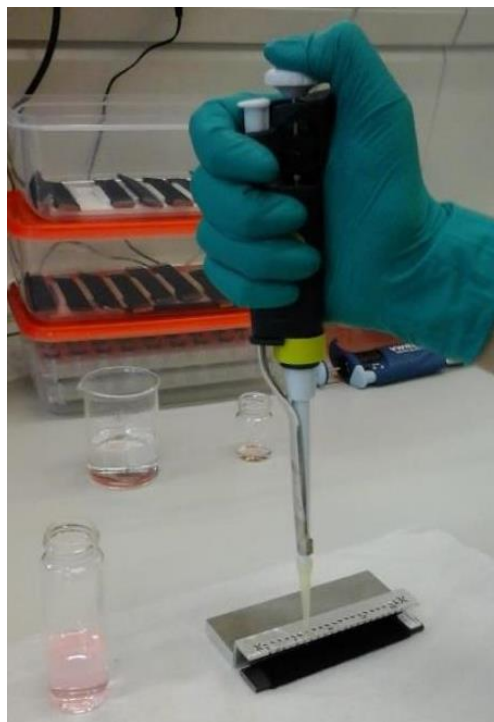


*Figure 11 Microspheres were deposited in a suspension of ethanol. Equally sized droplets were evenly distributed over the spool with threads.*

The concentration of the suspension was determined based on the demand that a circle of 10 mm diameter (surface area of the tape) should contain about 1000 microspheres. It was chosen to deposit the suspension by 4 droplets of 0.025 mL ethanol per sample circle (20 droplets on each spool), so this would result in an even more homogeneous trace distribution than when using one droplet. This led to a desired concentration of microparticles ( $9.2\text{E}4$  particles/mg [9]) in the suspension of 0.354 mg/mL, see calculations in Appendix F. An amount of microspheres

was weighed, enough to prepare all 60 textile samples ( $m_{\text{microspheres}} > 60 \cdot 3.54 \cdot 10^{-2} \text{ mg}$ ), see Figure 12. The microspheres were put in a jar and then ethanol was added so the suspension reached its desired concentration. Before the suspension was applied to the substrates, the suspension jar was put in an ultrasonic bath for 2 minutes at room temperature to break agglomerates of spheres into separated particles, see Figure 13.

Then the suspension was deposited on the substrate using a pipette that could deposit 0.025 mL droplets. The distance between droplets was controlled by pipetting through a self-designed tool that contained holes at every 4 mm (20 holes in total), see Figure 14. After the deposition of every 5 droplets the suspension jar was shaken, because otherwise the microspheres would sink down, and the pipette was rinsed two times with clear ethanol, so that the concentration would not increase over time due to particles remaining in the pipette tip.

When the deposition was finished, the substrates dried to the air for at least 24 hours before the samples were stubbed.



Figure 12 The microspheres were weighed at a digital mass weighing scale.



Figure 13 Before the suspension was deposited on the substrates the suspension jar was put in an ultrasonic bath (VWR ultrasonic cleaner) for 2 minutes at room temperature to break agglomerates of spheres.

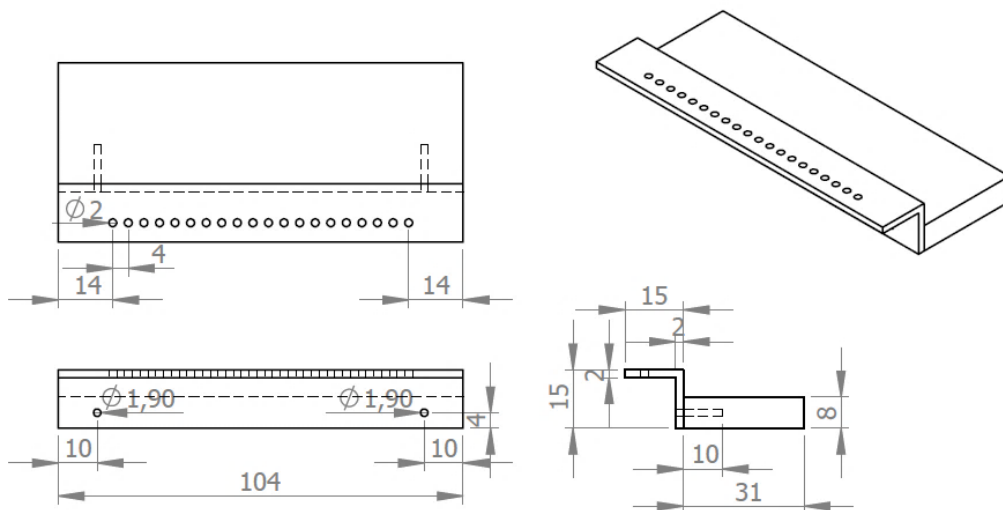


Figure 14 Technical drawing of the tool that was used to deposit droplets on the substrates (dimensions in mm). This tool contains 20 holes in which the pipette tip could be positioned to deposit a droplet of the suspension, see Figure 11.

## 2.5 Applied stubbing forces

The stubbing force is defined as the contact force between the tape and the sampled substrate during one tape application. If it is mentioned that a sample was stubbed with a stubbing force of for example 7 N, this means that the maximum stubbing force during the contact moment was 7 N. Note that it is basically the pressure between the tape and the sampled substrate that influences the collection efficiency. However, it is more practicable to control the stubbing force, because the pressure depends on the actual contact area over which the force is distributed, and the size of this area cannot exactly be determined. Moreover, the force is much easier to interpret when the experiments results are linked to the practice of stubbing.

### 2.5.1 Method of force application

An Instron tensile tester (model no.: 4505, serial no.: H2164) with a static load cell of  $\pm 100$  N (Instron, serial no.: 65883) was used to accurately impose a normal force on the stub under a fixed speed of application on and separation from the substrate.

To clamp the stub-pins directly to the load cell, a stub clamp was designed in which the stub-pins could be easily replaced, see Figure 15 and Figure 16.

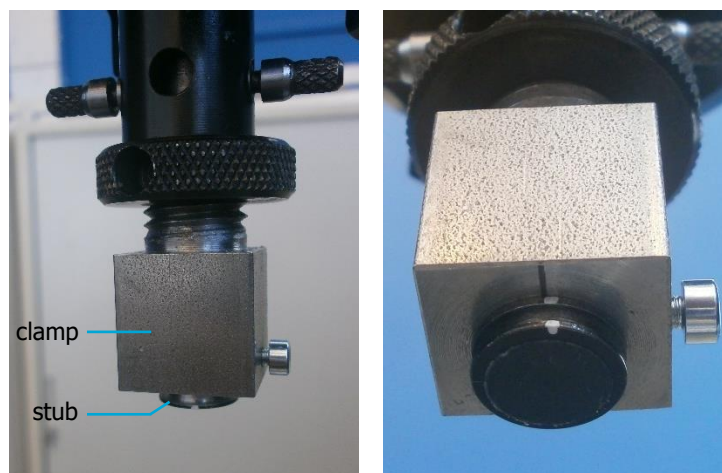


Figure 15 Stub clamp that was designed to connect the stub-pin with the load cell.

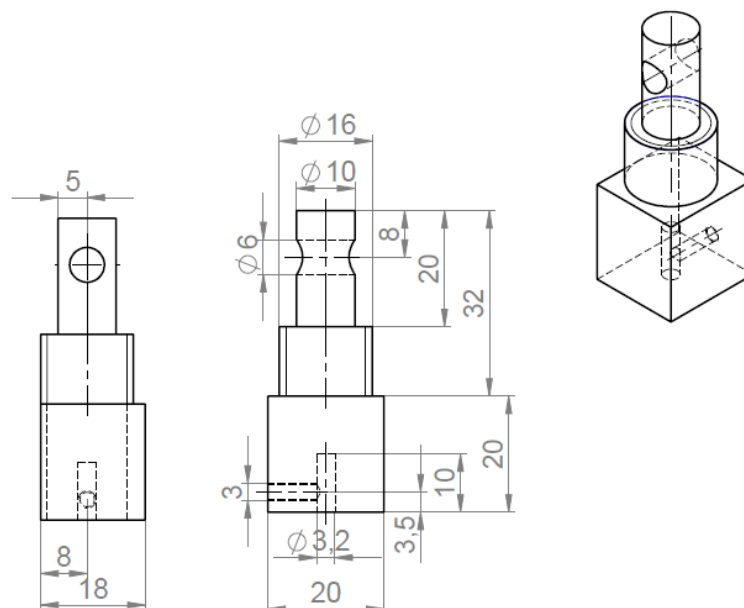


Figure 16 Technical drawing of the stub clamp that was used to connect the stub-pin to the load cell of the tensile tester (dimensions in mm).

To clamp the textile substrates tightly to the moving crosshead of the tensile tester, a substrate clamp was designed, see Figure 17 and Figure 18. In this clamp the substrates could be replaced and could be moved in the horizontal plane, so all 5 sample circles on one spool could be lined up with the stub.

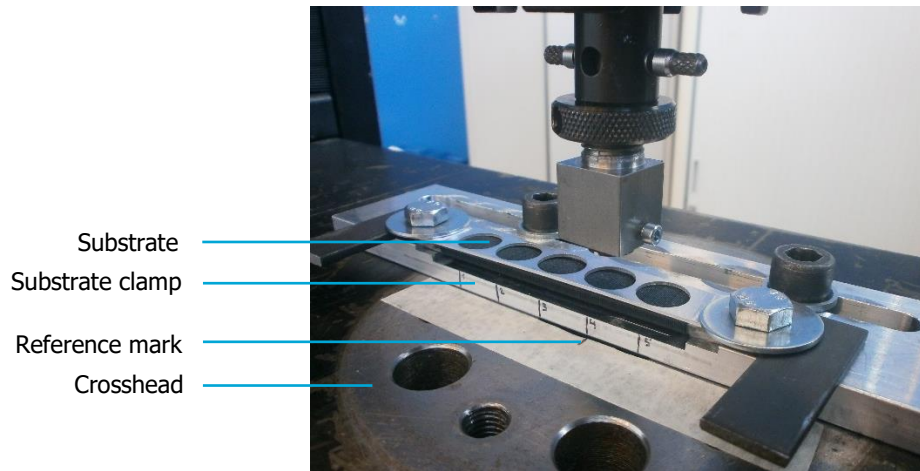


Figure 17 Substrate clamp to fix the substrate to the crosshead of the tensile tester. A piece of masking tape with a reference mark was attached to the crosshead, so the sample areas on the substrate could easily be aligned with the centre of the stub.

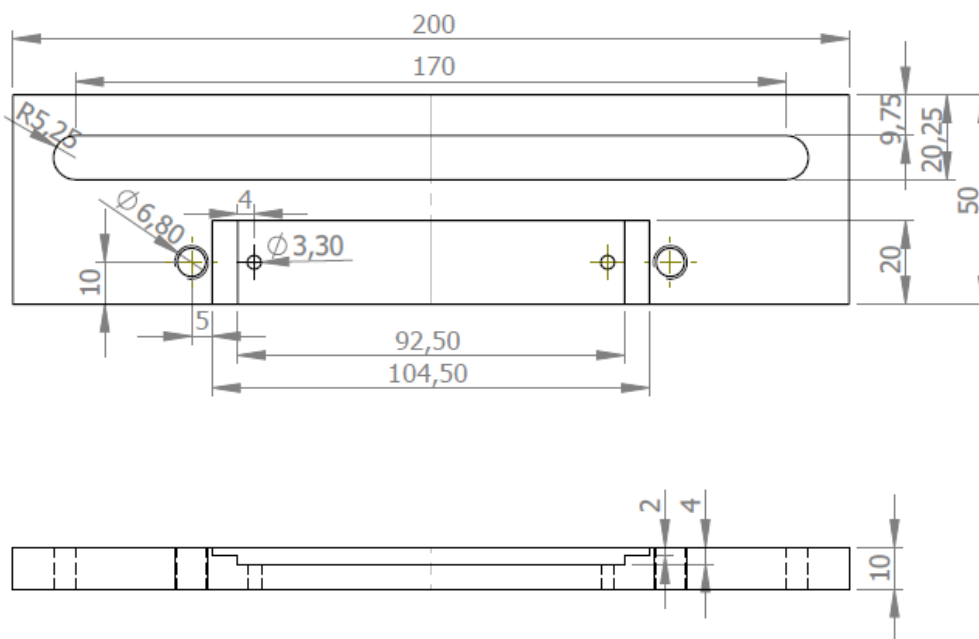


Figure 18 Technical drawing of the substrate clamp (dimensions in mm). It could be used to clamp a spool with fibres as in Figure 17, secured by two M8 bolts and fender washers, or to clamp a glass slide on the surface of 92.5x20 mm, secured by two M4 bolts and slides with rubber that press the glass to its support.

At the start of the experiments, the load cell was calibrated in the Instron software (which had to be done without external load) and then the stub holder was attached to it. The substrate holder was attached to the crosshead, see Figure 17. The sample areas on the substrates were absolutely not touched (apart from the intended contact with the stub).

For every tape-lift, the following actions were performed. Firstly, the stub with tape (still covered by the siliconized paper cover) was fastened in the stub clamp by tightening the small bolt

when the stub-pin is placed as deep as possible in the clamp. The white reference mark on the stub was aligned to the reference mark on the stub holder, see Figure 15, to roughly determine the position of the tape relative to the sample circle. Secondly, the substrate was fastened in the clamp and one of the sample circles was positioned under the stub in a way that the stub could not make contact with the sample cover. When the setup was properly aligned, the tape cover was removed and the stub was positioned close to the substrate. Finally, it was needed to 'zero' the crosshead and to 'balance' the load cell in the software, so the vertical starting position of the stub with respect to the substrate was defined as 0 mm and the measured starting force as 0 N.

During each tape-lift the same method of force application was used, see Figure 19. The stub approached the substrate with a speed of 0.02 mm/s until the maximum allowed stubbing force was reached. This speed was set low to avoid too much overshoot after the maximum allowed force was reached. Then, the contact was held for 0.5 s followed by separation with a speed of 1 mm/s to a position 10 mm above the starting position. The used stubbing force, substrate name and stub name were noted and the stub was placed back in the stock box.

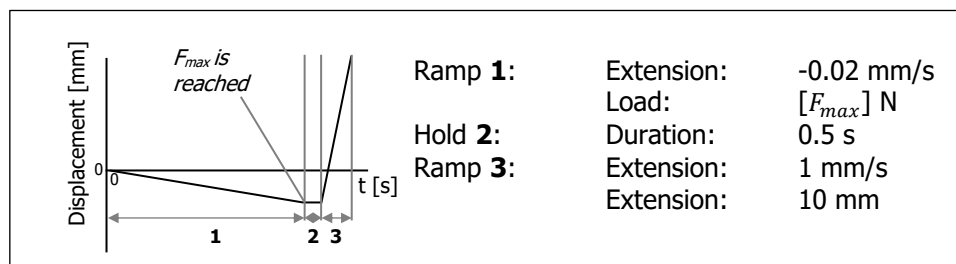


Figure 19 Method of force application conducted by the tensile tester.  $F_{max}$  was defined according to subparagraph 2.5.2.

The data that was obtained by using the tensile tester can be considered precise enough for what it is used for. Every 0.002 seconds a sample was taken. With the approaching velocity of 0.02 mm/s that was chosen, this resulted in resolution of  $2.5E4$  samples per millimetre displacement of the stub. This sample rate was maintained until the specified maximum force  $F_{max}$  was reached (defined in subparagraph 2.5.2). After this moment, the resolution decreased to 10 samples/mm. Considering the resolution, it is not likely that the resolution of the tensile tester was a limiting factor in the interpretation of the impression of the threads versus the stubbing force.

### 2.5.2 Magnitude of stubbing forces

Five different stubbing forces were selected in a way that the measured data for these forces properly describe the relation between stubbing force and micro-trace collection efficiency. It was hypothesised that the collection efficiency was proportional to the actual contact area between the tape and the substrate times the microparticle coverage on the actual contact area. Therefore, the stubbing forces were chosen in such a way that these measuring points together describe the trend of increasing contact area with increasing stubbing force. In this approach the particle distribution over the material was not taken into account yet.

To determine the relation between the stubbing force and the actual contact area between the tape and the sampled substrate, a pre-test with the tensile tester was performed to determine the relation between the stubbing force and the impression of the textile. A simplified calculation was subsequently used to estimate the actual contact area between the tape and the substrate based on the measured impression of the substrate.

The relation between the stubbing force and the impression of the textiles was defined over a force range from 0 to 9 N. To do so, the tensile tester was used and the same method of force application was used as described above, see Figure 19. On all three substrate materials, 3 trials were performed: in sample circles 1, 3 and 4 of the same spool of threads, see Figure 20. The trials were performed in succession without replacing the stub and/or tape. Before the

used trials, an additional trial was performed of which the resulting data was rejected. This was done because replacing of the stub gave errors to the first measurement, probably because the stub had to settle in the stub holder.

The resulting data was processed as follows. The moment of first contact was defined as the moment on which the measured force surpassed the noise in this signal ( $F > 0.005 \text{ N}$ ), see `'read_data.m'` in Appendix J. Note that the measured impressions were influenced by the deformation of the system that supports the tape and the textile. So, to know the impression of just the fibres and the tape under a certain stubbing force, the measured impression was reduced by the deformation of an empty metal spool and a stub without tape that was measured. It was taken into account that the system's deformation slightly differed between sample circles on the metal substrate base, see Figure 21. This was caused by the fact that the metal base was only supported at its ends (otherwise the impression of the textile threads at the bottom of the metal would be measured too). The measured absolute impressions of the textile threads and tape are represented in Figure 23. The  $F, d$ -plots of the individual trials can be found in Appendix H.

The system's deformation including the impression of the tape is shown in Figure 22. Here it can be seen that the measured deformation is much higher than for the same system without tape (Figure 21). This indicates that the measured absolute impressions, displayed in Figure 23, are indeed defined by the impression of the tape and the textile, and not only by the impression of the textile. It was checked if the measured deformation of the system, without tape and with tape, was influenced by the order of the measurements. It turned out that this had no effect. In Figure 22 the order of measurements is displayed.

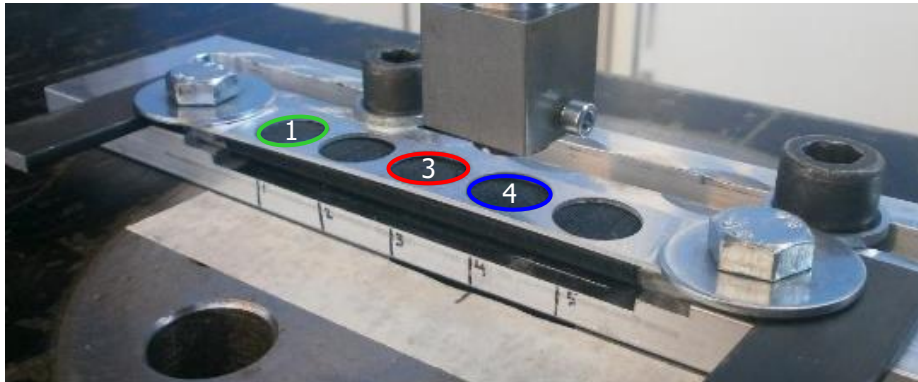


*Figure 20 Sample circles at location 1, 3 and 4.*

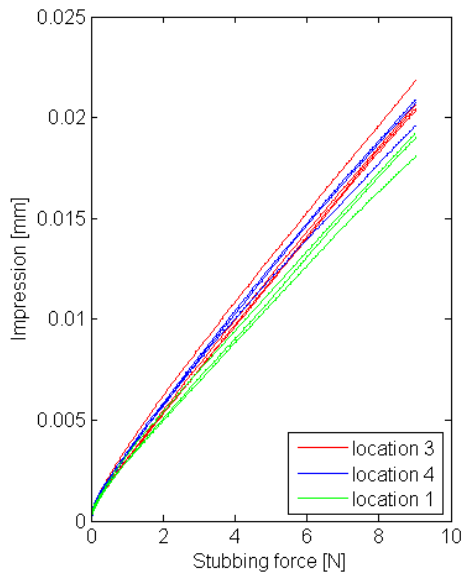


Figure 21 Deformation of the steel spool, the stub **without tape** and mounting under an applied force.

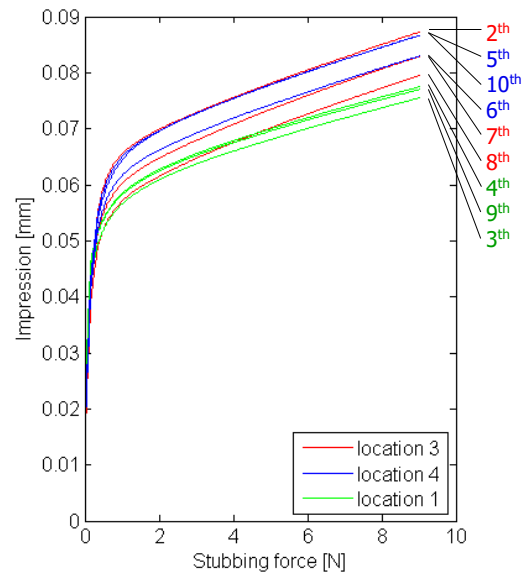


Figure 22 Deformation of the steel spool, the stub **with tape** ( $t = 0.1$  mm [6]) and mounting under an applied force.

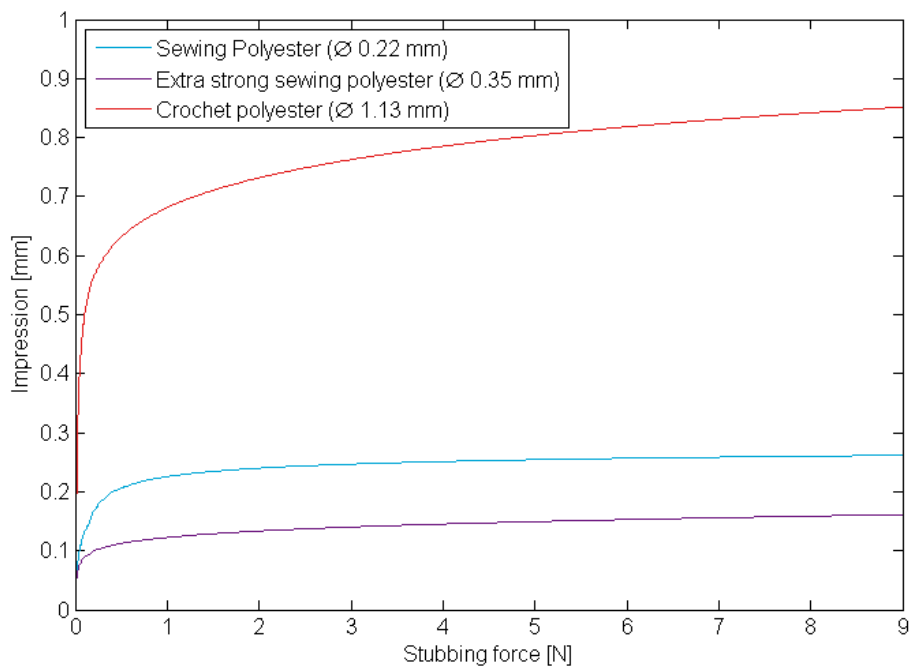


Figure 23 Mean absolute impression of the textile substrates and the tape (with a thickness of 0.1 mm according to the product specifications [6]) while stubbing with a 12.65 mm diameter aluminum stub-pin. The deformation of the system, see Figure 21, was subtracted from the measured data ( $n=3$  for each material).

A simplified approximation was used to relate the impression  $d$  of the textile substrates to the relative contact area between the tape and the substrates. The tape was approached as a rigid surface pressing in the thread which was approached as an elastic cylinder with a diameter equal to the measured thread thickness, see Figure 24. The thickness of the used polyester threads was measured under the microscope, see Appendix G.

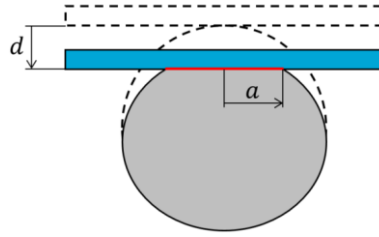


Figure 24 Figure that explains the used contact theory, for which the tape was considered as a flat rigid surface (in blue) and the threads were considered as cylinders (in grey). The indentation  $d$  of one thread results in a contact area with contact radius  $a$ .

The contact radius  $a$  in Figure 24 was calculated according to the classical solution for non-adhesive elastic contact between two cylinders with parallel axes [10]:

$$a = \sqrt{Rd} \quad \text{Eq. 2.1}$$

Where  $R$  can be calculated by:

$$\frac{1}{R} = \frac{1}{R_{\text{tape}}} + \frac{1}{R_{\text{thread}}} \quad \text{Eq. 2.2}$$

The tape was approached as a flat rigid surface,  $R_{\text{tape}} = \infty$ , and therefore  $R = R_{\text{thread}}$ .

If fibres are adjacent to each other without free space in between, the contact radius that relates to the apparent contact area is  $R_{\text{thread}}$ . Therefore, the relative contact area between the tape and the thread can be calculated as:

$$\text{Relative contact area} = \frac{a}{R_{\text{thread}}} \cdot 100 \% \quad \text{Eq. 2.3}$$

Together with the pre-test data, these calculations led to the relation between the relative contact area  $\frac{a}{R}$  and the stubbing force for all three different textiles, see Figure 25. In these calculations, the first contact between the tape and the top of the thread that was represented as a cylinder, was defined by the first moment of contact between the tape and the substrate measured by the tensile tester. However, as described above, this first moment of contact measured by the tensile tester was defined by contact with extruding fibres and irregularities in the substrate structure. The moment of contact between the tape and the top of the threads ( $d = 0 \text{ mm}$  in the calculation) could not be defined more accurately based on the measured data. At this moment, an abrupt change in the stiffness ( $\frac{\Delta F_{\text{stub}}}{\Delta d}$ ) was expected. However, this could not be observed in the data. If the moment contact with the thread tops could have been defined more accurate, the plots of the relative contact area would shift downwards and the steepness at the beginning of the plot would reduce.

Furthermore, for the calculation of the relative contact area it was assumed that the threads were so closely wound together that there was no distance between the threads, and therefore the radius that related to the apparent contact area was given by  $R_{\text{thread}}$ . However, in practice there was some free space between the threads, so the ratio between the real contact area and the apparent contact area would be lower in practice.

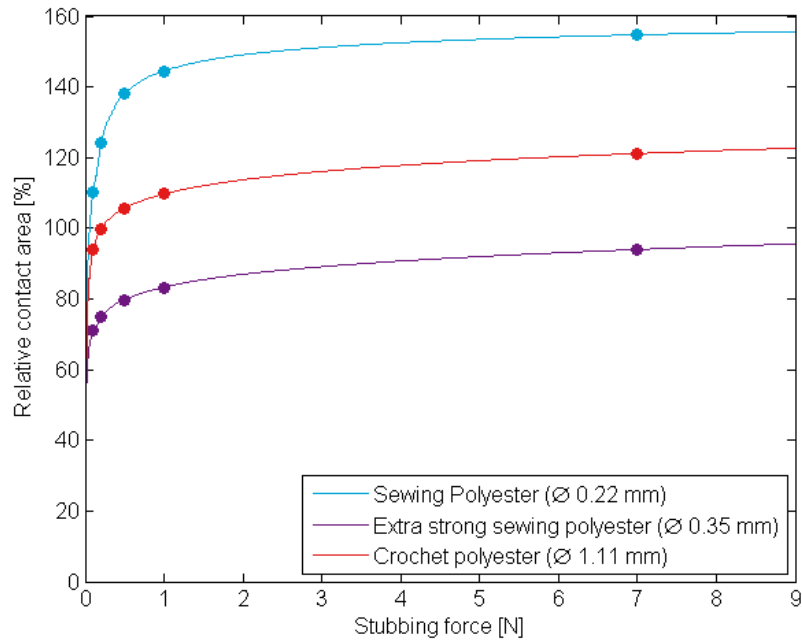


Figure 25 Calculated relative contact area versus the stubbing force, based on data from the tensile tester and simplified calculations. The relative contact area is a measure for the actual contact area relative to the apparent contact area between the tape and the textile. The dots represent the chosen stubbing forces for the current research.

The applied stubbing forces used during the experiments were chosen in a way that the data points related to these forces describe the trend of the calculated relative contact area well. The chosen stubbing forces were 0.1, 0.2, 0.5, 1.0 and 7.0 N, see the dots in Figure 25. A force overshoot was measured in the tensile tester, which was larger for the higher stubbing forces. So, to achieve the desired stubbing forces, the following values for  $F_{max}$  were set in the tensile tester software: 0.1, 0.2, 0.5, 0.97 and 6.73 N. The stubbing forces that are further mentioned in this report are the resulting forces and not the set forces.

## 2.6 Measurement of external factors

The ambient temperature and relative air humidity near the tensile tester were measured every half hour during stubbing, because changes in these conditions might influence the experiment results. The effects of these environmental conditions were not further analysed.



Figure 26 Digital thermometer (left) and analogue hygrometer (right).

## 2.7 Counting micro-traces

Microspheres were counted on the tapes after these were used to lift microspheres from the substrates. Before and after tape-lifting, microspheres were counted on the substrates as well. Counting was done as follows. Firstly, images of the tape and substrates were constructed by using a light microscope: the Keyence VHX-5000 Digital Microscope. Then the images were processed in Photoshop in order to discriminate the microspheres from the background. Finally, a self-made MATLAB script was used to automatically count the microparticles using image recognition routines.

### 2.7.1 Microscopy

To create pictures of the substrates and tapes, these were placed on the XY stage of the Keyence microscope under the 200x zoom lens. The substrate was positioned horizontally by placing the ends of the spools (where no threads were wound around) on two supporting metal strips. The stub was positioned horizontally in a self-made holder, see Figure 51 in Appendix B.

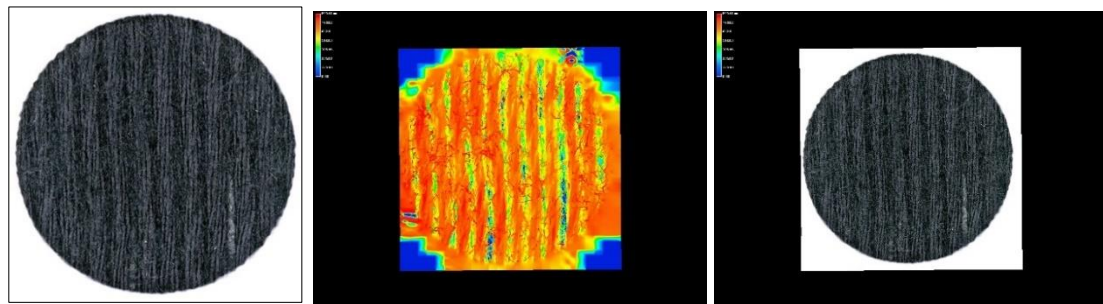
Tape and glass surfaces were captured by 2D image stitching: the microscope made multiple pictures and automatically stitched these pictures to one picture of the entire tape or sample area. For the textile substrates 3D image stitching was used. For this, the microscope not only stitched multiple pictures in the XY-plane together, but also in the Z-dimension. At each location in the XY-plane, the lens moved over the Z-axis while capturing the substrate at every 24  $\mu\text{m}$ . From these pictures with different focal planes, only the areas with in-focus data were extracted and combined to create a completely sharp picture that also included data of the height profile of the image [11].

For every picture, the same lighting, recording and stitching settings were used, which are displayed in Figure 27. The lighting was equal for textile substrates and the tape, but the glass was illuminated less, because the image would otherwise be overexposed due to the strong reflection of the glass. For 3D image stitching an upper and lower limit had to be specified. The upper limit was specified as the position of the lens at which the extruding fibres were in focus. The lower limit was defined as the position at which the steel substrate base was in focus. However, in some sample circles of the crochet polyester substrate, there was no steel visible. For these substrates, the lower limit was defined as the position in which even the deepest fibres were just out of focus.

<b>Lighting</b>	RGB:	[700 256 420]
	Light intensity:	Full ring Transmitted illumination: off Epi-illumination: 60 (textiles and tape) / 17 (glass)
	Shutter speed:	Manual, 15 ms
	Gain:	Manual, 2.5 dB
	HDR:	No
	<b>Rec settings</b>	Rec size:
<b>Stitching</b>	Set range:	(Top, right, bottom and left of the substrate's sample circle or the tape)
	Z set (only for 3D stitching):	
	Set upper:	(Extruding fibres in focus)
	Set lower:	(Metal substrate base in focus)
	Vertical Pitch:	Manual, 24 $\mu\text{m}$
<b>Settings for saving 3D images (height profile and reference picture)</b>		
	Height:	0 (display scale in height direction was set to 0, otherwise it would distort the 2D image)
	Scale:	OFF
	Save 3D data:	ON (height profile) / OFF (reference picture)

Figure 27 Used settings for the Keyence VHX-5000 Digital Microscope.

Before stubbing and after stubbing, three pictures of each sample circle were saved, see Figure 28. Firstly, the **original stitching result** was saved. This picture was used to detect the microspheres in it. Secondly, the picture was opened in the 3D menu, using the settings that are displayed in Figure 27. In this menu, the **height profile** was saved: an image with colours that indicate the height of the surface structure. To be able to overlay the normal image and the height profile accurately, the sample circle had to be detected in both images. In the height profile, this was not doable, because there was too little contrast between the sample cover and the substrate. Therefore, a **reference picture** was saved. This picture was similar to the height profile, but then with colours of the normal picture instead of the colours that indicate the height.



**Original stitching result**

**Height profile**

**Reference picture**

*PolcrochA1\_prestub\_normal.jpg*

*PolcrochA1\_prestub\_height.jpg*

*PolcrochA1\_prestub\_refheight.jpg*

*Figure 28 Example of the three resulting pictures from one sample circle on textile (crochet polyester before stubbing). From left to right: the original picture, that was detailed enough to detect the microspheres in it, the height profile, and the reference picture that was needed to overlay the height profile and the normal picture.*

After stubbing, pictures of the stub-tapes were saved too, see Figure 29 for an example.

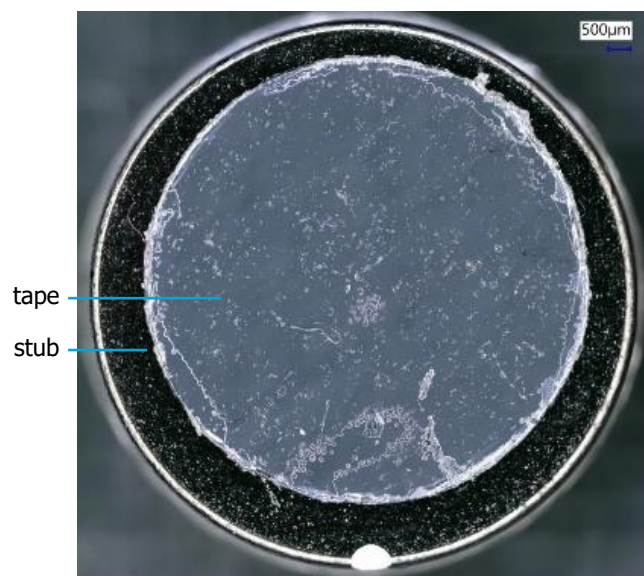


*Figure 29 Example of a picture of a stub after stubbing (Stub1A2.jpg).*

### 2.7.1.1 Tilt correction in the height profile picture

Some substrates were not situated completely horizontal relative to the lens, probably due to a fibre or another particle between the substrate and its metal supports. This could be seen by an incorrect colour gradient in the picture. This is demonstrated in the left picture in Figure 30, where the left part of this picture seemed to be higher (closer to red) than the right part. The '3D tilt correction' function was used to compensate the tilt in the height profile. Therefore, 3 points were selected that were defined in the same horizontal plane. If the adjustment resulted in a well-balanced colour profile, see for example the right picture in Figure 30, the image was corrected and then saved.

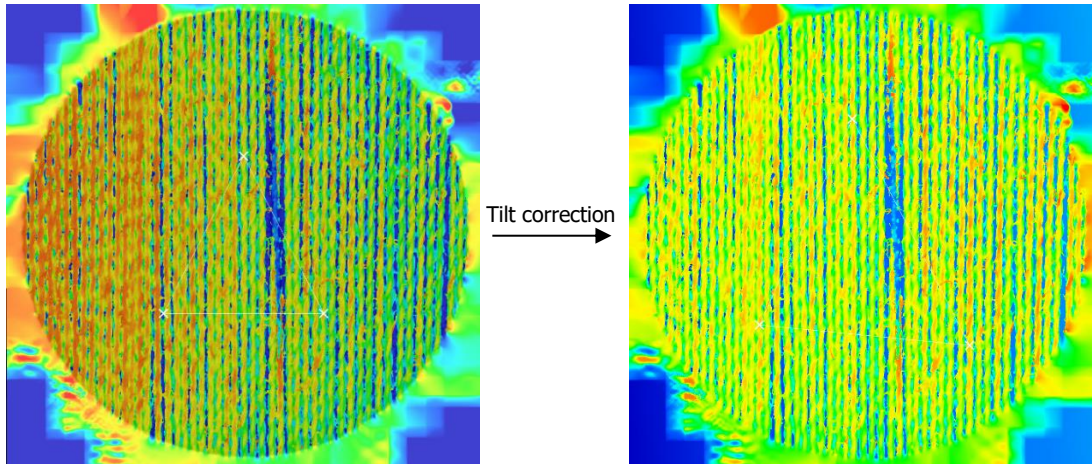


Figure 30 The left picture is tilted and should therefore be corrected. Tilt correction was done by selecting three points in the same horizontal plane (see white marks in the left picture).

### 2.7.2 Image processing in Photoshop

To simplify automatic counting of the microspheres, the microscope images of the tape and substrates were processed in Adobe Photoshop CS6. A succession of multiple image editing steps resulted in a binary image in which the microspheres could be discriminated from the background, see the transition from image 1 to 2 in Figure 31. These editing steps were recorded into a Droplet, which is an application made in Photoshop that repeats a processing sequence on a batch of photos by only dragging and dropping them to the Droplet application. The used editing steps and how the Droplet was created are described in Appendix I.

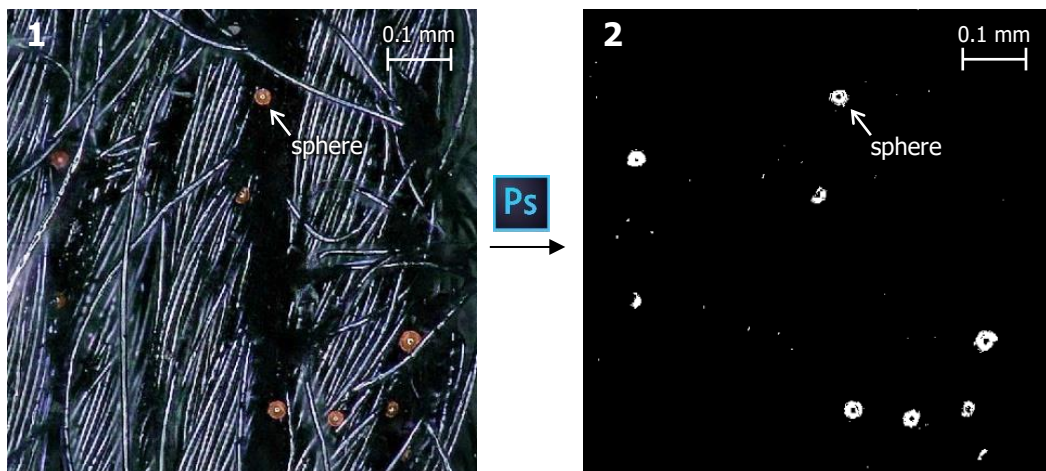


Figure 31 A section of a crochet polyester substrate with microspheres on it (PolcrochA1\_prestub): the original stitching result from the microscope (left) and the image that was processed by Photoshop (right).

### 2.7.3 Image processing in MATLAB

MATLAB was used to count the number of microspheres in the black and white images that resulted from the Photoshop processing, see Figure 32. The MATLAB function that was written for this, 'Define\_particle\_nr.m', is given in Appendix J. This function was called by 'Run\_define\_particle\_nr\_substrates.m' and 'Run\_define\_particle\_nr\_stubs.m', which are also given in Appendix J. The procedure was as follows.

1. The location of the tape centre or sample circle centre was detected in the normal microscope picture (the original stitching result). This location is identical to the location of the centre in the associated black and white image, because no changes were made in the size of the image in Photoshop.
2. The detected centre location was used as centre of the analysed circle in the black and white image. The area outside this circle was masked.
3. The 'noise' (i.e.: the smaller white spots that do not indicate spheres) in the black and white image from Photoshop was removed in MATLAB. This can be seen when comparing Figure 31 and Figure 32.
4. The microspheres were automatically detected by using the function 'imfindcircle'.
5. On some microspheres multiple circles were detected. To avoid double counting of these microspheres, a maximum tolerated overlap of the circles was set in the MATLAB code. If this maximum was exceeded, one of the two overlapping circles was removed. Figure 32 shows two examples of overlapping circles; the blue circles in the image were excluded from the counting because of the overlap with other circles.
6. To enable validation of the used method, the circles that indicated detected microspheres were displayed on the normal microscope image, see Figure 33.

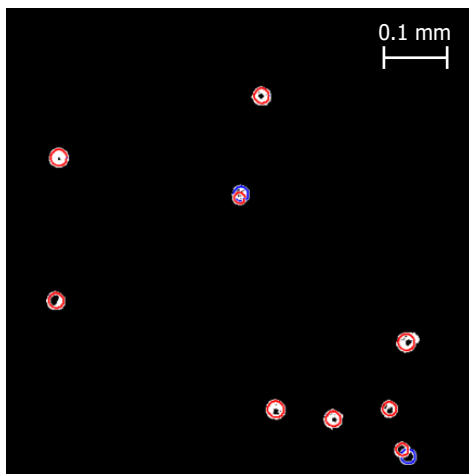


Figure 32 Particles were detected in the black and white image. The blue circles were not included in the particle counting, because the overlap was higher than tolerated.

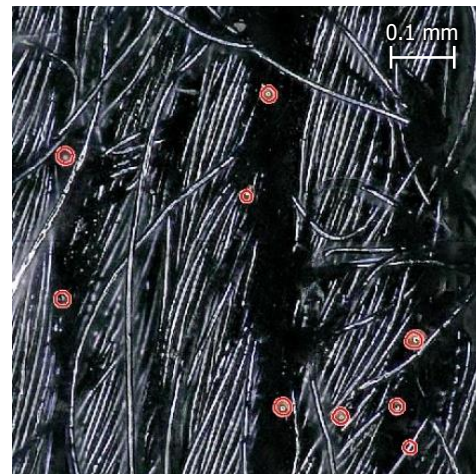


Figure 33 The circles that indicate detected microspheres were plotted in the normal microscope image.

The method that was used for counting the microspheres in the microscope images was validated. This was done by manually verifying the particle detection in different microscope images. The number of particles that were falsely detected by MATLAB and the number of particles that were undetected by MATLAB were counted based on visual observations. These numbers were both brought to an acceptable level by tweaking parameters in the MATLAB code, such as the range of the microsphere radius and the sensitivity of the circle detection, see Appendix L.

After particle counting by MATLAB, the resulting images (Figure 33 is a section of one of those images) were quickly scanned visually. When a closely packed group of falsely detected

microspheres was detected, for example on a red toned fibre, the number of these falsely detected microspheres was subtracted from the number of detected microspheres. An example is given in Figure 34: a picture of a tape sample on which a fibre was causing a lot of falsely detected fibres.

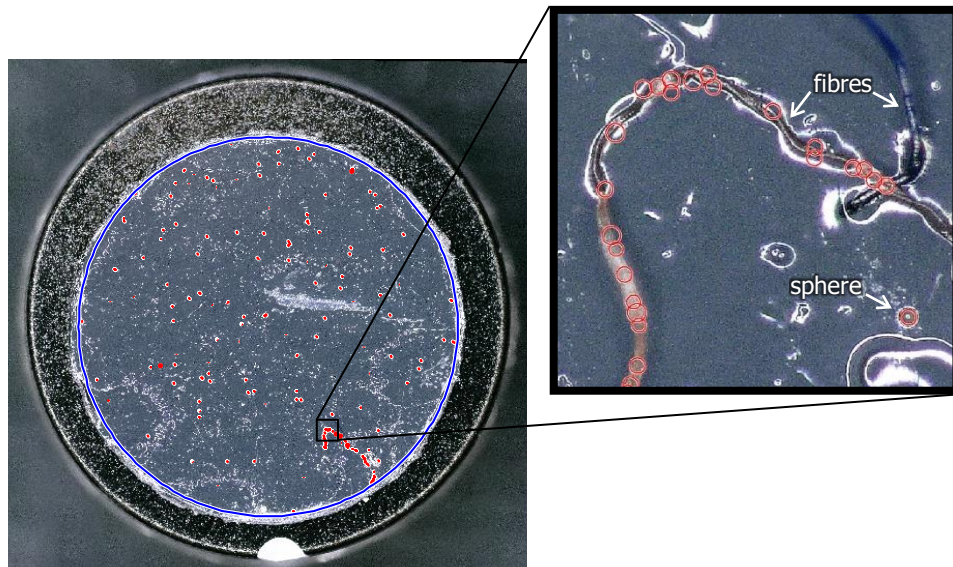


Figure 34 Example of microspheres that were falsely detected on a red toned fibre. The number of these falsely detected particles was manually subtracted from the total number of microspheres calculated by MATLAB.

The distribution of microparticles over the depth of the textile substrates, before and after stubbing, was examined to analyse the particle collection efficiency of microparticles from different depths in the substrate structure (research question 2). The MATLAB function that was written for this, 'Define\_particle\_height\_textiles.m', can be found in Appendix J. This function was called by 'Run\_define\_particle\_height\_textiles.m', which is also given in Appendix J. The procedure was as follows.

1. Only the part of the sample circle was analysed that was fully covered by the tape anyways. Because the placement of the tape was not exactly similar during every tape-lift, the fully covered area had to be determined according to Appendix K.
2. The normal microscope picture and the height profile picture were overlaid. Therefore, the location of the sample circle in the height profile image was determined by detecting the sample circle in the equally sized reference picture (see for example the third image in Figure 28). The analysed part of the sample circle in the height profile was masked, cut out and scaled to the same size as the normal microscope picture, see Figure 35. The normal microscope picture was masked and cut out as well.
3. The microspheres were counted according to the same procedure as in the function 'Define\_particle\_nr.m' (now only in the smaller, fully covered sample area). Subsequently, the locations of the detected microspheres could be plotted in the height profile image, see Figure 35.
4. The colour (i.e.: RGB-value) at the location of each detected microsphere centre in the height profile image was linked to a height value by selecting the best corresponding colour in the legend of the height profile image, see Figure 36. The colours in the legend colour bar were interpreted as follows. The maximum value in the legend colour bar was entered manually in MATLAB (899.41  $\mu\text{m}$  in the example of Figure 36). Based on this value, a height value was assigned to all 254 unique RGB-values in the legend colour bar by MATLAB.

- The absolute height of the microspheres do not offer useful information if the reference height deviates between different samples. Therefore, the minimum height measured in the sample circle was defined. This minimum height was the height of the steel base basically. However, as mentioned in subparagraph 2.7.1 the steel base was not visible in every substrate of crochet polyester, and therefore the minimum height was sometimes defined by the deepest detected fibres in these samples. This minimum height in the sample circles was subtracted from the absolute heights of the microspheres that was measured to get the relative distance from the substrate base (or relative distance from the deepest fibres for some crochet polyester substrates).

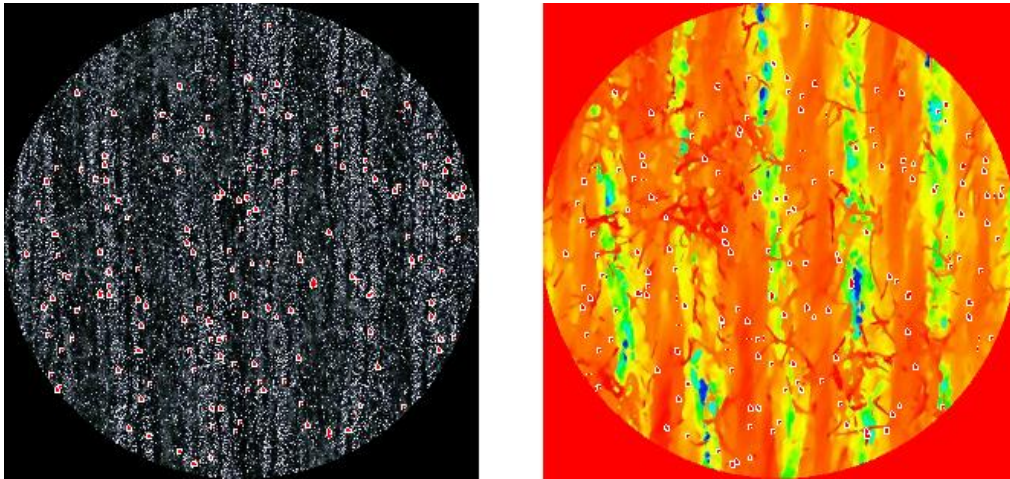


Figure 35 The microscope image was masked and cut out (left) and the corresponding height profile image was masked, cut out and scaled to the same size as the original stitching result. The microspheres that were detected in the image were plotted in both images.

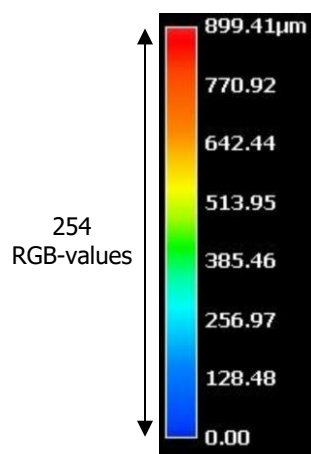


Figure 36 Legend colour bar of one of the height profile images. It consists of 254 unique RGB values that match to colours in picture. Every RGB-value on the legend was assigned a unique height value.

## 2.8 Data analysis

### 2.8.1 Collection efficiency for different stubbing forces

The collection efficiency of microspheres,  $\eta_{collection}$  [%], was calculated by dividing the number of microspheres detected on the stub tape by the number of microspheres that were present before stubbing at the substrate surface area that was covered by tape. However, this second number of microspheres could not be determined directly, because the exact placement location of the tape on the substrate is unknown. Therefore, the particle density on the substrate before stubbing,  $\rho_{substrate\ prestub}$  [#/ $mm^2$ ], was calculated by dividing the number of detected microspheres on the substrate before stubbing by the surface area that was analysed, see equation 2.4.

$$\rho_{substrate\ before\ stubbing} = \frac{n_{substrate\ before\ stubbing}}{A_{substrate}} \quad Eq. 2.4$$

The particle density was used to estimate the number of microspheres on the surface area of the substrate on which the tape was placed. Thereby, the collection efficiency could be calculated, see equation 2.5.

$$\eta_{collection} = \frac{n_{tape}}{A_{tape} \cdot \rho_{substrate\ before\ stubbing}} \cdot 100\% \quad Eq. 2.5$$

For each combination of substrate material and stubbing force, the mean collection efficiency of 3 trials was calculated. Statistical analysis of this data was not possible because of the limited amount of data points. Therefore, descriptive statistics was applied. Per substrate material, a curve was fitted to the mean collection efficiencies, to indicate the overall trend of collection efficiency over increasing stubbing force. These curves were compared to the graphs of the relative contact area vs. the used stubbing force.

Furthermore, it was analysed if there was a correlation between the collection efficiency of microparticles from a textile sample and the number of microparticles that were present on that sample before stubbing. This was done so that a potential difference in the number of microparticles on the substrates would not influence the test results without being noticed.

### 2.8.2 Distribution of microspheres over the height of the textile substrates before and after stubbing

The distribution of microspheres over the height of the textile structure before and after stubbing was compared. Therefore, five 'height levels' were distinguished per substrate material. These height levels defined equal height ranges between 0  $\mu m$  (which should indicate the height of the steel substrate base) and the height of the highest detected particle relative to the base (this can be larger than the diameter of the thread due to extruding fibres). The difference between the number of detected microspheres before and after sampling was calculated per height level, see equation 2.6. If the microspheres do not displace on the substrate, apart from being captured by the adhesive tape, this (negative) number indicates the number of collected microspheres per height level.

$$(n_{substrate\ after\ stubbing,i} - n_{substrate\ before\ stubbing,i}), \text{ where } i = 1 \dots 5 \quad Eq. 2.6$$

# 3.

## 3 Results

### 3.1 Adhesive performance of tape after UV irradiation

The mean maximum adhesive force between the 10 mm diameter adhesive tape and the glass substrate over each set of trials was calculated and the results were compared, see Table 2 and Figure 37. UV irradiation by both the setup of the NFI and the TU Delft turned out not to have a noteworthy effect on the maximum adhesive force between the tape and the glass. It can be seen that the variation in adhesive forces between the differently UV irradiated tapes is small, and not consistent over the various applied stubbing forces. Though, the UV irradiation had a notable effect on the colour of the tape, which indicates that there had been a physical change in the tape. It is possible that the colour change is a result of a chemical change in the backing of the glue, which is a UPVC film [6].

*Table 2 The measured maxima of the adhesive forces between adhesive tape and glass are displayed for not UV irradiated tape, tape that was UV irradiated at the TU Delft and tape that was UV irradiated at the NFI. The maximum adhesive forces that are measured with a stubbing force of 9 N are displayed together with their standard deviations.*

		UV irradiation		
		No UV	UV TUDelft	UV NFI
Stubbing force	1 N ( $n=3 \times 3$ )	2.55 N	2.35 N	2.65 N
	3 N ( $n=3 \times 3$ )	5.06 N	5.7 N	5.00 N
	9 N ( $n=6 \times 3$ )	8.45 ( $\pm 1.32$ ) N	8.02 ( $\pm 0.53$ ) N	8.83 ( $\pm 2.01$ ) N

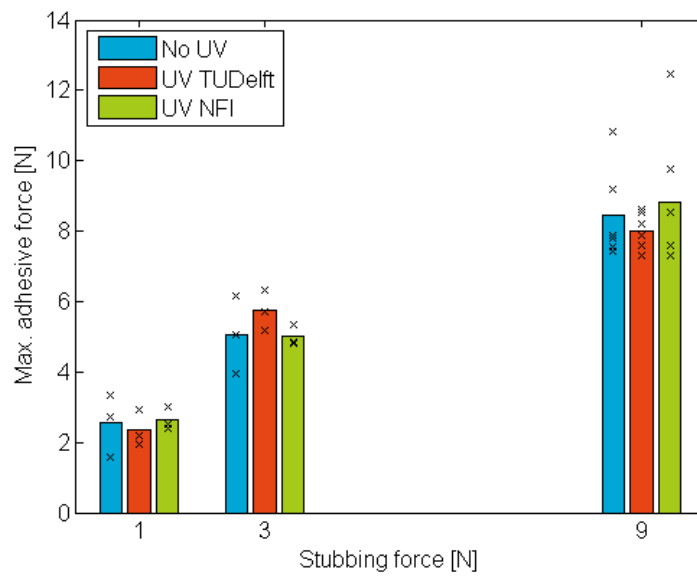


Figure 37 Mean maximum adhesive force measured between adhesive tape (10 mm diameter) and glass after stubbing with 1, 3 and 9 Newton. Three different tape types were tested: not UV irradiated tape (No UV), tape that was UV irradiated with the setup that was designed at the TU Delft (UV TUDelft), and tape that was UV irradiated according to the procedures of the NFI (UV NFI).

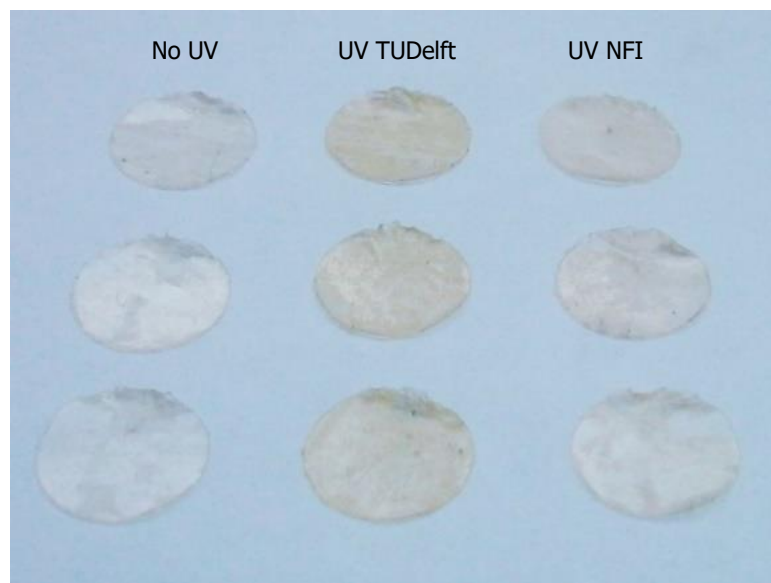


Figure 38 There was a notable colour difference between tape that was not UV irradiated (left column) and tape that was UV irradiated in the setup that was developed at the TU Delft (middle column). A smaller colour difference was visible between the tape that was not UV irradiated and the tape that was UV irradiated according to the procedures of the NFI (right column).

### 3.2 Collection efficiency for different stubbing forces

In Figure 39 the collection efficiency of microparticles can be found for all used stubbing forces on three different substrate materials. It can be seen that some stubbing forces were not exactly equal to the intended stubbing forces. This was due to overshoot in the tensile tester. This overshoot was already considered when the maximum force was set in the software that actuates the tensile tester. However, it can be seen that the force overshoot differed between substrate materials and between trials. The collection efficiencies were calculated based on the raw experiment data that is displayed in Appendix M.

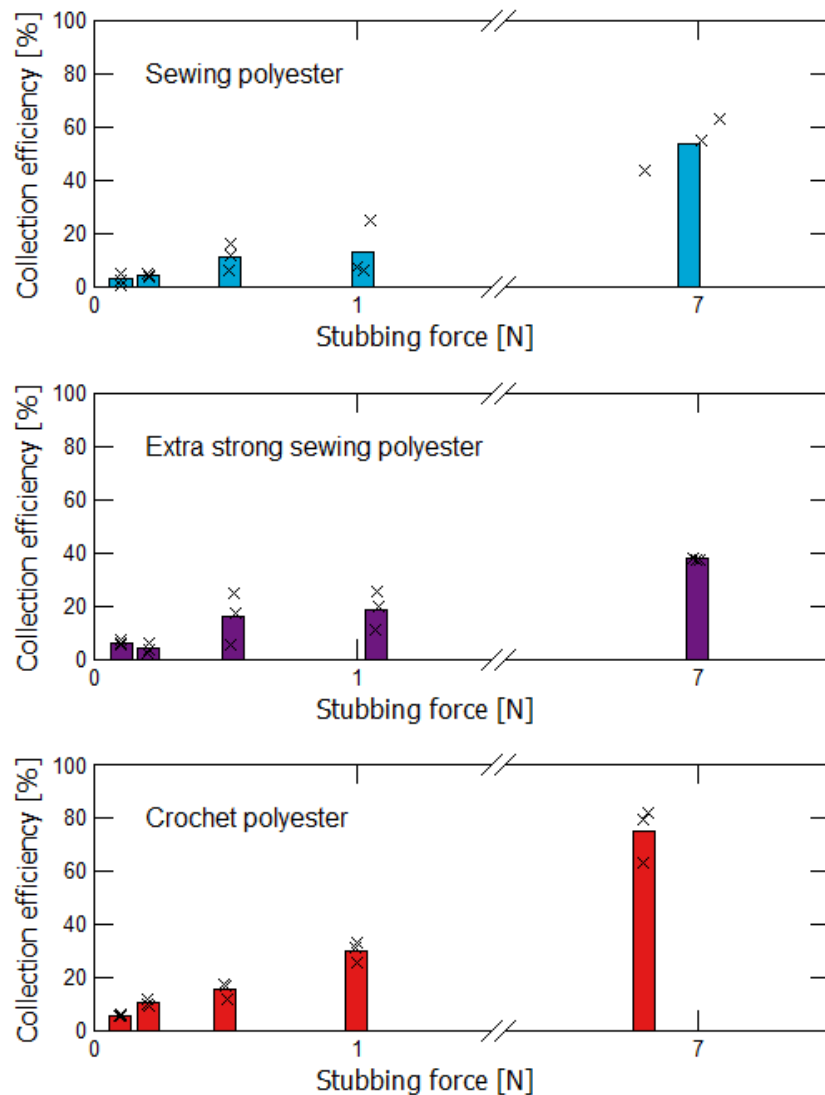


Figure 39 Collection efficiencies of microspheres when stubbing at about 0.1, 0.2, 0.5, 1 and 7 N. The x-marks indicate the individual trials (n=3). Results are displayed for all three substrate materials.

A curve was fitted through mean collection efficiencies according to an exponential behaviour  $y = -a \cdot e^{-b \cdot x} + c$ , see Figure 40. This plot shows the overall trend that was specified by the data points.

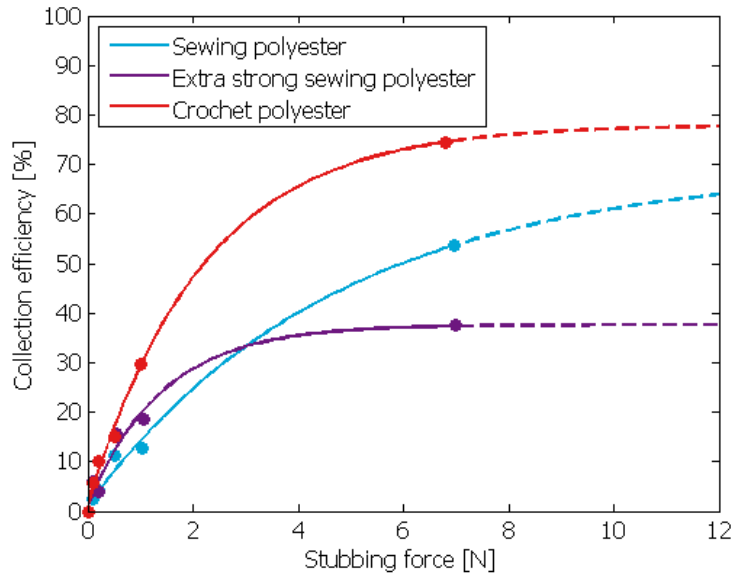


Figure 40 Curves were fitted through the mean collection efficiencies that were plotted over the used stubbing forces (represented by the dots in the graph) according to the expected behaviour, which is increasing and which stagnates at a certain force ( $y = -a \cdot e^{-b \cdot x} + c$ ), using the least squares method.

The correlation between the number of microspheres on the substrates before stubbing and the collection efficiency when stubbing from these substrates is visually displayed in Figure 41.

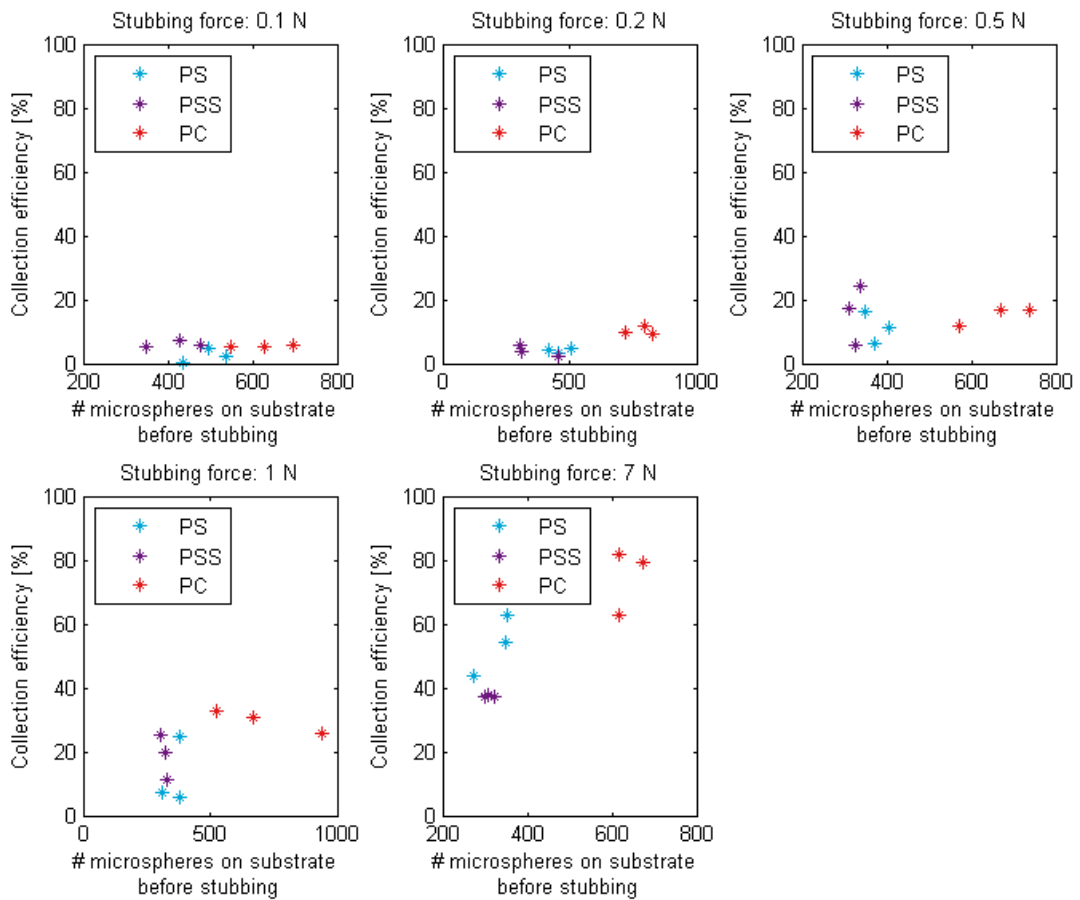


Figure 41 Collection efficiency versus the number of microspheres on the substrate before stubbing for the different textiles: sewing polyester (PS), extra strong sewing polyester (PSS) and crochet polyester (PC).

### 3.3 Distribution of microspheres over the height of the textile substrates before and after stubbing

Microscope images of the textile substrates before and after stubbing were compared using MATLAB. An example of how this was visualised is displayed in Figure 42.

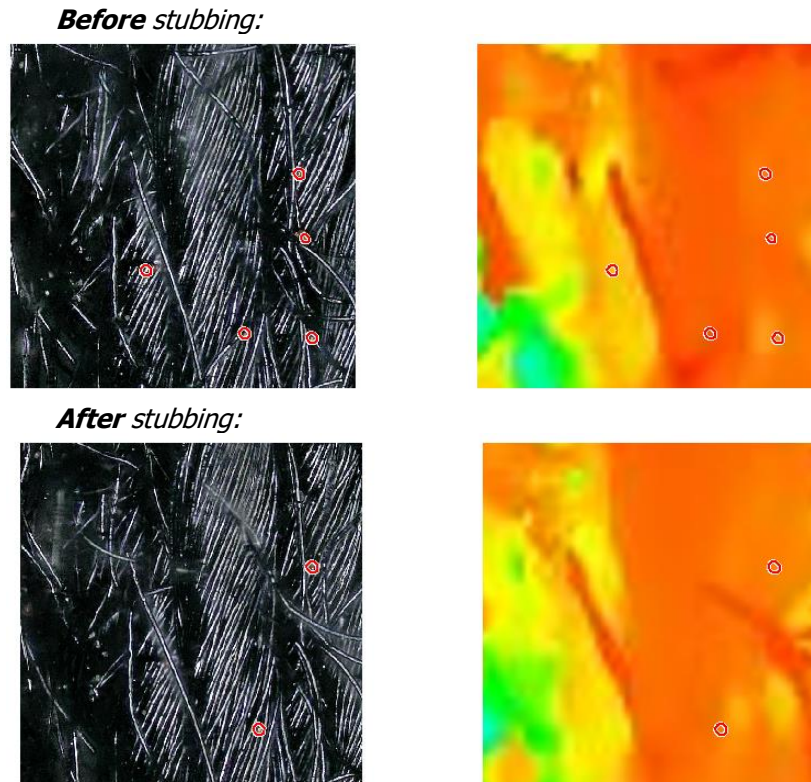


Figure 42 Example of resulting images after particle detection and overlap with the height profile before and after stubbing (PolcrochA1). In this example it can be seen that three particles are disappeared and two are not moved.

The difference between the number of detected microspheres before and after stubbing ( $n_{after\ stubbing} - n_{before\ stubbing}$ ) on sewing polyester was displayed per height level, Figure 43. This data is based on 3 trials per stubbing force. The raw data of these trials is displayed in Table 7 in Appendix N. The difference in number of detected microspheres over all five height levels together is displayed in the legend of Figure 43. To support the interpretation of this data, the mean distribution of microparticles on sewing polyester substrates before stubbing is displayed in Figure 44. For the other substrate materials similar results were obtained and these are displayed in Appendix N.

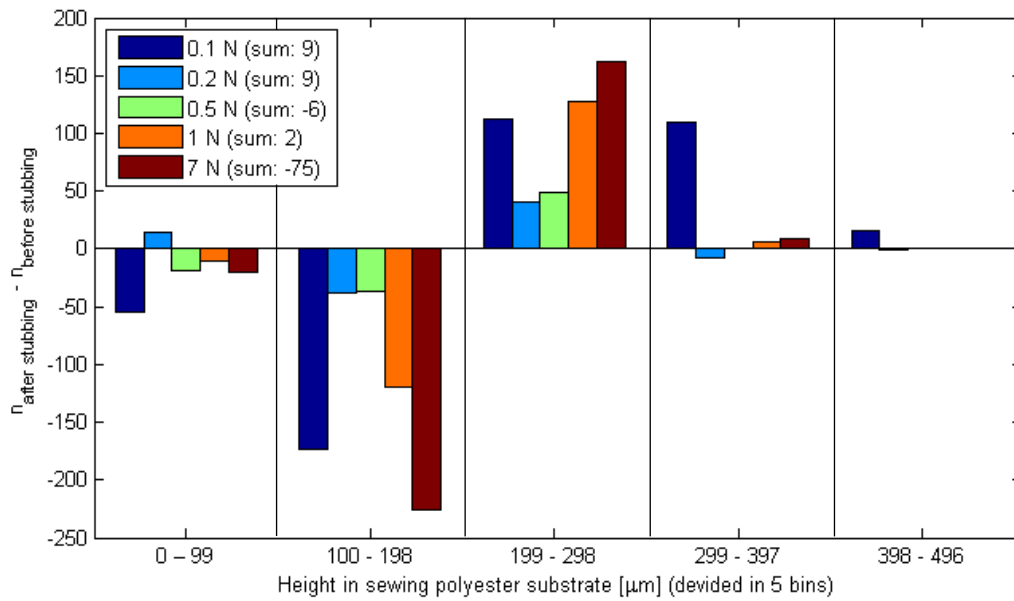


Figure 43 The difference between the number of microparticles after and before stubbing on sewing polyester. In the sample circles, only the area was analysed that was fully covered by tape (n=3).

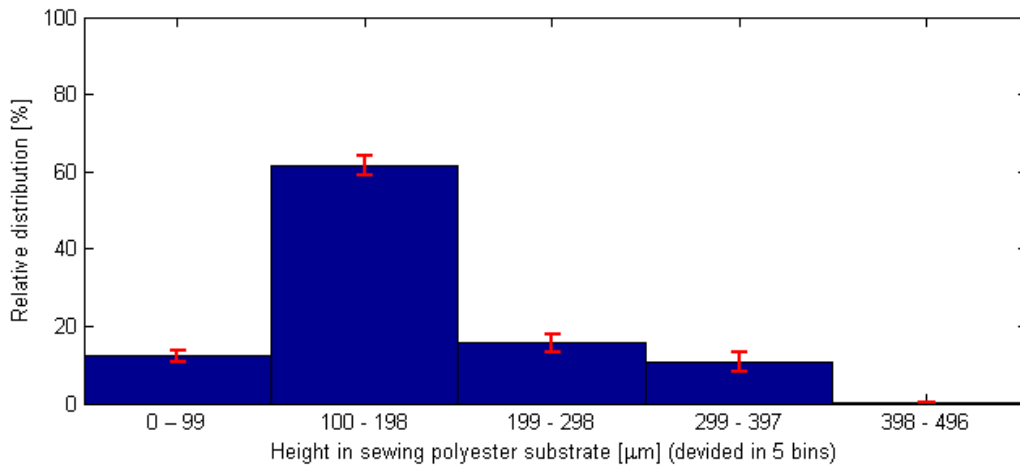


Figure 44 Mean distribution of microparticles on sewing polyester substrates over the height levels before stubbing (n=3x5). The red lines indicate the standard deviation between the trials.

### 3.4 Other measured external factors

During stubbing, the ambient temperature varied between 21 and 24 degrees Celsius. The relative humidity of ambient air varied between 38 and 36 % ( $\pm 5$  %).

# 4.

## 4 Discussion

---

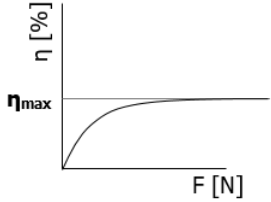
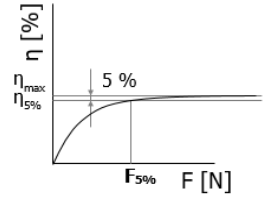
Microspheres were deposited on different textile substrates, and collected from these substrates by using stubs. The influence of the used stubbing force, that was applied using a tensile tester, on the trace collection efficiency was analysed. The trace collection efficiency was determined using visual quantification of the microspheres on the substrates and the stub-tapes. The results showed an increase of collection efficiency with an increasing stubbing force, which is discussed in paragraph 4.1. The collection efficiency from selective heights in the substrate structures was analysed to see if layered collection would be possible, see paragraph 4.2. Recommendations are given in paragraph 4.3. Finally, the results of this research are placed in its wider context and recommendations for future research are given in paragraph 4.4.

### 4.1 Collection efficiency for different stubbing forces

On all textile substrates, the mean efficiency of the collection of microspheres increased with increasing stubbing force in a concave down increasing function. This matched the expectation that the collection efficiency would increase in a similar manner as the actual contact area between the tape and the substrate. A more detailed comparison between the collection efficiencies (Figure 40) and relative contact areas (Figure 25) was not made, because the calculated relative contact areas were not accurate enough, as described on page 26. Moreover, the collection efficiency was not only defined by the contact area, but also by the distribution of microspheres over the depth of the substrate material.

The collection efficiency of microspheres increased most quickly among low stubbing forces up to about 1 N. The rise of collection efficiency with increasing stubbing force stagnated between 3 and 12 N according to the fitted curves, see Table 3. These results indicate that stubbing with a stubbing force higher than 12 N would not be really useful when requiring a maximum collection efficiency on the variety of substrate materials that was tested. However, based on the fitted curves, the theoretical maxima of the collection efficiencies are far below 100%. These results suggest that it might be more useful to stub multiple times on the same location of a substrate when the goal is to collect as much as possible than to further increase the stubbing force.

*Table 3 Theoretical maxima of the collection efficiencies and calculated stubbing forces at which the increase of collection efficiencies stagnated (defined as 5% (absolute number) from theoretical maximum) for different substrate materials.*

	<b>Theoretical maximum collection efficiency</b>	<b>Stubbing force at stagnation of collection efficiency (5 % below theoretical maximum)</b>
		
<b>Sewing polyester</b>	69 %	12 N
<b>Extra strong sewing polyester</b>	38 %	3 N
<b>Crochet polyester</b>	78 %	6 N

When the particles were counted, deviations of the counted number of particles with respect to the true number of visible particles were caused in two ways: particles were undetected by the used method or particles were falsely detected (for example on a red toned fibre as in Figure 34). The number of undetected particles depends on the number of present particles (if no particles are present in a sample, there can be no undetected particles). The number of falsely detected particles depends on the size of the area that was analysed more than the number of visible particles. Therefore, the proportion of falsely detected particles relative to the number of present particles is especially high for low collection efficiencies.

To calculate the collection efficiencies, several assumptions were made. Firstly, a visual method was used to quantify the number of particles. This means that particles present at the textile substrates could be invisible, because these were covered by fibres or other particles. On the tape, particles could only be overlapped by other particles. This suggests that there are probably much more undetected particles on the substrates than on the tape, and therefore the true collection efficiency was probably lower than displayed in Figure 39 and Figure 40.

Another assumption that was made, was that the tape and the substrate were two parallel surfaces, what would result in a homogeneous pressure distribution over the tape. However, the observable inhomogeneous distribution of microspheres over the surface of the tape after sampling glass indicate there was no homogeneous pressure distribution in the contact between tape and glass, see Appendix O. Therefore it is likely that the surface of the tape and the textile substrates were tilted relative to each other as well during stubbing. However, this was not notable when observing the tapes that sampled the textile substrates. The deformability of the textile resulted in a more equal pressure distribution between the tape and the substrate than between the glass and the tape.

#### 4.1.1 Number of microspheres on the substrate before stubbing vs. trace collection efficiency

Figure 41 shows that the number of microspheres on the substrates before stubbing differed among different samples. The intention of the used material deposition method was to deposit about 1000 microspheres on the surface area of the sample that was to be covered by tape, which indicates that there should be about  $1.6E3$  particles in the analysed part of the sample circle before stubbing. However, in practice there were much less particles detected on the analysed parts of the sample circles on the substrates (on average 673 on crochet polyester, 402 on sewing polyester and 346 on extra strong sewing polyester). One of the causes for this is that the suspension of ethanol was spread out so fast, that the liquid also penetrated in the textile on the other side of the spool, which is known because moisture was detected beneath the spools after material deposition. This caused the particles to be distributed over a larger surface area than was intended when this method was designed. An additional explanation is that some particles were undetectable by the microscope, because these were covered by the threads.

Within sets of 3 trials (same stubbing force and same substrate material used), there was no consistent trend in the relation between the collection efficiency and the number of microspheres present on the substrate before stubbing, see Figure 41. Therefore, it was assumed that the existing differences in particle density on the substrates before stubbing did not influence the collection efficiencies.

## 4.2 Collection efficiencies at different height levels of the substrate structure

The number of detected microparticles in defined height levels of the substrates differed after and before stubbing. This had several potential causes. Firstly, if this difference is negative ( $n_{after\ stubbing} < n_{before\ stubbing}$ ), material was possibly collected by tape. However, there are several other possible explanations. Microparticles could have been moved over the substrate material, and end up in another height level. Furthermore, particles may have become visible or invisible by displacement of the fibres. This latter phenomenon was also visually detected, see Figure 45. This phenomenon affirms that stubbing one the same location on the evidentiary item more than once can be beneficial to optimize the overall collection efficiency. Moreover, the displacement of microspheres and fibres results in the fact that the applied method is not suitable for determining from what height the collected particles originated. This is only possible when the initial locations of the collected particles can be deduced. To do so, a new method should be designed.

Though, the acquired data of the impression of the polyester threads and adhesive tape under an increasing stubbing force already gave some insight in the collection efficiency from different height levels. When stubbing with 1 N, the impression of the tested substrate materials almost reached its maximum. This means that it is likely that contact with deeper layers of the substrate is made when applying 1 N, by which it is possible that material is collected from deeper layers of the substrate. Therefore, it is likely that selective collection of superficial traces is only possible when using a stubbing force far below 1N.

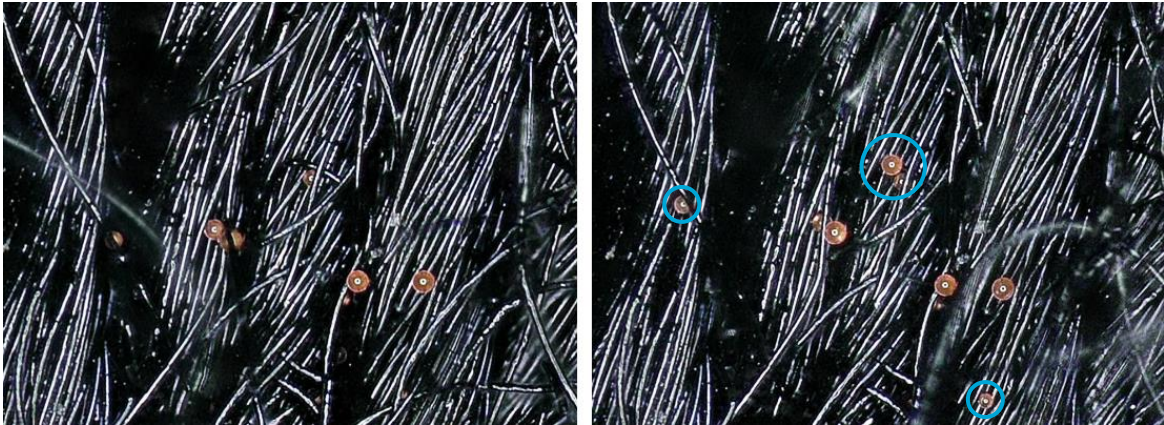


Figure 45 A crochet polyester substrate before (left) and after (right) stubbing. It can be seen that by displacement of the fibres and the microspheres, some microspheres moved to a more superficial position in the substrate (indicated by the blue circles in the right image).

#### 4.2.1 Inaccuracies

There were falsely detected and undetected particles in the images of the substrate as discussed above. When the overall collection efficiency (from all heights in the substrate together) was calculated, the falsely detected particles on large irregularities could be manually subtracted from the sum of detected microspheres. However, when the height of detected particles was of interest, this was not feasible, because therefore the height information of each individual particle that was falsely detected should be determined and should be removed from the total data manually. Another observation was that the number of falsely detected particles was larger after stubbing than before stubbing. Oxidation of the steel substrate base could possibly be an explanation for this phenomenon, because hereby the metal would get a more red tone, similar to the colour of the microspheres, see Figure 46. However, not only on the metal, but also on the fibres more particles were detected. An explanation for this phenomenon cannot be given, because all settings of the microscope, Photoshop CS6 and MATLAB that were used to analyse the samples before and after stubbing were equal, except from the exact upper and lower limit of Z-range over which the microscope lens moved. However, this difference does not offer an explanation for the observed difference in falsely detected particles before and after stubbing.

The resolution of the height profile image was limited compared to the normal image. However, 1 pixel in the height profile was smaller than the size of a microparticle, so considering this the height profile image could be used as indication of the height of a particle.

Furthermore, the overlap between the normal photo, that was used for particle detection, and the height profile was limited, because the centre of the sample circle that was detected in the normal picture did not always exactly match the centre that was detected in the height profile (by using the reference picture, see Figure 28). An inaccuracy of this resulted in the fact that particles were not projected on the right spot in the height profile.

Finally, the reference height in the height profile image could not always be defined by the height of the steel base. In samples of crochet polyester (the thickest thread, with least free space between the threads) the lowest detected height in the profile was defined as reference height. However, this height can be different between samples, and therefore this gives a deviation when comparing the results of multiple samples.

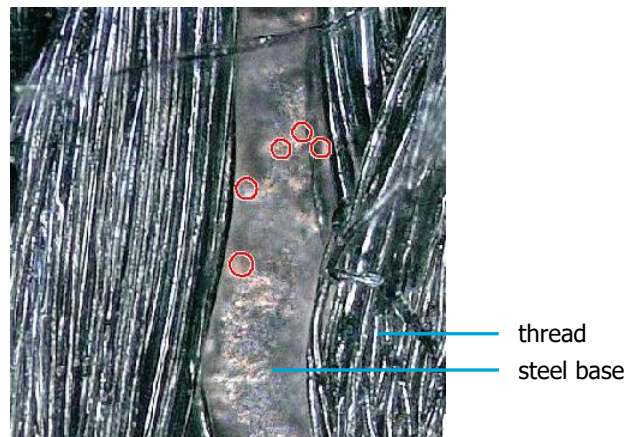


Figure 46 Oxidation of the steel substrate base resulted in falsely detected particles (PolsewstrA1 before stubbing). Possibly, further oxidation in the time between the pictures taken before stubbing and after stubbing resulted in a higher total number of falsely detected particles on the metal substrate base after stubbing.

Most of the mentioned limitations can be solved by some changes in the used method. These recommendations are given in paragraph 4.3.

## 4.3 Recommendations to improve the used method

### 4.3.1 Improve particle detection

A better distinction between microspheres and the background could be improved by the following adjustments. The steel substrates have to be painted black, just as the stub-pins. A large proportion of the falsely detected microspheres was detected on the steel, because of its red tone. The number of falsely detected microspheres on the fibres could probably be reduced by using a lower light intensity of the microscope light. This should reduce the red tone in the fibres resulted by the over-exposure of light. When reducing these risks of falsely detecting particles, the sensitivity used in the particle detection method could probably be set higher, what will subsequently result in less undetected particles on the textile substrates as well.

In this method, a well-considered choice was made to deposit the microparticles on the substrates by using a solvent. This resulted in a homogeneous distribution without agglomerations of particles. However, the disadvantage of this method is that particles can penetrate in the fibres, by which the particles get invisible, what leads to an inaccuracy in the quantification of particles. One alternative to solve this, is to find a new method to equally distribute dry particles upon the substrate. Another alternative would be to know the concentration of microspheres in the solvent that is deposited (just as it was known in these experiments) and to know on which surface area this solvent spreads out (which was unknown, because the solvent flowed beyond the edges of the substrate spools). A potential way to set this surface area, is by using water in the solvent instead of ethanol. It was observed that a water droplet did not flow out over the used substrates well. This is caused by the higher surface tension of water relative to ethanol. If a droplet of a water-based solvent evaporates, particles in the solvent will be distributed over the surface area of the droplet.

### 4.3.2 Improve determination of particle depth location

Close to every sample circle there should be a visible part of the metal support, so this could be defined as reference height. By a consistent definition of the reference height, the height of microparticles relative to this reference can be compared properly between different samples.

The overlap between the detected sample circle in the normal microscope image and the height profile would probably be more accurate if the edge of the circle in the sample cover was smoother. In these experiments, the sample circles had rippling edges as a result of the

low accuracy of the laser cutter by which the sample covers were produced. This also reduced the detection accuracy for this circle. Another solution would be to place reference marks on the sample cover that can visually be detected by MATLAB.

More insight is specifically desired in the way how traces can selectively be collected from merely the top layer of the substrate. This is most likely only possible when using low stubbing forces, and thus when the collection efficiencies are low as well. The difference between the number of particles that can be found on the substrate before and after stubbing will therefore be really small, so even small inaccuracies in the used method would have a large impact. Therefore, it is relevant that if more insight is desired in the collection of traces from selective depths of textile, the used method has to be considerably accurate.

#### 4.4 Future research

To see how the results of the current study can be implemented further, this experiment was placed in its wider context, see Figure 47. Based on this context, recommendations are given for future studies on the five topics that are also displayed in Figure 47.

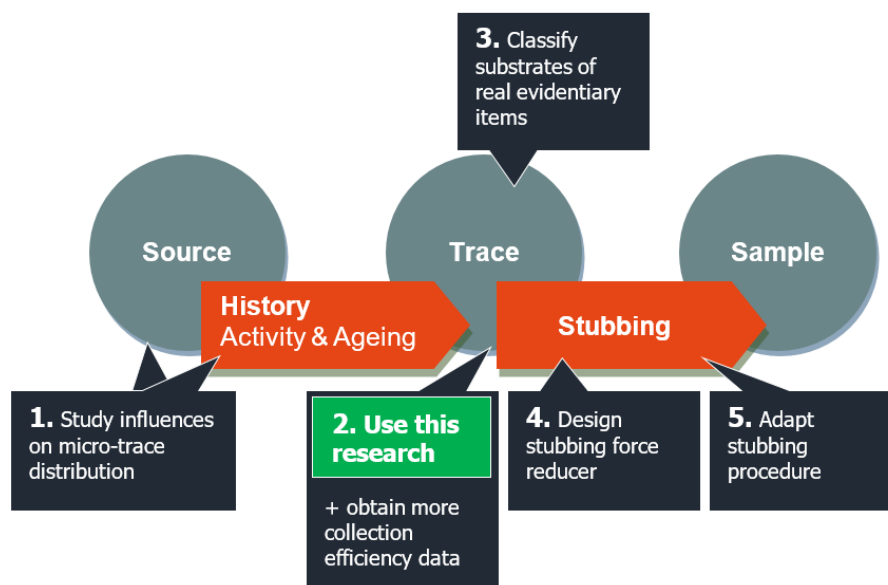


Figure 47 DNA transfer process from a DNA source to a sample. The numbered remarks indicate the recommendations for future studies.

##### 1. Study influences on micro-trace distribution

To the best of our knowledge, there are no studies that analysed the distribution of trace DNA (or other micro-traces) on textiles or other substrates. However this distribution will determine to what extent it would be possible to selectively collect a targeted trace from a substrate by adapting the stubbing force. A similar particle detection method as used in this research (with adjustments as recommended in paragraph 4.3) can probably be used to analyse trace compositions.

The distribution of traces over textile is influenced by multiple factors: the DNA source, the activity by which DNA is transferred and ageing of the trace. The material properties of the DNA-containing material that is secreted by the **DNA source** is not unambiguously. Trace DNA can consist of different body secretions: skin cells, DNA carried by sweat or sebum and highly nucleated body fluids from the eyes, nose or mouth [1]. It is likely that these different body

secretions are distributed differently over a substrate. Wet traces could for example penetrate deeper in the substrate material than dry traces.

The **activity** indicates all actions by which DNA is transferred. Goray et al. [12] demonstrated that in general significantly more trace DNA was transferred by friction than by passive or pressured contact (from one to another substrate). Ladd et al. [13] demonstrated that prolonged contact time during dynamic contact (what means that contacting surfaces slide over each other) does increase the amount of DNA that is transferred from a DNA source to a substrate. This statement is not true for static contact [14][15]. In short, of multiple distinguishable activities it is known that they influence the amount of transferred DNA traces. However, something that is useful to know as well is the distribution of traces over the depth of the substrates after different activities. If this is known, the collection technique can be adapted to it in order to increase the ratio between targeted trace and noise in the sample. In practice there are usually multiple DNA deposits on an evidentiary item. Therefore, it is also useful to test the influence of the deposition of a second trace on the distribution of an earlier deposited trace. To do this, distinguishable traces should be used.

**Ageing** indicates all influences on the DNA trace in the time between the trace application and collection. To implement knowledge about the relation between activity and trace distribution into stubbing procedures, it is of high importance to investigate how actions of the forensic investigators would change the trace distribution, for example by packing and transporting an evidentiary item in a paper bag.

Finally, **substrate properties** will not only affect how traces are removed from it, but also how traces are distributed by the deposition.

## 2. Obtain more collection efficiency data

This research gives new insight in the increase of micro-trace collection efficiency with increasing stubbing force for the tested materials. However, the collection efficiency should be defined for a wider variety of substrate materials and micro-traces too, because these materials influence the trace collection by various properties, as illustrated in Figure 48. The thickness and bulk stiffness of the textile determine the impression of the textile with a certain stubbing force. The structure of the substrate, such as the weaving type, determines the actual contact area between the tape and the textile that is achieved by a particular impression of the textile. The adhesive properties of the substrate and the micro-traces determine the relation between the actual contact area and the trace collection efficiency.

The microspheres used in this experiment differed from DNA-containing particles in size, shape and other mechanical properties, what influenced the adhesive bonding and thereby the trace collection efficiency. However, to make a statement about collection efficiency of trace DNA under specific conditions in general is not doable, because the content of trace DNA can also vary a lot [1].

A new method should be designed to study the relation between the used stubbing force and the possibility of collecting traces from specific depths in the substrate structure (deep or superficial), see recommendations in paragraph 4.2. Selective collection is expected to be related to the relative impression of the textile, which indicates the impression of the textile relative to its thickness. Therefore, it will be useful to measure the relation between the relative impression and the substrate depth from which traces are collected at the same time.

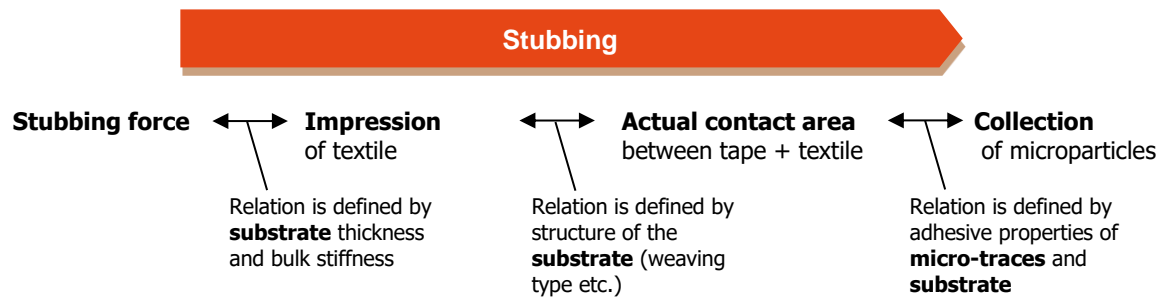


Figure 48 Visualisation of how properties of the substrate and micro-particles influence the trace collection when stubbing.

### 3. Classify substrates of real evidentiary items

To give an estimation of the stubbing force that should be used to selectively collect micro-traces from the top layer of a textile evidentiary item, a method should be found to measure the relative impression of textile with increasing stubbing force. Based on the relation between the relative impression and the trace collection on the tested substrates, the stubbing force can be defined to collect material from a certain depth in the substrate. To enable measurement of the impression of textiles, it is really important how the moment of initial contact is defined, which is not unambiguously due to extruding fibres and irregularities in the surface structure. When determining the relative impression for a textile, it should be taken into account that there are exceptions, such as textiles with superficial prints on it. For these textiles, the impression would influence the collection of micro-traces differently.

The overall collection efficiency of micro-traces from textile depends on many substrate properties. These properties can widely vary between evidentiary items. Therefore, it is not practical to classify the substrates based on all these specific properties and to determine the relation between the stubbing force and the trace collection efficiency for all these substrates. However, based on data that will be obtained, a statement for a more general group of substrates (in terms of structure and adhesive properties) can be given about the minimum stubbing force that is needed to approach the theoretical maximum collection efficiency (>95% of the theoretical maximum). The exact stubbing force when requiring as much of the traces as possible from a textile is not of noteworthy influence anyhow.

### 4. Design stubbing force limiter

The results of this research suggest that the efficiency of the collection of micro-traces from textile, as well as the estimated actual contact area between the tape and the substrates, particularly increases among stubbing forces up to 1 N. The estimated actual contact area was considered to be nearly complete at a stubbing force of 1 N. Therefore, selective collection of material from the top layer is probably only possible far below 1 N. Forensic investigators now seem to use a stubbing force in the range between 1 and 10 N. This force range is based on a study of Wendt in 2013 [4], in which the stubbing force was measured that was used by forensic investigators during stubbing on different textiles that were placed over mock-up skin. There was a lot of variation in stubbing forces between repeating trials, which indicates that it is hard to control the stubbing force manually. Moreover, the stubbing forces that can probably be used to collect traces from selective layers of the substrate are much lower than investigators seem to use, so a limiter of the stubbing force will be needed to enable selective trace collection.

Wendt [4] designed a stubbing force indicator that could be coupled to a stub holder. In this mechanism there was an adjustable spring to set the desired stubbing force. An indicator light in the mechanism turned on when the desired stubbing force was reached. This instrument had a force range between 5.9 and 8.8 N. In 2014 an improved stubbing force limiter was designed by a BSc. project group at the TU Delft [16]. This design could mechanically limit the

stopping force by using a pressure reducing valve. The range of stopping forces that could be achieved with this mechanism was 2.10 to 30 N, with a standard deviation of about 0.5 N. Based on what is known now, the force range must be even lower and standard deviation should be much smaller to use a stopping force limiter to collect traces from only the top layers of textiles. However, the exact range of stopping forces is yet to be defined based on knowledge of trace distributions, textile properties and collection efficiencies that should be obtained first. A mechanical force limiter is recommended, because when requiring really low stopping forces, the chance of exceeding this force limit is very high if only an indication light is used.

### **5. Adapt stopping procedure**

When all previously mentioned issues are investigated, together these results may answer the following question: If multiple DNA sources deposited trace DNA on the same substrate, how does the use of different stopping forces influence the collected amounts of these different DNA traces and the ratio between it?

If it turns out that traces are totally mixed up instead of being layered, the only goal is just to collect as much material as possible. Therefore, a stopping force of at least 3 to 12 N can be used. The exact force does not matter because the collection efficiency does not significantly differ in the higher range of stopping forces. It should be taken into account that there might be other material, or fibres of the substrate itself, that are undesired to be collected in the DNA sample. Some materials inhibit the further processing of the DNA sample by which a DNA profile is created, for example denim, leather, and various soiled items [17]. If these kind of materials are present on the substrate, this might change the desired stopping technique.

If a targeted DNA trace is positioned on top of other traces, a low stopping force should be used. If a targeted DNA trace is positioned below other traces, it might be useful to stop twice: first with a low stopping force to remove the top traces, and subsequently with a higher stopping force to collect the desired trace from deeper layers in the substrate.

# 5.

## 5 Conclusion

---

The experiment results suggest that the collection efficiency of microspheres increases with increasing stubbing force in a concave down increasing function. This was tested on three textile substrate materials: flat spools of sewing polyester, extra strong sewing polyester and crochet polyester threads. The results were in line with the expectations, because the collection efficiency is related to the contact area between the tape and the substrate, which increases in a similar manner with increasing stubbing force. According to a fit through the measured collection efficiencies (measured for stubbing forces of 0.1, 0.2, 0.5, 1 and 7 N), the collection efficiencies seemed to stagnate at 3, 6 and 12 N (for extra strong sewing polyester, sewing polyester and crochet polyester, respectively). Stubbing with a force higher than 3 to 12 N (depending on the substrate material) does not notably influence the collection efficiency. However, because the theoretical maxima of the collection efficiencies were far from 100%, it is highly likely that stubbing multiple times on the same spot of a substrate increases the total collection efficiency. This is caused by displacement of substrate fibres and microparticles during stubbing, which was visually observed in the microscope images, causing unreachable traces become reachable for the tape.

The designed method was too inaccurate to define the trace collection efficiency from different depth locations in the substrate structure. Various recommendations were proposed. Yet, the acquired data of the impression of the polyester threads and adhesive tape with increasing stubbing force showed that when using a stubbing force of 1 N, the impression almost reached its maximum. Thereby, it is likely that material from deeper layers of the substrate is collected when applying a stubbing force of 1 N. Therefore, selective collection of superficial traces is probably only possible when using a stubbing force below 1N, which is far below the range of stubbing forces that are currently used.

The distribution of trace DNA in different scenarios should be analysed to see to what extent layered trace deposition can occur. This distribution is defined by multiple factors, which influences should be studied: the type of deposited material, the activity by which a trace was transferred, the ageing process of the trace, and the type of substrate material. More data should be collected over a wider variety of textiles to investigate the effect of the relative impression (the impression relative to thickness) of the substrate under a stubbing force, the substrate structure and other adhesive properties of the substrate on the micro-trace collection. The stubbing force limiter prototype should be redesigned to allow stubbing with a much lower and more accurate stubbing force (< 1 N).

This research is, to the best of our knowledge, the first research that provided insight in the relation between the used stubbing force and the collection of microparticles from textile. It will contribute to a collection method by which micro-traces on a victim's jacket that are left by the perpetrator can be collected as effectively as possible.

# Bibliography

---

- [1] S. van Berkel, "Improving the stubbing technique for DNA collection," Delft University of Technology, 2016.
- [2] B. Bhoelai, F. Beemster, and T. Sijen, "Revision of the tape used in a tape-lift protocol for DNA recovery," *Forensic Sci. Int. Genet.*, vol. 4, pp. e270–e271, 2013.
- [3] T. J. Verdon, R. J. Mitchell, and R. a H. Van Oorschot, "Evaluation of tapelifting as a collection method for touch DNA," *Forensic Sci. Int. Genet.*, vol. 8, no. 1, pp. 179–186, 2014.
- [4] R. Wendt, "Onderzoek stubapparaat," The Hague, 2013.
- [5] D. Satas, *Handbook of pressure sensitive adhesive technology*, Second Edi. New York: Van Nostrand Reinhold, 1989.
- [6] Scapa, "Technical Data Scapa 4405," 2007. [Online]. Available: <http://www.hadleigh-tapes.co.uk/Handlers/fileServer.ashx?fileID=1752&d=1456754392448>. [Accessed: 29-Feb-2016].
- [7] C. Windmeijer, E. Versteeg, A. Nouar, and K. Visser, "DNA-vrij maken van bemonsteringstape met behulp van UV-licht," Delft, 2015.
- [8] Genetic Science Learning Center, "Cell Size and Scale," 2010. [Online]. Available: <http://learn.genetics.utah.edu/content/cells/scale/>. [Accessed: 15-Oct-2016].
- [9] Distrilab B.V., "Fluoro-Max Green and Red Dry Fluorescent Particles," 2016. [Online]. Available: <http://www.distrilabparticles.com/products/fluorescent-microspheres/fluoro-max-green-and-red-dry-fluorescent-particles/>. [Accessed: 23-Sep-2016].
- [10] V. L. Popov, *Contact mechanics and friction: Physical principles and applications*. Berlin: Springer-Verlag Berlin Heidelberg, 2010.
- [11] KEYENCE CORPORATION, "Keyence Digital Microscope," 2016. [Online]. Available: <http://www.keyence.com/ss/products/microscope/vhx5000/feature/>. [Accessed: 02-Nov-2016].
- [12] M. Goray, R. J. Mitchell, and R. a H. Van Oorschot, "Investigation of secondary DNA transfer of skin cells under controlled test conditions," *Leg. Med.*, vol. 12, no. 3, pp. 117–120, 2010.
- [13] C. Ladd, M. S. Adamowicz, M. T. Bourke, C. a Scherzinger, and H. C. Lee, "A systematic analysis of secondary DNA transfer.," *J. Forensic Sci.*, vol. 44, no. 6, pp. 1270–1272, 1999.
- [14] R. A. H. van Oorschot and M. K. Jones, "DNA fingerprints from fingerprints," *Nature, Sci. Corresp.*, vol. 387, p. 767, 1997.
- [15] M. K. Balogh, J. Burger, K. Bender, P. M. Schneider, and K. W. Alt, "Fingerprints from fingerprints," *Int. Congr. Ser.*, vol. 1239, pp. 953–957, 2003.
- [16] J. Van Eck, G. v.d. Hart, R. Goudriaan, and B. Koppenol, "Begrenzing van drukkracht voor bemonstering van DNA-sporen," Delft, 2014.
- [17] M. Barash, A. Reshef, and P. Brauner, "The use of adhesive tape for recovery of dna from crime scene items," *J. Forensic Sci.*, vol. 55, no. 4, pp. 1058–1064, 2010.

---

## Appendices

---

Appendix A - <i>Stub-tape cutting procedure</i>	p. 53
Appendix B - <i>Technical drawings of stub-pin holders</i>	p. 55
Appendix C - <i>List of available party hoses at HEMA</i>	p. 56
Appendix D - <i>Considerations for the substrate material choice</i>	p. 57
Appendix E - <i>Procedure to produce the spools of threads</i>	p. 59
Appendix F - <i>Calculation of the concentration of microspheres in the suspension</i>	p. 61
Appendix G - <i>Measured diameters of the used textile threads</i>	p. 62
Appendix H - <i>Graphs of the substrate impression versus the stubbing force</i>	p. 63
Appendix I - <i>Photoshop editing procedure</i>	p. 64
Appendix J - <i>MATLAB files</i>	p. 66
Appendix K - <i>Determination of the substrate area that was fully covered by tape</i>	p. 77
Appendix L - <i>Validation of microspheres counting by MATLAB</i>	p. 78
Appendix M - <i>Datasheet experiment results</i>	p. 80
Appendix N - <i>Collection efficiency at different substrate structure heights (PSS and PC)</i>	p. 81
Appendix O - <i>Collection efficiency on glass</i>	p. 84

# Appendix A

## *Stub-tape cutting procedure*

---

**Required:**

1. Arc punch of 10 mm diameter (see Figure 49)
2. Wooden plate (see Figure 49)
3. Steel hammer (see Figure 49)
4. Tweezers (see Figure 49)
5. Scissor
6. Hand gloves
7. Cleanroom wipes (or paper towels)
8. Black-painted stub-pins (12.6 mm diameter)
9. Double sided adhesive Scapa 4405 tape (see Figure 49) (The edges of the tape roll had been UV irradiated at the NFI, because this is how the tape rolls are stored there. The tape roll was packed in plastic to protect it against contamination.)
10. Single sided adhesive tape (width: 19 mm, brand unspecified)
11. Holder for the stubs in a box (see Figure 50 in Appendix B)
12. Holder for a single stub (see Figure 49 and Figure 51)
13. Mass with flat base of 2.1 kg (see Figure 49)



*Figure 49 Some of the tools that are used to cut the tape. The numbers refer to the list above.*

**Procedure:**

- Wear hand gloves.
- Clean the tools and the working environment with cleanroom wipes and some ethanol.
- Clean the stub-pins with a cleanroom wipe and ethanol and put these in the holder in the box.
- Cut a piece of double sided tape with the scissor. Only the ends of the tape can be touched by the scissor and tweezers, for these are not punched out.
- Place a piece of the double sided tape, with the protective silicone paper sticking to it at one side, on the wooden plate. The silicone paper should be situated at the bottom side, in contact with the wood. If needed, use single-sided tape to stick it to the wood.
- Clean the inside of the arc pinch by pulling a cleanroom wipe through it (using tweezers) up to the half of the towel and then turn the towel around so loose particle insides the arc pinch are removed.
- Place the cutting edge of the arc pinch on the tape on the location where a full(!) circle should be punched out.
- Hit the back of the arc punch with the steel hammer only once heavily.
- Push the tape out of the arc punch after pressing it from the inside of the arc punch with the tip of the tweezers.
- The round tape can be lifted out of the arc punch using tweezers and placed with the sticking side to a clean stub-pin in the holder for a single stub.
- Press the tape gently with the side of the tweezers to the stub.
- Press the tape firmly to the stub-pin by placing a mass for a few seconds on the silicon paper (which still covers the tape). Make sure the bottom side of the mass is horizontal to the surface of the stub-pin.
- Remove the silicon paper from the double sided tape using tweezers. Avoid unnecessary contact between the tweezers and the adhesive tape.
- Place the stub-pin in the holder and close it to protect it from dust etc. from the environment.
- For every new stub, repeat step 6 to 14.

## Appendix B

### *Technical drawings of stub-pin holders*

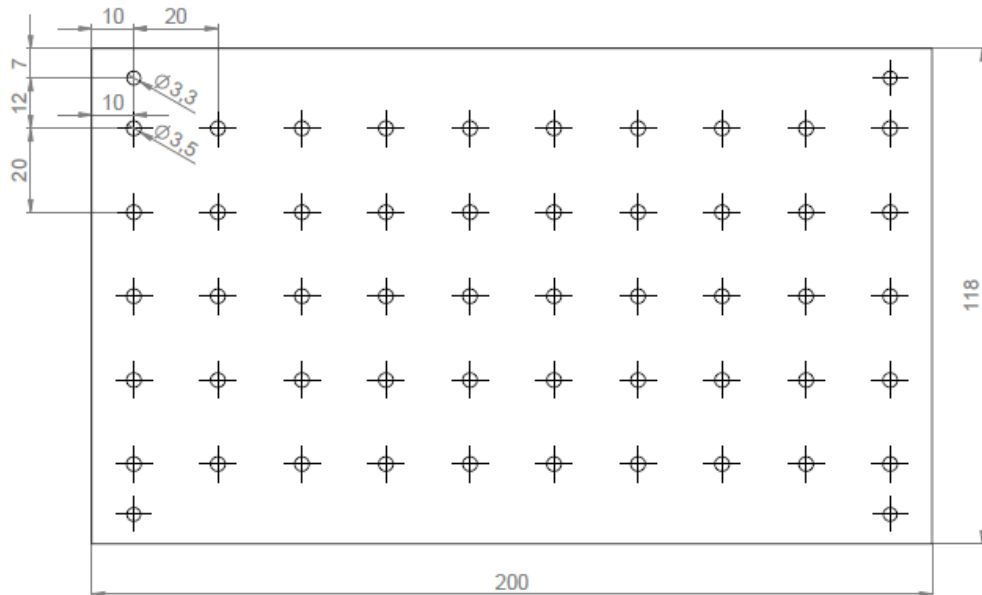


Figure 50 Holder to store 50 stub-pins, made of 8mm thick acrylate (dimensions in mm). The four holes at the corners were used to screw this plate to a similar plate that did not contain holes for the stub-pins, so the holder was closed at the bottom side. Between the plates a paper was placed on which the stub names were displayed.

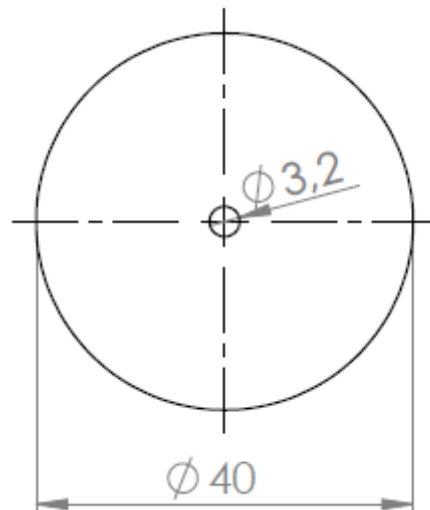


Figure 51 Holder made from 8mm thick acrylate (dimensions in mm). Used to position the stub-pin horizontal when the double sided tape is stuck to it, and when the tape is analysed under the microscope.

## Appendix C

### *List of available panty hoses at HEMA*

Table 4 Panty hoses available at HEMA B.V.

Item number	Description (Dutch)	Denier	Colour	Material		Remarks
				Polyamide (%)	Elastane (%)	
4062500	Panty	15	black	90	10	-
4052501	Hold-up panty	15	black	86	14	Slightly glossy
4061204	Panty	15	black	100	0	Smooth
4061303	Panty	20	black	95	5	Mousse
4053404	Push-up panty	20	black	83	17	
4000041	Panty	20	black	90	10	-
4053514 / 4053512	Corrigerende panty	20	black	85	15	Lycra leg care
4051679	Panty	30	black	100	0	-
4095204	Panty	40	black	93	7	Made from recycled yarns
4097301	Corrigerende panty	40	black	93	7	
4000052	Panty	40	black	92	8	Opaque, special 'body conditioning' treatment to avoid sweating
4052039	Steunpanty	40	black	82	18	
4048021	Panty opaque	50	black	87	13	Silky smooth and very elastic
4000023	Corrigerende panty	60	black	94	6	
4060904	Panty	60	black	87	13	Very elastic
4000087	Panty ecocare	80	black	96	4	Made from recycled yarns

Optional combinations to test are given the same colour:



The ratio between polyamide and elastane is approximately equal for these three panty types. The linear mass density of fibres are 15, 30 and 60 denier.



The ratio between polyamide and elastane is approximately equal for these three panty types. The linear mass density of fibres are 15, 20, 50 and 60 denier.

# Appendix D

## Considerations for the substrate material choice

Table 5 All considerations for the choice of a substrate material are summed up in this table. The main requirements are emphasised in bold. The colours give a quick overview of the rating of an optional substrate for a specific requirement: green indicates a good score, yellow a medium score and red a bad score.

		Fabrics	Spool of threads	Modified plastic surfaces	Panty hoses
Related to the contribution to research question	Good representation of samples that are usually stubbed?	<b>Yes. However, many more different textile materials are encountered in practice.</b>	<b>Quite good. The same material as in real fabrics is used, but this substrate is not woven as usually encountered substrates, so the surface roughness is not influenced by the weaving type.</b>	<b>No, a different material than textile is used. This material has a different roughness and different properties such as surface free energy, etc. Furthermore, milling is unsuitable for soft materials, because then the milling head presses away the material.</b>	<b>Quite good, but panty hoses are made from another textile than cotton or polyester.</b>
	Can the substrate be varied systematically?	<b>No, between different textiles more properties vary simultaneously.</b>	<b>With the available threads this is possible to a certain extend.</b>	<b>Yes, by changing the macroscopic roughness and/or microscopic roughness.</b>	<b>No, between different textiles more properties vary simultaneously.</b>
	Can different substrate depths be distinguished under the microscope?	<b>Yes, different depths in the substrate can be distinguished by the digital microscope.</b>	<b>Yes, areas with different depths can be distinguished in the 2D-plane, for example by marking the different levels with a specific colour.</b>	<b>Yes, depths in the substrate can be distinguished by the digital microscope.</b>	<b>Yes, depths in the substrate can be distinguished by the digital microscope.</b>
Related to the consistency of the experiments	Can the substrate be damaged by the tape?	No, not after one contact moment at least.			
	Is the surface consistent?	Yes, it is made by very accurate machines.	Pretty good if winding of the threads around the spool is done consistently.	Yes.	Yes, but only when it is equally stretched.
	Does the material sink into the substrate?	Yes.		No.	Yes.

(Continued on next page)

(Cont'd)		Fabrics	Spool of threads	Modified plastic surfaces	Panty hoses
Practical considerations	Is it available or manufacturable?	<b>Available.</b>	<b>Threads are available and spools are manufacturable.</b>	<b>Manufacturable, but it will take a lot of time to investigate how to do this.</b>	<b>Available.</b>
	Is it possible for future research to obtain or manufacture the same substrate (i.e.: is the experiment repeatable)?	<b>It will be hard, or even impossible, to obtain textiles in the future that are equal to textiles bought for this research, especially when no manufacturer is known.</b>	<b>Buying threads from the same brand with the same description is probably doable in the future.</b>	<b>Yes, when the production process is described very detailed.</b>	<b>It will be possible to find similar panties, but it is not guaranteed that the production of the specific used panties will be continued.</b>
	Is the substrate reusable?	Yes, it can be washed. This might change the material properties of the substrate, so cleaning should also be done before the first use.			

# Appendix E

## *Procedure to produce the spools of threads*

### 1. Produce the spool bases

- Produce the steel base according to Figure 52.

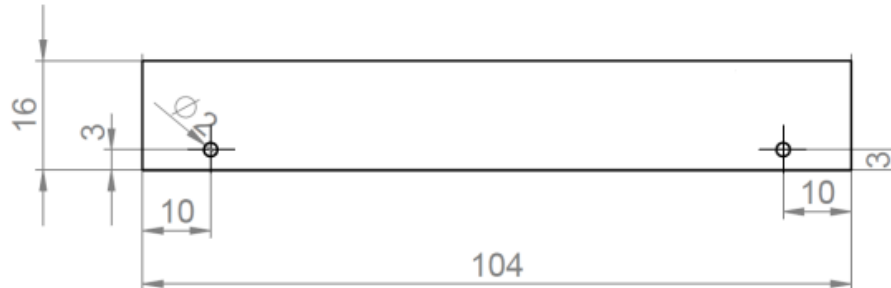


Figure 52 Dimensions of the base of the spools, made from steel of 3 mm thickness (dimensions in mm).

### 2. Warp the threads around the spool

14. Knot the thread through one of the holes in the base, using tweezers to get the thread through this hole.
15. For every single winding, turn the metal spool (and not the threads around the spool, otherwise the yarns in the thread would be twined or untwined). Always keep the thread under tension during winding. Do not let the thread slide through your hands, for this would also cause untwining of the thread, but grip a new part of the thread when needed.
16. Make sure that every new winding is adjacent to the previous winding. If there is a 'gap' between neighbouring windings that is visible with the naked eye), then push the threads together, but avoid overlapping of adjacent thread.

### 3. Clean the substrate

- Hold all four long edges of the spool for about 10 seconds under a warm, fast running water tap. Move the spool back and forth during this to make sure the water flows over the whole surface.
- Dry the spool by rolling it into a disposable towel and compress it. Then dry the spool in the air, under room temperature for at least 12 hours, with all sides of the substrate free to dry.

### 4. Name the substrates

- The substrates should be named so these can be distinguished during the experiments. The names consist of the abbreviation of the thread type followed by one of the letters A to D, because there are 4 pieces of each substrate type, and then followed by "1-5", because every substrate consists of 5 sample location. The abbreviations that are used for sewing polyester, extra strong sewing polyester and crochet polyester are 'Pol.sew', 'Pol.sew.str' and 'Pol.croch' respectively. The location closest to the name label is sample location 1 and the furthest location from the label is sample location 5.

**5. Cover the substrate to distinguish the sample locations**

- After micro-traces are deposited on the substrate the spools can be overlaid by a cover containing circular gaps of 14mm diameter, so that the 5 sample locations can be distinguished. The cover was attached to the spool at both ends by 19 mm wide adhesive tape.

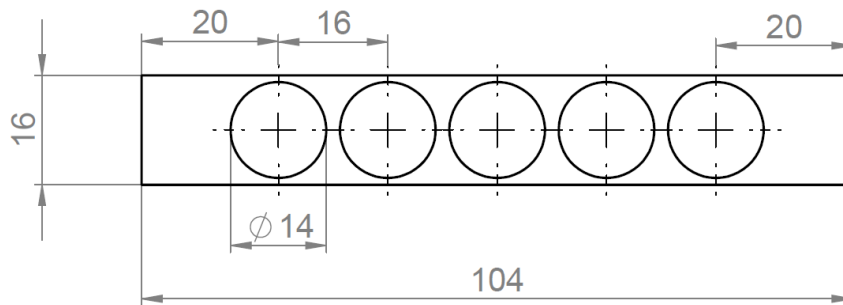


Figure 53 Dimensions of the sample cover, made from aluminium of 0.5 mm thickness (dimensions in mm).

The final results are depicted in Figure 54.

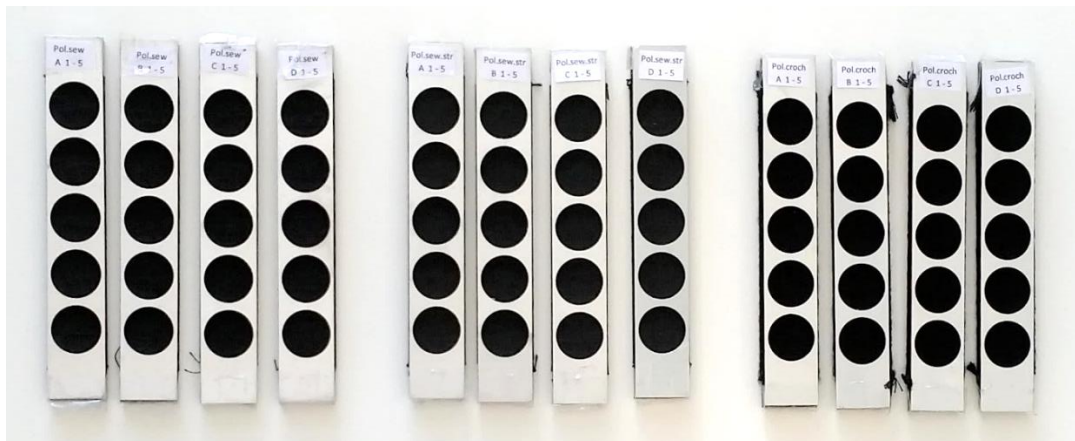


Figure 54 Resulting textile samples.

## Appendix F

### *Calculation of the concentration of microspheres in the suspension*

---

The number of particles per gram is  $9.2E4$  particles/mg [9].

<b>Needed particles per sample circle</b>	
Desired number of particles in Ø10 mm circle	<b>1000</b>
Surface area Ø10 mm circle	<b><math>78.54 \text{ mm}^2</math></b>
Surface area of material deposition (including area around circle: 16x16mm)	<b><math>256 \text{ mm}^2</math></b>
Desired number of particles on 16x16mm surface	$\frac{256}{78.54} \cdot 1000 = 3259$
Needed weight of microspheres per sampled area	$\frac{3259}{9.2 \cdot 10^4 / \text{mg}} = 3.54 \cdot 10^{-2} \text{ mg}$
<b>Needed volume of ethanol per sample circle</b>	
Desired number of droplets for textiles	<b>4</b>
Desired number of droplets for glass	<b>2</b>
Volume of one droplet	<b><math>0.025 \text{ mL}</math></b>
Total volume of ethanol for textile per sample	<b><math>0.1 \text{ mL}</math></b>
Total volume of ethanol for glass	<b><math>0.05 \text{ mL}</math></b>

For textile substrates: concentration of  $\frac{3.54 \cdot 10^{-2} \text{ mg}}{0.1 \text{ mL}} = 0.354 \text{ mg/mL}$

For glass substrates: concentration of  $\frac{3.54 \cdot 10^{-2} \text{ mg}}{0.05 \text{ mL}} = 0.708 \text{ mg/mL}$

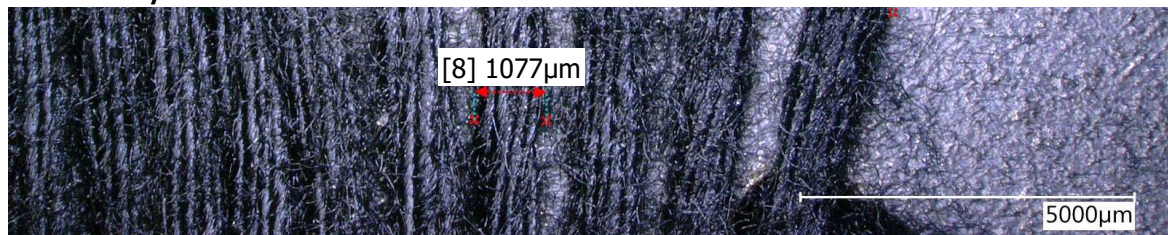
## Appendix G

### *Measured diameters of the used textile threads*

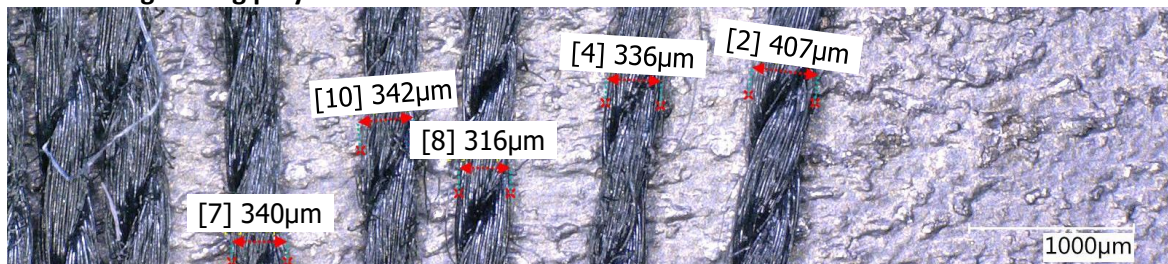
Table 6 Measured thread diameters and the calculated mean diameter of the threads. The threads were measured as represented in Figure 55.

Measurement	Thread diameter [mm]		
	Crochet Polyester	Sewing polyester	Extra strong sewing polyester
1	1.006	0.217	0.373
2	1.221	0.214	0.407
3	1.115	0.205	0.392
4	1.206	0.209	0.336
5	1.113	0.202	0.316
6	1.248	0.202	0.336
7	0.873	0.198	0.340
8	1.077	0.222	0.316
9	1.030	0.253	0.370
10	1.175	0.238	0.342
<b>Mean:</b>	<b>1.132</b>	<b>0.216</b>	<b>0.353</b>

#### Crochet Polyester



#### Extra strong sewing polyester



#### Sewing polyester



Figure 55 Some examples of the measured thread diameters for crochet polyester, extra strong sewing polyester and sewing polyester.

## Appendix H

### *Graphs of the substrate impression versus the stubbing force*

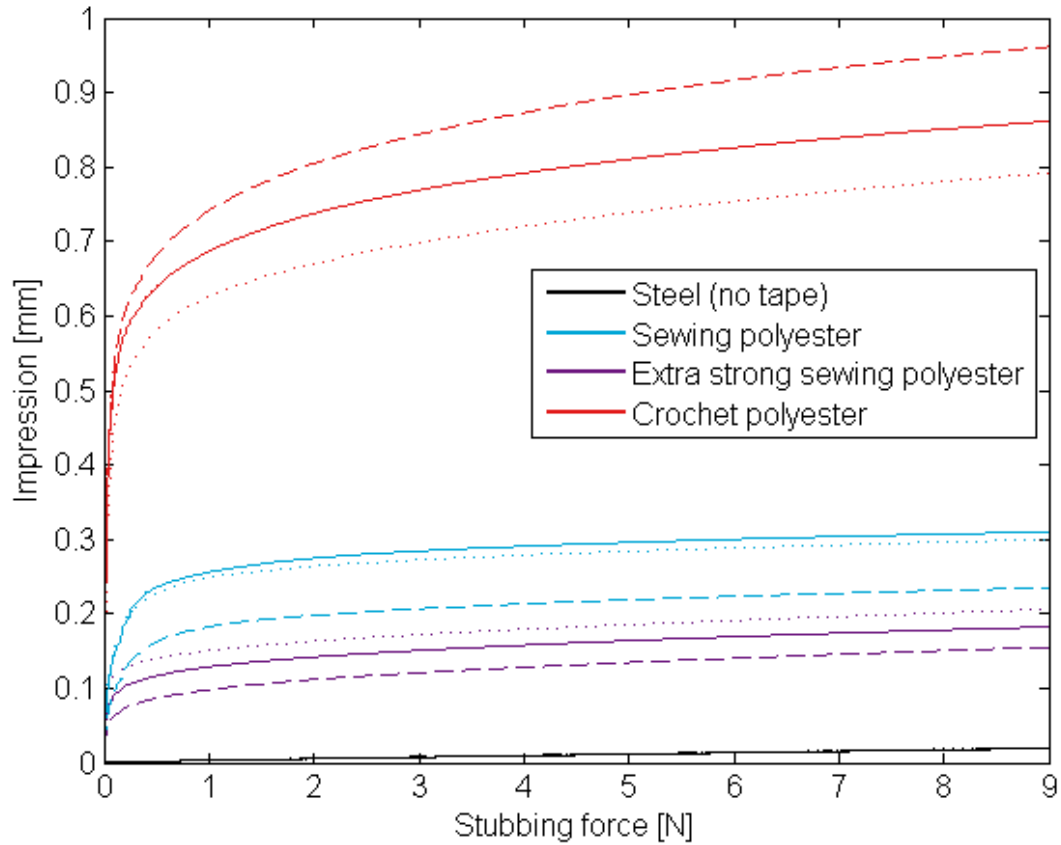


Figure 56 Measured impression on the substrates under an applied stubbing force (including the system's deformation). The different line types indicate the three different sample circles where the data was measured (circle 1: —, circle 4: ---, circle 3: ...), see Figure 20.

# Appendix I

## *Photoshop editing procedure*

---

A 'Droplet' was created in Photoshop. In this application, images could be dragged and dropped to be edited according to the actions that are embedded in the Droplet. Hereby, a lot of images can be edited in the same way very fast and easily.

A droplet can be created as follows:

- Select "New Action" in the Action panel menu (if this is not visible, click on: "Window" > "Actions")
- Name your action and click "Record"
- Execute the actions that should be embedded in the droplet (see descriptions below)
- Click on: "File" > "Automate" > "Create Droplet".
  - o Select the name of your action.
  - o Choose the file destination of the new Droplet and the files that will be created by this Droplet.
  - o Define the document name of the edited picture as "Document name + \_PS + extension"

### **Actions to edit images of the textile substrate:**

- **Image > Adjustments > Invert**
- **Image > Adjustments > Hue/Saturation**  
Cyans: Saturation +80%
- **Image > Adjustments > Selective color**  
Reds, Yellows, Greens, Magentas, Whites and Neutrals: black +100% (absolute)
- **Image > Adjustments > Threshold**  
All channels: Threshold Level: 40
- **Image > Adjustments > Black & White**  
(Default settings)
- **Save**  
(Maximal quality)

### **Actions to edit images of the tape:**

- **Image > Adjustments > Invert**
- **Image > Adjustments > Hue/Saturation**  
Cyans: Saturation +100%
- **Image > Adjustments > Selective color**  
Reds, Yellows, Greens, Magentas, Whites and Neutrals: black +100% (absolute)
- **Image > Adjustments > Threshold**  
All channels: Threshold Level: 55
- **Image > Adjustments > Black & White**  
(Standard settings)
- **Save**  
(Maximal quality)

**Actions to edit images of the glass substrates:**

- **Image > Adjustments > Invert**
- **Image > Adjustments > Brightness/Contrast**  
Brightness: +100%
- **Image > Adjustments > Hue/Saturation**  
Cyan: Saturation +100%
- **Image > Adjustments > Selective color**  
Reds, Yellows, Greens, Magentas, Whites and Neutrals: black +100% (absolute)
- **Image > Adjustments > Threshold**  
All channels: Threshold Level: 55
- **Image > Adjustments > Black & White**  
(Standard settings)
- **Save**  
(Maximal quality)

(!) Caution: the Droplet overwrites the original file, so always use a copy of your original file in the Droplet!

# Appendix J

## *MATLAB files*

---

<b>Read_data.m</b>	<i>This function was used to read data from the tensile tester.</i>	p. 67
<b>Run_define_particle_nr_substrates.m</b>	<i>This code was used to calculate the number of detected microspheres on the substrates before stubbing by calling the function Define_particle_nr.m</i>	p. 68
<b>Run_define_particle_nr_stubs.m</b>	<i>This code was used to calculate the number of detected microspheres on the tape after stubbing by calling the function Define_particle_nr.m</i>	p. 69
<b>Define_particle_nr.m</b>	<i>This function was used to calculate the number of detected microspheres in an image by first masking and editing the image.</i>	p. 70
<b>Run_define_particle_height_textiles.m</b>	<i>This code was used to determine the height of detected microspheres on a textile before and after stubbing by calling Define_particle_height_textiles.m.</i>	p. 72
<b>Define_particle_height_textiles.m</b>	<i>This function was used to determine the height of detected microspheres by overlapping the normal image and the resized height profile of the image.</i>	p. 74

**Read\_data.m**

```

function [x,F,max_error_F] = read_data(data_material,material)
t = data_material(:,1); % Time [s]
x = -data_material(:,2); % Displacement of the crosshead from start position [mm]
F = data_material(:,3); % Force measured by the load cell [N]

% Variables to process the data
lower_limit_F = 0.005; % The data is cut off if the force comes below this value,
% for this small measured forces can be a result of noise [N]
upper_limit_F = 9; % After this contact force was reached, the stub moved back
% from the substrate again [N]
smooth_span = 600; % Data is smoothed using the average of this number of points

if material(1:2) == 'SN'
    smooth_upper_limit = 0.005; % Up to this force the graph is smoothed [N]
elseif material(1:2) == 'ST'
    smooth_upper_limit = 0.02; % Up to this force the graph is smoothed [N]
else
    smooth_upper_limit = 0.05; % Up to this force the graph is smoothed [N]
end

%% Smooth Force data
% Define the indexes of forces below the smooth upper limit:
for k = 1:length(F)
    if F(k) > smooth_upper_limit
        break
    end
end
index_Fsmooth_lim = k;

Fsmooth1 = smooth(F(1:index_Fsmooth_lim),smooth_span);
Fsmooth = [Fsmooth1; F(index_Fsmooth_lim+1:end)];

errors = abs(F-Fsmooth);
[max_error_F,i_max_error] = max(errors);

Fold = F;
F = Fsmooth;

%% Delete data that was obtained after maximum force was reached
for i = 1:length(F)
    if F(i) > upper_limit_F
        break
    else
        i = length(F);
    end
end
index_Fmax = i;

x = x(1:index_Fmax);
F = F(1:index_Fmax);

%% Delete data that was obtained before contact was made between the tape and the
substrate
% Only include data that is reached after the lower limit is definitely passed:
for j = length(F):-1:1
    if F(j) < lower_limit_F
        break
    else
        j = 1;
    end
end

index_x0 = j+1;
val_x0 = x(index_x0);
x = x(index_x0:end)-val_x0;
F = F(index_x0:end);
end

```

**Run\_define\_particle\_nr\_substrates.m**

```

%%%%%%%%%%%%%%%%%%%%%%%%%%%%%%%%%%%%%%%%%%%%%%%%%%%%%%%%%%%%%%%%%%%%%%%%
%% Define the number of detected microspheres          %%
%% on the substrates before stubbing                  %%
%% By Selma Damsteeg - van Berkel 2016                %%
%%%%%%%%%%%%%%%%%%%%%%%%%%%%%%%%%%%%%%%%%%%%%%%%%%%%%%%%%%%%%%%%%%%%%%%%
clear all; clc; close all;

%%%%%%%%%%%%%%%%%%%%%%%%%%%%%%%%%%%%%%%%%%%%%%%%%%%%%%%%%%%%%%%%%%%%%%%%
%% Paths to images and matlabfiles:
addpath('G:\Keyence_microscope\20160809_prestub');
addpath('G:\Keyence_microscope\20160809_prestub_PS');
addpath('C:\Users\Selma\Documents\Graduation');

%%%%%%%%%%%%%%%%%%%%%%%%%%%%%%%%%%%%%%%%%%%%%%%%%%%%%%%%%%%%%%%%%%%%%%%%
%% Particle density on textile substrates
% Set variables:
R_spheres_textile = [8 13]; % Range of microsphere radius [px]
range_R_textile = [6000 6300]; % Range of the sample circle radius [px]
R_textile = 6200-550; % Radius of analysed area of the sample circle [px]
polarity_textile = 'dark'; % Setting for finding the sample circle with
                        'imfindcircle'
sens_textile = 0.97; % Detection sensitivity of microspheres in
                    'imfindcircle'
tol_overlap_textile = 3; % Tolerated overlap of detected microspheres [px]
nr_bwareaopen_textile = 40; % Setting used to remove noise in the Photoshop image
                        with the function 'bwareaopen'

[num_xls,text_xls]=xlsread('DATA_EXPERIMENTS.xlsx');
textile_names = char(text_xls(28:33,2)); % Polcroch
% textile_names = char(text_xls(34+5:48,2)); % Polsew
% textile_names = char(text_xls(49+3:63,2)); % Polsewstr

% (!) For Polsew, some settings are different than for Polcroch and Polsewstr:
% R_spheres_textile = [7 13];
% sens_textile = 0.945;
% nr_bwareaopen_textile = 100;

% Calculate particle density by using 'Define_particle_nr.m':
particle_nrs = [];
for i = 1:length(textile_names(:,1))
    name = textile_names(i,:);
    image_prestub = imread([name '_prestub_normal.jpg']); % Image of the substrate
    [H,W,RGB]
    PS_image_prestub = imread([name '_prestub_normal_PS.jpg']); % Image edited by Photoshop
    name_prestub = [name ' before stubbing'];
    [particle_nr,centers_prestub,radii_prestub] = ...
        Define_particle_nr(image_prestub,PS_image_prestub,range_R_textile,R_textile,...
            polarity_textile,R_spheres_textile,sens_textile,tol_overlap_textile,...
            nr_bwareaopen_textile,name_prestub);

particle_nrs = [particle_nrs; particle_nr];
end

%%%%%%%%%%%%%%%%%%%%%%%%%%%%%%%%%%%%%%%%%%%%%%%%%%%%%%%%%%%%%%%%%%%%%%%%
%% Particle density on glass substrates
% Set variables:
R_spheres_glass = [5 8]; % Range of microsphere radius [px]
range_R_glass = [6000 6300]; % Range of the sample circle radius [px]
R_glass = 6200 - 550; % Radius of analysed area of the sample circle [px]
polarity_glass = 'dark'; % Setting for finding the sample circle with
                        'imfindcircle'
sens_glass = 0.975; % Detection sensitivity of microspheres in
                    'imfindcircle'
tol_overlap_glass = 8; % Tolerated overlap of detected microspheres [px]
nr_bwareaopen_glass = 40; % Setting used to remove noise in the Photoshop image
                        with the function 'bwareaopen'

%
% glass_names = ['GlassA1'; 'GlassA2'; 'GlassA3'; 'GlassB2';
%               'GlassC1'; 'GlassC2'; 'GlassC3'; 'GlassD1'; 'GlassD2'; 'GlassD3';
%               'GlassE1'; 'GlassE2'; 'GlassE3'; 'GlassF1'; 'GlassF2'; 'GlassF3'];
%
% Calculate particle density by using 'Define_particle_nr.m'
particle_nrs = [];
for i = 1:length(glass_names(:,1))
    name = glass_names(i,:);
%
% image_prestub = imread([name '_prestub.jpg']); % Image of the substrate [H,W,RGB]

```

```

% PS_image_prestub = imread([name '_prestub_PS.jpg']); % Image edited by Photoshop
% name_prestub = [name ' before stubbing'];
% [particle_nr,centers_prestub,radii_prestub] = ...
%     Define_particle_nr(image_prestub,PS_image_prestub,range_R_glass,R_glass,...
%     polarity_glass,R_spheres_glass,sens_glass,tol_overlap_glass,...
%     nr_bwareaopen_glass,name_prestub);
%
% particle_nrs = [particle_nrs; particle_nr];
% end

```

### Run\_define\_particle\_nr\_stubs.m

```

%%%%%%%%%%%%%%%%%%%%%%%%%%%%%%%%%%%%%%%%%%%%%%%%%%%%%%%%%%%%%%%%%%%%%%%%
%% Define the number of detected particles on the stub tapes      %%
%% By Selma Damsteeg - van Berkel 2016                          %%
%%%%%%%%%%%%%%%%%%%%%%%%%%%%%%%%%%%%%%%%%%%%%%%%%%%%%%%%%%%%%%%%%%%%%%%%
clear all; clc; close all;

% Paths to images and matlabfiles:
addpath('G:\Keyence_microscope\20160816_stubbed');
addpath('G:\Keyence_microscope\20160816_stubbed_PS');
addpath('C:\Users\Selma\Documents\Graduation\Matlab\Particle count');
addpath('C:\Users\Selma\Documents\Graduation');

% Set variables:
R_spheres_tape = [9 13]; % Range of microsphere radius [px]
range_R_tape = [4300 4700]; % Range of the tape radius [px]
R_tape = 4400; % Radius of analysed area of the tape (no edges) [px]
polarity_tape = 'bright'; % Setting used for finding the round tape with
% 'imfindcircle'
sens_tape = 0.975; % Detection sensitivity of microspheres in 'imfindcircle'
tol_overlap_tape = 8; % Tolerated overlap of detected microspheres[px]
nr_bwareaopen_tape = 40; % Setting used to remove noise in the Photoshop image with
% the function 'bwareaopen'

[num_xls,text_xls]=xlsread('DATA_EXPERIMENTS.xlsx');
tape_names = char(text_xls(2:18,3));



---


%% Particle number on stubs
nrs_tape = [];
for i = 1:length(tape_names(:,1))
    name_tape = tape_names(i,:);
    image_tape = imread([name_tape '.jpg']);
    PS_image_tape = imread([name_tape '_PS.jpg']);
    [nr_tape,centers_tape,radii_tape] = ...
        Define_particle_nr(image_tape,PS_image_tape,range_R_tape,R_tape,...
            polarity_tape,R_spheres_tape,sens_tape,tol_overlap_tape,...
            nr_bwareaopen_tape, name_tape);
    nrs_tape = [nrs_tape;nr_tape];
end

```

**Define\_particle\_nr.m**

```

function [particle_nr,true_centers,true_radii] = ...
    Define_particle_nr(image,PS_image,range_Rsample,R_sample,...
        polarity_sample,R_spheres,sensitivity,tolerance_overlap,nr_bwareaopen,name)

H = length (PS_image(:,1,1));
W = length(PS_image(1,(:,1)));           % Size of picture
downscale = 0.1;
scaled_image = imresize(image,downscale);



---


%% Detect sample area using the normal picture
if name(1:7) == 'stub2B5'
    % Change the RGB picture to a black-white picture, so the tape can be detected
    adj_level = 0.5;
    scaled_image_adj = im2bw(scaled_image,adj_level);
elseif name(1:7) == 'stub1F5'
    adj_level = 0.5;
    scaled_image_adj = im2bw(scaled_image,adj_level);
elseif name(1:5) == 'Glass'
    adj_level = 0.5;
    scaled_image_adj = im2bw(scaled_image,adj_level);
else
    % For all other pictures: change the RGB picture to a grayscale picture
    scaled_image_adj = rgb2gray(scaled_image);
end

[center_sample_scaled, radius_sample_scaled] = ...
    imfindcircles(scaled_image_adj,downscale*range_Rsample,'ObjectPolarity',...
        polarity_sample, 'Sensitivity',0.995);
center_sample_scaled = round(center_sample_scaled); % (x_center y_center)

% Check if exactly 1 circle is found:
if length(center_sample_scaled(:,1)) < 1
    disp('Error! No sample circle is detected in the image.')
    return
elseif length(center_sample_scaled(:,1)) == 1
    disp('A sample circle is detected in the image.')
elseif length(center_sample_scaled(:,1)) > 1
    disp('More than one sample circle is detected in the image. (The circle with the
highets circle strength is used.)')
end

% Scale back to real scale:
center_sample = center_sample_scaled(1,:)./downscale;
radius_sample = R_sample;



---


%% Mask PS_image
% Create mask:
[xx,yy] = ndgrid((1:W)-center_sample(1), (1:H)-center_sample(2));
mask_sample = uint8((xx.^2 + yy.^2) < radius_sample^2);
mask_sample = mask_sample.'; % Invert the mask to change x,y to y,x, so this
corresponds with (height,width)

% Apply mask to images:
final_PS_image = mask_image(mask_sample,PS_image);



---


%% Find location of microspheres in the Photoshop image
% Use image operations to make the PS image more suitable for detection of microspheres
% Change image to a BW image to enable the other operations:
final_PS_image = im2bw(final_PS_image);
% Changes black (0-valued) pixels to white (1-valued) pixels if they have
% two white neighbors that are not connected:
BW_PS_image = bwmorph(final_PS_image,'bridge');
% Apply erosion followed by a dilation, using the same structuring element:
se = [0 1 0 ; 1 1 1]; % Structuring element neighbourhood
BW_PS_image = imopen(BW_PS_image,se);
% Remove all connected components(white objects) that have fewer than P pixels:
BW_PS_image = bwareaopen(BW_PS_image,nr_bwareaopen);
% Find the location of the microspheres:
[centersBW, radiiBW] = imfindcircles(BW_PS_image,R_spheres,'ObjectPolarity','bright',
'Sensitivity',sensitivity);
% Remove overlapping circles, for these are (mostly) an incorrect representation of
the microspheres:
[centers,radii]=RemoveOverLap(centersBW,radiiBW,tolerance_overlap,1);

```

```

centers = round(centers);
radii = round(radii);



---


%% All found circles outside the mask area should be deleted!
% Even though the image is masked, circles are falsely detected on the outer edge of
% the masked area. Obviously, these circles have to be removed.
i_centers = [];
for i = 1:length(centers(:,1))
    if mask_sample(centers(i,2),centers(i,1)) == 1
        i_centers = [i_centers; i];
    end
end

true_centers = centers(i_centers,:);
true_radii = radii(i_centers,:);

particle_nr = length(true_centers(:,1)); % Total nr. of detected particles



---


%% Show image with microspheres
figure
imshow(image)
% hold on; viscircles(centersBW,radiiBW,'edgeColor','b');
hold on; viscircles(true_centers,true_radii,'edgeColor','r');
hold on; viscircles(center_sample,radius_sample,'edgeColor','b');
title([num2str(particle_nr) ' detected microspheres on ' name])
saveas(gcf,['G:\Keyence_microscope\Particles_detected \' name'],'fig')
saveas(gcf,['G:\Keyence_microscope\Particles_detected \' name'],'png')

end

```

## Run\_define\_particle\_height\_textiles.m

```

%%%%%%%%%%%%%%%%%%%%%%%%%%%%%%%%%%%%%%%%%%%%%%%%%%%%%%%%%%%%%%%%%%%%%%%%
%% Define the height of the particles in the textile structures %%
%% before and after stubbing %%
%% By Selma Damsteeg - van Berkel 2016 %%
%%%%%%%%%%%%%%%%%%%%%%%%%%%%%%%%%%%%%%%%%%%%%%%%%%%%%%%%%%%%%%%%%%%%%%%%
clear all; clc; close all;

%%%%%%%%%%%%%%%%%%%%%%%%%%%%%%%%%%%%%%%%%%%%%%%%%%%%%%%%%%%%%%%%%%%%%%%%
%% Paths to images and matlabfiles:
addpath('G:\Keyence_microscope\20160809_prestub');
addpath('G:\Keyence_microscope\20160809_prestub_PS');
addpath('G:\Keyence_microscope\20160816_stubbed');
addpath('G:\Keyence_microscope\20160816_stubbed_PS');
load('C:\Users\Selma\Documents\Graduation\Matlab\Particle count\height_max')

%%%%%%%%%%%%%%%%%%%%%%%%%%%%%%%%%%%%%%%%%%%%%%%%%%%%%%%%%%%%%%%%%%%%%%%%
%% Set variables:
R_spheres_textile = [8 13]; % Range of microsphere radius [px]
range_R_textile = [6000 6300]; % Range of the sample circle radius [px]
R_textile = 3150; % Radius of the area that was fully covered by tape
[px]
polarity_textile = 'dark'; % Setting used for finding the round tape with the
fuction 'imfindcircle'
sens_textile = 0.97; % Detection sensitivity of microspheres in the fuction
'imfindcircle'
tol_overlap_textile = 3; % Tolerrated overlap of detected microspheres[px]
nr_bwareaopen_textile = 40; % Setting used to remove noise in the Photoshop image
with the function 'bwareaopen'

textile_names = ['PolcrochA1 '; 'PolcrochA2 '; 'PolcrochA3 '; 'PolcrochA4 '; 'PolcrochA5 ';
'PolcrochB1 '; 'PolcrochB3 '; 'PolcrochB4 ';
'PolcrochC1 '; 'PolcrochC2 '; 'PolcrochC3 '; 'PolcrochC5 '; 'PolcrochD1 ';
'PolsewstrA1'; 'PolsewstrA2'; 'PolsewstrA3'; 'PolsewstrA4'; 'PolsewstrA5';
'PolsewstrB1'; 'PolsewstrB2'; 'PolsewstrB3'; 'PolsewstrB4'; 'PolsewstrB5';
'PolsewstrC1'; 'PolsewstrC2'; 'PolsewstrC3'; 'PolsewstrC4'; 'PolsewstrC5'];

% % (!) For Polsew, some settings are different than for Polcroch and Polsewstr:
% R_spheres_textile = [7 13];
% sens_textile = 0.945;
% nr_bwareaopen_textile = 100;
%
% textile_names=['PolsewA1 '; 'PolsewA2 '; 'PolsewA3 '; 'PolsewA4 '; 'PolsewA5 ';
% 'PolsewB1 '; 'PolsewB2 '; 'PolsewB3 '; 'PolsewB4 '; 'PolsewB5 ';
% 'PolsewC2 '; 'PolsewC3 '; 'PolsewC4 '; 'PolsewC5 '; 'PolsewD1 '];

for i = 1:length(textile_names(:,1))
    name = strtok(textile_names(i,:));

%%%%%%%%%%%%%%%%%%%%%%%%%%%%%%%%%%%%%%%%%%%%%%%%%%%%%%%%%%%%%%%%%%%%%%%%
%% Before stubbing
image_prestub = imread([name '_prestub_normal.jpg']); % Original image [H,B,RGB]
PS_image_prestub = imread([name '_prestub_normal_PS.jpg']); % Image edited by Photoshop
height_prestub = imread([name '_prestub_height.jpg']); % Height profile image

height_prestub_max = eval(['height_max.' name '_prestub']);
refheight_prestub = imread([name '_prestub_refheight.jpg']); % Image with the same size
as the height profile, needed to detect the sample circle in height properly
name_prestub = [name ' before stubbing'];
if name_prestub(1:10) == 'PolcrochA3' % (This image deviated from others)
    scale_PCA3 = 4642/6200;
    image_prestub = imresize(image_prestub,1/scale_PCA3);
    PS_image_prestub = imresize(PS_image_prestub,1/scale_PCA3);
end

[final_height_prestub, final_image_prestub, nr_prestub, height_centers_prestub, ...
centers_prestub, radii_prestub, height_zero_prestub] = ...
Define_particle_height_textiles(image_prestub, PS_image_prestub, height_prestub, ...
refheight_prestub, range_R_textile, R_textile, R_spheres_textile, sens_textile, ...
tol_overlap_textile, nr_bwareaopen_textile, name_prestub, height_prestub_max);

%%%%%%%%%%%%%%%%%%%%%%%%%%%%%%%%%%%%%%%%%%%%%%%%%%%%%%%%%%%%%%%%%%%%%%%%
%% After stubbing
image_stubbed = imread([name '_stubbed_normal.jpg']);
PS_image_stubbed = imread([name '_stubbed_normal_PS.jpg']);
height_stubbed = imread([name '_stubbed_height.jpg']); % Height profile image
(information about the roughness of the substrate)
height_stubbed_max = eval(['height_max.' name '_stubbed']);

```

```

refheight_stubbed = imread([name '_stubbed_refheight.jpg']);% Image with the same size
as the height profile, needed to detect the sample circle in height properly
name_stubbed = [name ' after stubbing'];

[final_height_stubbed,final_image_stubbed,nr_stubbed,height_centers_stubbed,...
centers_stubbed,radii_stubbed,height_zero_stubbed] = ...
Define_particle_height_textiles(image_stubbed,PS_image_stubbed,height_stubbed,...
refheight_stubbed,range_R_textile,R_textile, R_spheres_textile, sens_textile,...
tol_overlap_textile,nr_bwareaopen_textile,name_stubbed,height_stubbed_max);

```

---

```

%% Figures
figure
subplot(2,2,1)
imshow(final_image_prestub);
hold on; viscircles(centers_prestub,radii_prestub, 'edgeColor','r');
title([num2str(nr_prestub) ' detected microspheres on ' name_prestub])
hold on
subplot(2,2,2)
imshow(final_height_prestub);
hold on; viscircles(centers_prestub,radii_prestub, 'edgeColor','r');
subplot(2,2,3)
imshow(final_image_stubbed);
hold on; viscircles(centers_stubbed,radii_stubbed, 'edgeColor','r');
title([num2str(nr_stubbed) ' detected microspheres on ' name_stubbed])
hold on
subplot(2,2,4)
imshow(final_height_stubbed);
hold on; viscircles(centers_stubbed,radii_stubbed, 'edgeColor','r');
AX = findall(gcf,'Type','axes');
linkaxes(AX,'xy')

```

---

```

%% Save data for histograms
saveas(gcf,['C:\Users\Selma\Documents\Graduation\Matlab\Particle
count\Height_particles\Height_particles_' name],'fig')

save(['C:\Users\Selma\Documents\Graduation\Matlab\Particle
count\Height_particles\h_prestub_' name '.mat'],'height_centers_prestub')
save(['C:\Users\Selma\Documents\Graduation\Matlab\Particle
count\Height_particles\h_zero_prestub_' name '.mat'],'height_zero_prestub')

save(['C:\Users\Selma\Documents\Graduation\Matlab\Particle
count\Height_particles\h_stubbed_' name '.mat'],'height_centers_stubbed')
save(['C:\Users\Selma\Documents\Graduation\Matlab\Particle
count\Height_particles\h_zero_stubbed_' name '.mat'],'height_zero_stubbed')

end

```

**Define\_particle\_height\_textiles.m**

```

function [final_height,final_image,particle_nr,...
height_centers_rel,centers,radii,height_zero] = ...
    Define_particle_height_textiles(image,PS_image,height,refheight,range_Rsample,...
    R_sample,range_Rspheres,sensitivity,tolerance_overlap,nr_bwareaopen,name,...
    height_max)

```

---

```

%% Dimensions of images
H = length (PS_image(:,1,1)); % Height of the normal picture [px]
W = length(PS_image(1,:,1)); % Width of the normal picture [px]
Hh = length(height(:,1,1)); % Height of the height profile image [px]
Wh = length(height(1,:,1)); % Width of the height profile image [px]

% The normal image should be scaled down, so the sample circle can be
% detected by using imfindcircles:
downscale = 0.1;
scaled_image = imresize(image,downscale);

```

---

```

%% Detect sample circle in Photoshop image (using the normal image)
scaled_image_gray = rgb2gray(scaled_image); % Change RGB picture to grayscale picture
[center_sample_PS_scaled, radius_sample_PS_scaled] = ...
    imfindcircles(scaled_image_gray,downscale*range_Rsample, ...
    'ObjectPolarity','dark','Sensitivity',0.999);
center_sample_PS_scaled = round(center_sample_PS_scaled); % (x_center y_center) [px]

% Check if exactly 1 circle is found:
if length(radius_sample_PS_scaled) < 1
    disp('Error! No sample circle is detected in the picture.')
    return
elseif length(radius_sample_PS_scaled) == 1
    disp('A sample circle is detected in the picture.')
elseif length(radius_sample_PS_scaled) > 1
    disp('More than one sample circle is detected in the image. (The circle with the
    highest circle strength is used.)')
end

% Scale coordinates back to normal picture size and, if more than one circle is
% detected, select the circle with the highest circle strength:
center_sample_PS = center_sample_PS_scaled(1,:)./downscale;
radius_sample_PS = R_sample;

```

---

```

%% Mask Photoshop image and normal image
% Create mask:
[xx,yy] = ndgrid((1:W)-center_sample_PS(1),(1:H)-center_sample_PS(2));
mask_PS = uint8((xx.^2 + yy.^2) < radius_sample_PS^2);
mask_PS = mask_PS.';

% Apply mask to images:
masked_PS_image = mask_image(mask_PS,PS_image);
masked_image = mask_image(mask_PS,image);

```

---

```

%% Detect sample area in the height profile (using the reference picture)
adj_level = 0.9;
refheight_adj = im2bw(refheight,adj_level); % Change the RGB picture to a blackwhite
picture, so the sample circle can be detected.
[center_sample_hp, radius_sample_hp] = imfindcircles(refheight_adj,[400
500],'ObjectPolarity','dark','Sensitivity',0.99);

% Check if exactly 1 circle is found:
if length(radius_sample_hp) < 1
    disp('Error! No sample circle is detected in the height profile.')
    return
elseif length(radius_sample_hp) == 1
    disp('A sample circle is detected in the height profile.')
elseif length(radius_sample_hp) > 1
    disp('More than one sample circle is detected in the image. (The circle with the
    highest circle strength is used.)')
end

% If more than one circle is detected, choose the circle with the highest circle
strength:
center_sample_hp = round(center_sample_hp(1,:)); % (x_center y_center) [px]
radius_sample_hp = round(radius_sample_hp(1)); % [px]
scale = 905/max(H,W); % In the height profile, the image fits in a box of 905x905
pixels

```

```

radius_sample_hp = scale*radius_sample_PS;      % The radius of the sample circle is
kept constant. The number 0.0681 is based on measurements: (D_hp/D_normal)

%% Mask height profile
% Create mask:
[xx,yy] = ndgrid((1:Wh)-center_sample_hp(1),(1:Hh)-center_sample_hp(2));
mask_height = uint8((xx.^2 + yy.^2) < radius_sample_hp^2);
mask_height = mask_height.';

% Apply mask to image:
masked_height = mask_image(mask_height,height);
% Recolour the black mask into red (needed for defining the minimum height)
masked_height(:,:,1)==0 & masked_height(:,:,2)==0 &
masked_height(:,:,3)==0) = 255;

%% Scale values of height profile to Photoshop image
center_sample_hp = center_sample_hp.*(1/scale);
radius_sample_hp = radius_sample_hp.*(1/scale);
refheight = imresize(refheight,(1/scale));
masked_height = imresize(masked_height,(1/scale));
Wh = Wh*(1/scale);
Hh = Hh*(1/scale);

%% Cut images to the circle to make them equally sized
final_PS_image = masked_PS_image(...
center_sample_PS(2)-radius_sample_PS : center_sample_PS(2)+radius_sample_PS,...
center_sample_PS(1)-radius_sample_PS : center_sample_PS(1)+radius_sample_PS,:);
final_image = masked_image( ...
center_sample_PS(2)-radius_sample_PS : center_sample_PS(2)+radius_sample_PS,...
center_sample_PS(1)-radius_sample_PS : center_sample_PS(1)+radius_sample_PS,:);
final_height = masked_height(...
center_sample_hp(2)-radius_sample_hp : center_sample_hp(2)+radius_sample_hp,...
center_sample_hp(1)-radius_sample_hp : center_sample_hp(1)+radius_sample_hp,:);

%% Show masked and cut images
figure
subplot(2,2,1); imshow(image)
hold on; viscircles(center_sample_PS,radius_sample_PS, 'edgeColor','b');
title(['Detect sample area in image of ' name]); hold on
subplot(2,2,2); imshow(final_PS_image)
title('Masked and cut PS image'); hold on
subplot(2,2,3); imshow(refheight)
hold on; viscircles(center_sample_hp,radius_sample_hp, 'edgeColor','b');
title('Detect sample area in refheight'); hold on
subplot(2,2,4); imshow(final_height)
title('Masked, resized and cut heightprofile')

%% Find location of microspheres in the Photoshop image
% Use image operations to make the Photoshop image more suitable for detection of the
microspheres
% Change image to a BW image to enable the other operations:
final_PS_image = im2bw(final_PS_image);
% Changes black (0-valued) pixels to white (1-valued) pixels if they have
% two white neighbors that are not connected:
BW_PS_image = bwmorph(final_PS_image,'bridge');
% Apply erosion followed by a dilation, using the same structuring element:
se = [0 1 0 ;1 1 1]; % Structuring element neighbourhood
BW_PS_image = imopen(BW_PS_image,se);
% Remove all connected components(white objects) that have fewer than P pixels:
BW_PS_image = bwareaopen(BW_PS_image,nr_bwareaopen);

% Find the location of the microspheres:
[centersBW, radiiBW] = ...
imfindcircles(BW_PS_image,range_Rspheres,'ObjectPolarity','bright', ...
'Sensitivity',sensitivity);

% Remove overlapping circles, for these are (mostly) an incorrect representation of the
microspheres:
[centers,radii]=RemoveOverLap(centersBW,radiiBW,tolerance_overlap,1);
centers = round(centers);
radii = round(radii);
particle_nr = length(centers(:,1)); % Total nr. of detected particles

%% Interpret colours in height profile
% Load the RGB values of the legend colour bar (which are read from the colour bar
automatically in 'Check_height.m')

```

```

load('C:\Users\Selma\Documents\Graduation\Matlab\Particle count\RGB_values')
% Define the heights related to the colours in the legend colour bar. Therefore,
% calculate the height difference between sequential colours in the colour bar
% (height_max is the maximum height in the legend [um]):
heightdiff_colordiff = height_max/length(RGB_values(:,1)); % [um]
% Define heights values [um] that correspond to the colours in the legend:
height_values = [];
for i = length(RGB_values(:,1))+1:-1:1
    height_value = heightdiff_colordiff*length(1:i-1);
    height_values = [height_values; height_value];
end

%% Find the absolute height in the substrate structure of each microsphere (center)
height_centers_abs = [];
for k = 1:length(centers)
    i = centers(k,2);
    j = centers(k,1);
    % Find RGB value in final_height image of the pixel at the k'th center:
    RGB_center = double(final_height(i,j,:));
    % Check the index of the best matching colour in the colour bar:
    [Y,indexRGB] = min(abs(RGB_center(1)-RGB_values(:,1)) + ...
        abs(RGB_center(2)-RGB_values(:,2)) + abs(RGB_center(3)-RGB_values(:,3)));
    % Use this index to find the height that corresponds to the colour of the center:
    height_center_abs = height_values(indexRGB); % [um]
    % Put all heights together in a vector:
    height_centers_abs = [height_centers_abs; height_center_abs];
end

%% Define the relative height in the substrate structure of each microsphere (center)
% Correct the center heights by subtracting the minimal height detected in the sample
% circle (this isn't always zero, because the incorrect height values detected on the
% sample cover can be zero!)The minimal height can be found by finding the pixel with
% the minimum sum of the Red and Green value:
% (!) This is only valid if min. height is indicated by a colour between
% dark blue [0 41 228] and yellow [0 251 252].
lower_lim_RG = min(min(final_height(:,1)+final_height(:,2))); % Minimum of the sum
of Red and Green values of one pixel.)
lower_lim_RG = double(lower_lim_RG);
% Find Red and Green values in the legend closest to the found values:
diff_lower_lim_RG = (RGB_values(:,1)+RGB_values(:,2)) - lower_lim_RG;
[val, index_RGB_lower_lim] = min(diff_lower_lim_RG);
% Use this index to find the minimum height in the sample:
height_zero = height_values(index_RGB_lower_lim); % [um]

% Calculate the height of the centers relative to the minimum height that was found in
the sample:
height_centers_rel = height_centers_abs - height_zero; % [um]

end

```

## Appendix K

### *Determination of the substrate area that was fully covered by tape*

To analyse the particle distribution over the height of the textile substrates (before and after stubbing), only the circle that was analysed that was fully covered by the tape anyhow. This circle, centred in the sample circle, was determined by assuming the 'worst-case scenario', in which the tape could have been placed most far from the centre of the substrate, see Figure 57. The radius of the circle that was fully covered by tape, even in this situation, was calculated by using Figure 58. The radius turned out to be 3150 pixels in the microscope image, see equation K.1.

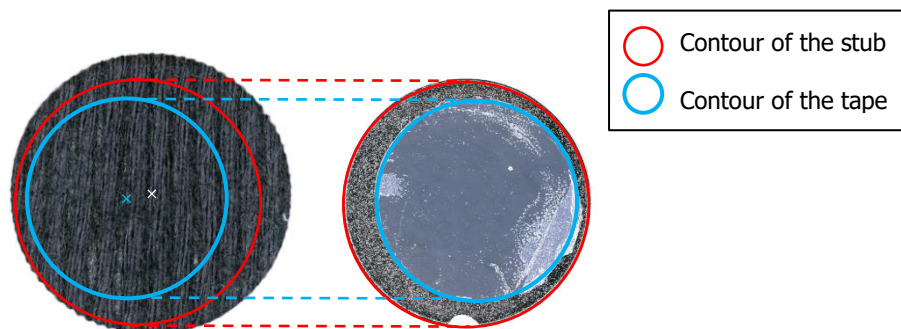


*Figure 57 The tape could have been placed most far from the centre of the substrate if the stub was placed on the substrate directly against the substrate cover, and the stub was used for which the distance between tape and the edge of the stub was the shortest (which was true for stub 1G3, with about 0.59 mm (550 pixels) between the tape and the edge of the stub).*

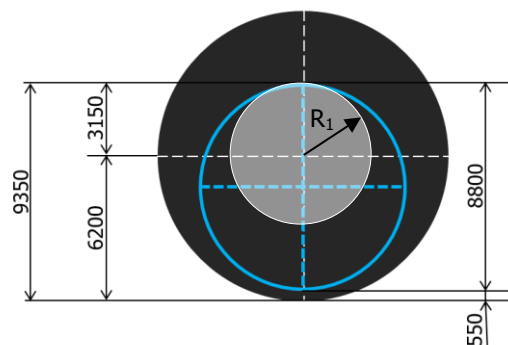


*Figure 58 The white circle indicates the region centred in the sample circle that was fully covered by tape during every tape-lift. The dimensions are expressed in the number of pixels in the microscope image. The sample circle had a radius of 6200 pixels and the tape had a radius of 4400 pixels.*

$$R_1 = 550 + 8800 - 6200 = 3150 \text{ pixels}$$

*Eq. K.1*

## Appendix L

### *Validation of microspheres counting by MATLAB*

---

The microspheres that are visually present in the microscope images are counted by MATLAB. Deviations in the quantification can occur in two ways: particles can be falsely detected and particles can be undetected. These deviations had to be minimalised. This was done by visually analysing part of the pictures<sup>5</sup>. To do this structurally, the images were overlapped by a grid, see Figure 59.

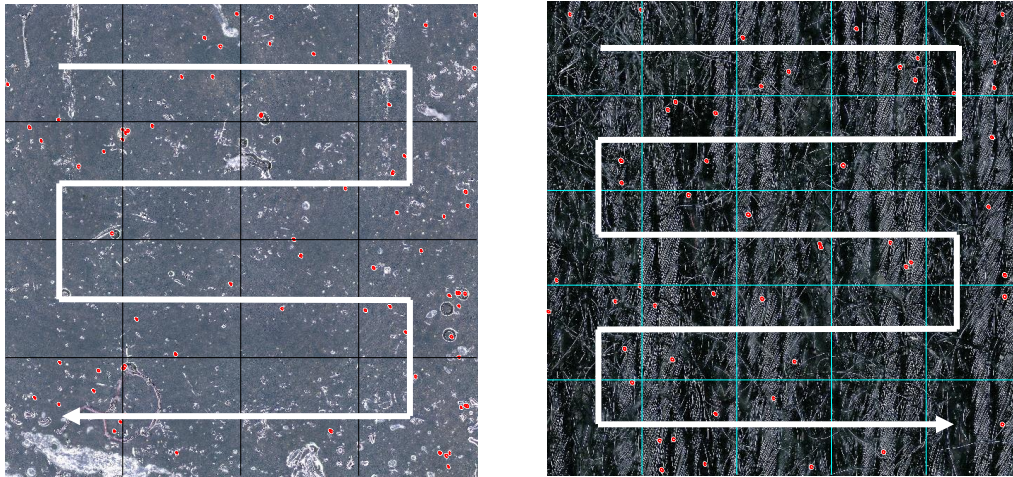


Figure 59 Areas of 4000x4000 pixels in the picture of the tape (left) and substrates (right) were manually analysed to validate the method that was used for particle counting. The areas were subdivided by a grid in equal squares, so the image could be structurally analysed while zooming in. The white arrow indicates the order in which the squares were analysed.

The following parameters in the MATLAB code were tuned to optimize the performance of this method:

- R\_spheres: Range of microsphere radius in the image [px]
- tolerance\_overlap: Tolerated overlap of the detected microspheres [px]
- sensitivty: Detection sensitivity of microspheres in the fuction 'imfindcircle'
- nr\_bwareaopen: Setting used to remove noise in the Photoshop image with the function 'bwareaopen'

The number of falsely detected particles can be given in the expected number of false particles per surface area (pixels<sup>2</sup> in the photo), because this number is independent of the number of present particles on a surface. The number of falsely detected particles on the tape or on the substrate area that is covered by the tape,  $n_{falsely\ detected\ tape}$  can be calculated by equation L.1. Here,  $A_{analysed}$  is the number of analysed tapes times the surface area of 4000x4000 pixels, see Figure 59. The surface area of the tape is  $A_{tape} = \pi \cdot 4400^2$ .

$$n_{falsely\ detected\ tape} = n_{falsely\ detected} \cdot \frac{A_{tape}}{A_{analysed}} \quad Eq. L.1$$

The number of undetected particles,  $n_{undetected}$ , depends on the number of present particles, and can therefore be given in an average percentage of the present particles in the analysed area,  $n_{present}$ , see equation L.2. The number of present particles in the analysed area is calculated by equation L.3.

---

<sup>5</sup> To do this, 'Evaluate\_Run\_define\_particle\_nr\_stubs.m' and 'Evaluate\_Run\_define\_particle\_nr\_substrates.m' were used to run 'Evaluate\_define\_particle\_nr.m'. These codes were not included in this report.

$$\%_{undetected} = \frac{n_{undetected}}{n_{present}} \cdot 100 \% \quad \text{Eq. L.2}$$

$$n_{present} = n_{detected} - n_{falsely\ detected} + n_{undetected} \quad \text{Eq. L.3}$$

Multiple combinations of parameters were applied and the results were analysed. The parameters that resulted in the best performance can be found in the tables below.

### Tape

Settings	Picture	n <sub>detected</sub>	n <sub>falsely det.</sub>	n <sub>undetected</sub>	n <sub>present</sub>
R_spheres = [9 13]; tol_overlap_tape = 8; sens_tape = 0.975; nr_bwareaopen_tape = 40;	Stub1C4	76	3	4	77
	Stub1D1	71	7	2	66
	Stub1J1	21	1	1	21
	Stub2D1	402	12	49	439
	Stub1C3	28	5	0	23
	Stub1C2	47 (excl. 7 on fibre)	7 (excl. 7 on fibre)	5	45
	Stub2D2	116	12	26	130
<b>Total:</b>		<b>761</b>	<b>47</b>	<b>87</b>	<b>801</b>

$$\text{Falsely detected particles on tape: } 47 \cdot \frac{\pi \cdot 4400^2}{7 \cdot (4000 \cdot 4000)} = 25.5$$

$$\text{Percentage of undetected particles on tape: } \frac{87}{801} \cdot 100\% = 10.9\%$$

### Sewing polyester

Settings	Picture	n <sub>detected</sub>	n <sub>falsely det.</sub>	n <sub>undetected</sub>	n <sub>present</sub>
R_spheres_textile = [7 13]; tol_overlap_textile = 3; sens_textile = 0.945; nr_bwareaopen_textile = 100;	PolsewA1_prestub	63	6	10	6
	PolsewB2_prestub	88	8	13	93
	PolsewA1_stubbed	66	11	9	64
	PolsewB2_stubbed	77	9	12	80
<b>Total:</b>		<b>294</b>	<b>34</b>	<b>44</b>	<b>304</b>

$$\text{Falsely detected particles: } 34 \cdot \frac{\pi \cdot 4400^2}{4 \cdot (4000 \cdot 4000)} = 32.3$$

$$\text{Percentage of undetected particles beneath tape: } \frac{44}{304} \cdot 100\% = 14.5\%$$

### Crochet polyester

Settings	Picture	n <sub>detected</sub>	n <sub>falsely det.</sub>	n <sub>undetected</sub>	n <sub>present</sub>
R_spheres_textile = [8 13]; tol_overlap_textile = 3; sens_textile = 0.97; nr_bwareaopen_textile = 40;	PolcrochA1_prestub	100	6	4	98
	PolcrochA4_prestub	148	7	0	141
	<b>Total:</b>	<b>248</b>	<b>13</b>	<b>4</b>	<b>239</b>

$$\text{Falsely detected particles: } 13 \cdot \frac{\pi \cdot 4400^2}{2 \cdot (4000 \cdot 4000)} = 24.7$$

$$\text{Percentage of undetected particles beneath tape: } \frac{4}{239} \cdot 100\% = 1.7\%$$

### Extra strong sewing polyester

Settings	Picture	n <sub>detected</sub>	n <sub>falsely det.</sub>	n <sub>undetected</sub>	n <sub>present</sub>
R_spheres_textile = [8 13]; tol_overlap_textile = 3; sens_textile = 0.97; nr_bwareaopen_textile = 40;	PolsewstrA2_prestub	81	9	3	75
	PolsewstrA4_prestub	67	3	10	74
	<b>Total:</b>	<b>148</b>	<b>12</b>	<b>13</b>	<b>149</b>

$$\text{Falsely detected particles: } 12 \cdot \frac{\pi \cdot 4400^2}{2 \cdot (4000 \cdot 4000)} = 22.8$$

$$\text{Percentage of undetected particles beneath tape: } \frac{13}{149} \cdot 100\% = 8.7\%$$

# Appendix M

## Datasheet experiment results

Substrate	Stub	Trial	Envir. temp. [°C]	Rel. humidity of ambient air [%]	Obtained stubbing force [N]	Measured stubbing force [N]	Measured adhesive force [N]	# Detected microspheres before stubbing on substrate	- # on irregularities	# Detected microspheres before stubbing on substrate corrected	# Detected microspheres on tape	- # on irregularities (fibres/bubbles/edges)	# Detected microspheres on tape corrected
PolcrochA1	stubIA2	1	21	38	0.1	0.10	0.15	549	0	549	18	0	18
PolcrochA2	stubIA3	2	21	38	0.1	0.10	0.14	704	9	695	25	0	25
PolcrochA3	stubIA4	3	21	38	0.1	0.10	0.15	630	0	630	21	0	21
PolcrochA4	stubIA5	4	21	38	0.2	0.20	0.28	863	66	797	56	0	56
PolcrochA5	stubIB1	5	21	38	0.2	0.20	0.29	733	16	717	50	7	43
PolcrochB1	stubIB2	6	21	38	0.2	0.21	0.25	858	28	830	59	13	46
PolcrochB3	stubIB4	8	21	38	0.5	0.50	0.42	671	0	671	69	0	69
PolcrochB4	stubIB5	9	21	38	0.5	0.50	0.49	586	13	573	40	0	40
PolcrochD1	stubID2	16	22	38	0.5	0.50	0.44	752	15	737	74	0	74
PolcrochB5	stubIC1	10	22	38	1	1.00	0.86	941	0	941	146	0	146
PolcrochC1	stubIC2	11	22	38	1	0.99	0.53	667	0	667	152	27	125
PolcrochC2	stubIC3	12	22	38	1	1.00	0.78	606	82	524	108	4	104
PolcrochC3	stubIC4	13	22	38	7	6.81	2.59	617	0	617	325	19	306
PolcrochC4	stubIC5	14	22	38	7	6.79	2.57	674	0	674	339	16	323
PolcrochC5	stubID1	15	22	38	7	6.79	3.08	618	0	618	235	0	235
PolsewB2	stubIE4	23	23	37	0.1	0.10	0.12	559	22	537	15	7	8
PolsewB3	stubIE5	24	23	37	0.1	0.10	0.09	502	6	496	22	7	15
PolsewB4	stubIF1	25	23	37	0.1	0.11	0.11	436	0	436	5	4	1
PolsewA4	stubIE1	20	23	37	0.2	0.21	0.26	509	0	509	15	0	15
PolsewA5	stubIE2	21	23	37	0.2	0.21	0.12	432	12	420	11	0	11
PolsewB1	stubIE3	22	23	37	0.2	0.21	0.20	489	33	456	47	38	9
PolsewA1	stubID3	17	23	37	0.5	0.52	0.50	442	37	405	28	0	28
PolsewA2	stubID4	18	23	37	0.5	0.52	0.45	358	8	350	34	0	34
PolsewA3	stubID5	19	23	37	0.5	0.51	0.25	382	11	371	17	3	14
PolsewB5	stubIF2	26	23	36	1	1.05	0.91	383	0	383	58	0	58
PolsewC2	stubIF4	28	23	36	1	1.00	0.50	323	9	314	28	14	14
PolsewD1	stubIG3	32	23	36	1	1.02	0.33	381	0	381	22	9	13
PolsewC3	stubIF5	29	23	36	7	6.80	1.12	330	58	272	150	78	72
PolsewC4	stubIG1	30	23	36	7	7.01	3.05	348	0	348	123	8	115
PolsewC5	stubIG2	31	23	36	7	7.08	3.26	426	72	354	199	64	135
PolsewstrA1	stubIG4	33	23	36	0.1	0.10	0.14	349	0	349	20	9	11
PolsewstrA2	stubIG5	34	23	36	0.1	0.11	0.17	507	28	479	21	4	17
PolsewstrA3	stubIH1	35	23	36	0.1	0.11	0.14	465	35	430	26	7	19
PolsewstrA4	stubIH2	36	23	36	0.2	0.21	0.09	453	0	453	24	18	6
PolsewstrA5	stubIH3	37	23	36	0.2	0.21	0.19	304	0	304	16	5	11
PolsewstrB1	stubIH4	38	23	36	0.2	0.21	0.13	314	0	314	7	0	7
PolsewstrB2	stubIH5	39	23	36	0.5	0.54	0.42	310	0	310	32	0	32
PolsewstrB3	stubII1	40	23	36	0.5	0.52	0.35	342	14	328	33	22	11
PolsewstrB4	stubII2	41	23	36	0.5	0.54	0.48	345	8	337	57	7	50
PolsewstrB5	stubII3	42	23	36	1	1.07	0.81	302	0	302	60	14	46
PolsewstrC1	stubII4	43	23	36	1	1.07	0.66	354	25	329	22	0	22
PolsewstrC2	stubII5	44	23	36	1	1.08	0.91	334	11	323	39	0	39
PolsewstrC3	stubIJ1	45	23	36	7	6.98	2.36	307	0	307	73	3	70
PolsewstrC4	stub2A1	46	23	36	7	6.99	2.03	402	81	321	73	0	73
PolsewstrC5	stub2A2	47	23	36	7	7.00	1.99	342	43	299	68	0	68

## Appendix N

### *Distribution of microspheres over the height of the textile substrates before and after stubbing*

*Table 7 The number of microspheres that was detected in the different height levels before stubbing (blue column) and after stubbing (grey column) is displayed for all sewing polyester samples. Furthermore, the used stubbing forces, the names of the sample circles, and the reference heights before and after stubbing are displayed. The reference height is the lowest measured height in the sample circle, which basically indicates the metal substrate base. The height levels that are given are relative to this reference height.*

Stubbing force	Sample circle	Reference height [ $\mu\text{m}$ ]		Height of microspheres in substrate relative to reference height [ $\mu\text{m}$ ]									
				0 – 99 $\mu\text{m}$		100 – 198 $\mu\text{m}$		199 – 298 $\mu\text{m}$		299 – 397 $\mu\text{m}$		398 – 496 $\mu\text{m}$	
0.1 N	PolsewB2	1.79	2.57	0	0	36	11	37	30	110	125	0	8
0.1 N	PolsewB3	1.27	2.08	27	9	112	57	37	98	2	18	0	8
0.1 N	PolsewB4	1.27	1.97	38	1	105	12	0	58	0	78	0	0
0.2 N	PolsewA4	1.28	1.56	8	22	134	121	7	5	0	0	0	0
0.2 N	PolsewA5	1.11	2.04	4	5	58	30	74	105	0	8	0	0
0.2 N	PolsewB1	1.81	1.71	0	0	8	11	15	27	80	64	1	0
0.5 N	PolsewA1	1.28	1.44	20	14	93	47	9	55	0	0	0	0
0.5 N	PolsewA2	1.27	1.18	39	18	76	101	0	2	0	0	0	0
0.5 N	PolsewA3	1.27	1.56	22	30	101	85	7	8	0	1	0	0
1 N	PolsewB5	1.61	1.68	3	1	5	6	116	95	24	26	0	0
1 N	PolsewC2	1.31	1.59	19	13	73	10	7	85	2	6	0	0
1 N	PolsewD1	1.10	1.24	6	3	138	80	2	72	0	0	0	0
7 N	PolsewC3	1.18	1.38	23	36	59	57	7	21	0	3	0	0
7 N	PolsewC4	1.18	1.38	12	2	124	42	2	72	0	1	0	0
7 N	PolsewC5	1.18	1.56	32	9	142	0	0	78	0	5	0	0

	Before stubbing
	After stubbing

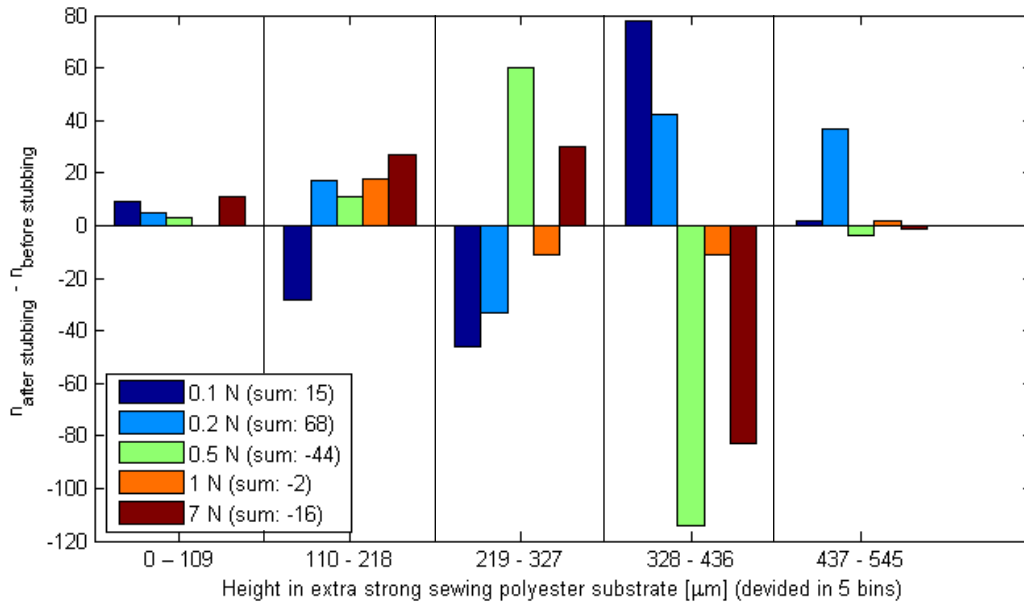


Figure 60 The difference between the number of microparticles after and before stubbing on extra strong sewing polyester. The total difference in the number of detected microspheres is displayed in the legend per stubbing force. In the sample circles, only the area was analysed that was fully covered by tape ( $n=3$ ).

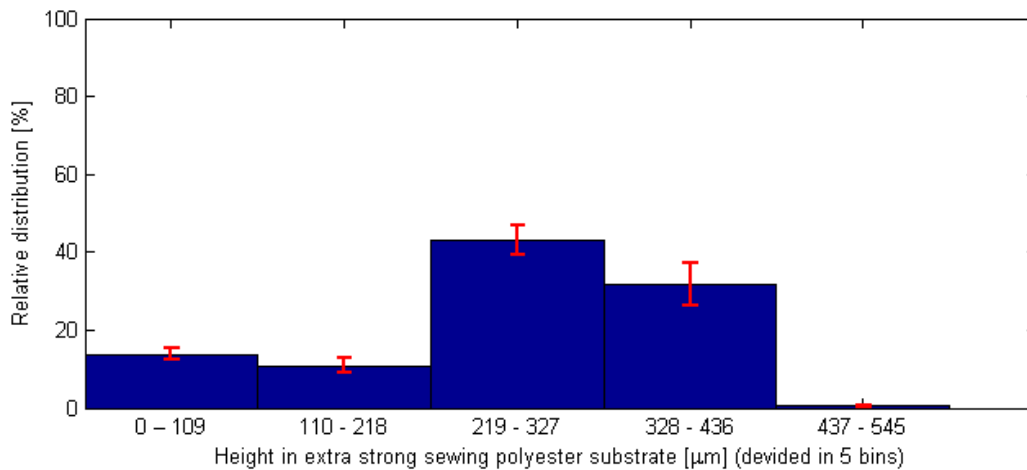


Figure 61 Mean distribution of microparticles on extra strong sewing polyester substrates over the height levels before stubbing ( $n=3 \times 5$ ). The red lines indicate the standard deviation between the trials.

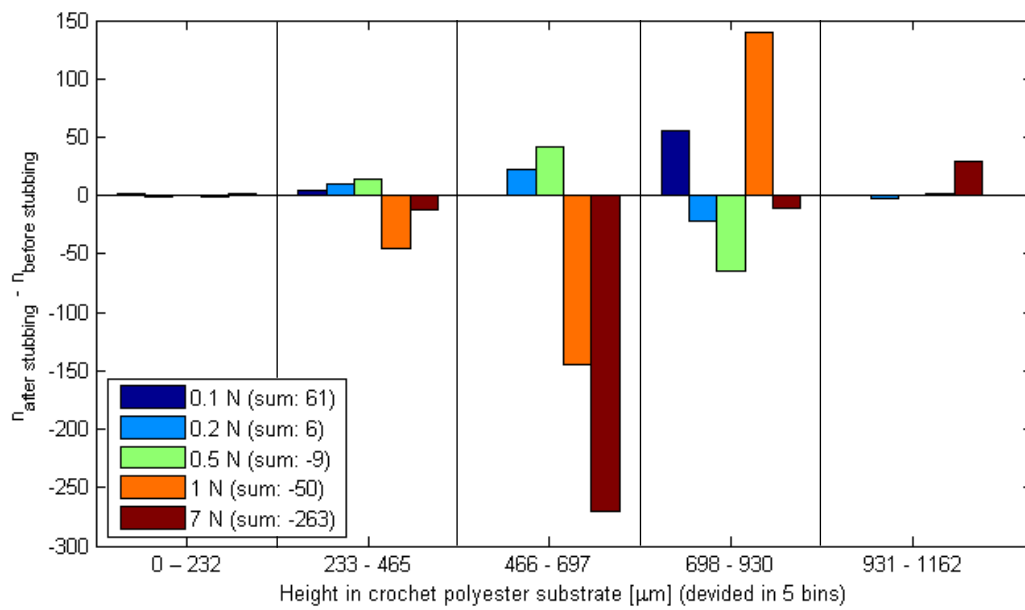


Figure 62 The difference between the number of microspheres after and before stubbing on crochet polyester. The total difference in the number of detected microspheres is displayed in the legend per stubbing force. In the sample circles, only the area was analysed that was fully covered by tape ( $n=3$ ).

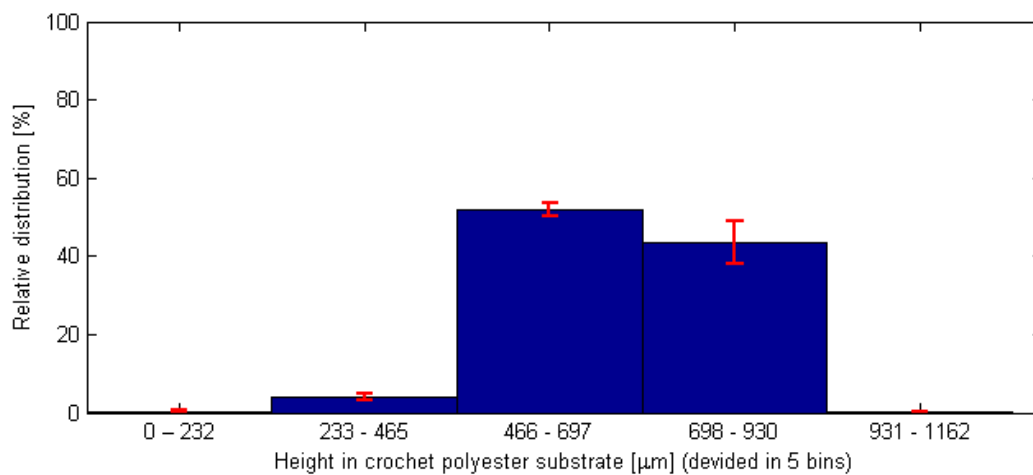


Figure 63 Mean distribution of microspheres on crochet polyester substrates over the height levels before stubbing ( $n=3 \times 5$ ). The red lines indicate the standard deviation between the trials.

## Appendix O

### Collection efficiency on glass

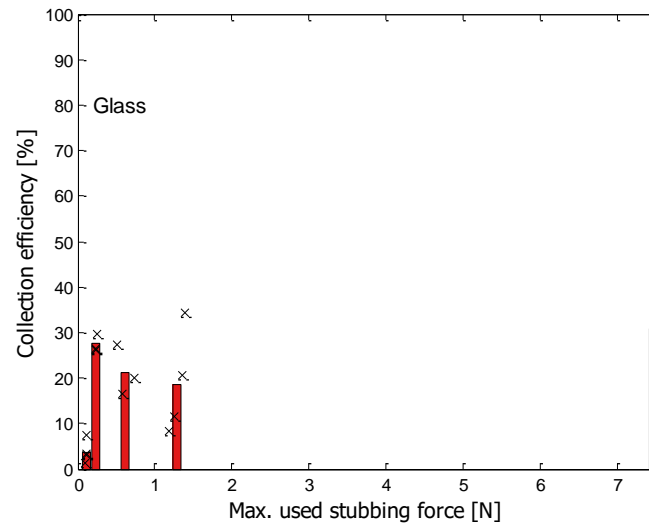


Figure 64 Collection efficiency of microspheres from a glass substrate when sampling with 0.1, 0.2, 0.5, 1 and 7 N.

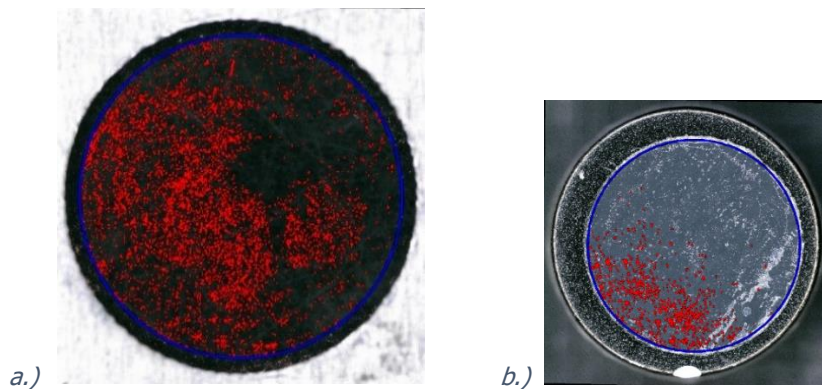


Figure 65 a.) A glass sample before stubbing with detected microspheres (GlassB2).

b.) Stub that was used to collect particles from this sample circle with a stubbing force of 0.2 N (stub2B1). The image of the glass sample was mirrored in such a way that the particles detected on the tape could be overlaid with the particles on the glass resulting in a match. This image indicates that the surfaces of the glass and the tape were not exactly parallel during stubbing.

The microspheres on the glass sample circle were **not equally distributed**. However, to calculate the trace collection efficiency, the mean density of microspheres on the substrate before stubbing was used. Because the unequal distribution of microspheres on glass, it was of significant influence where the stub was placed on the glass.

Probably the stub or the support of the glass slide was placed **under a slight angle**, because the results indicate that the tilt angle was similarly oriented every sample (and the glass slide itself was replaced every 3 measurements). Because of this tilt, the force was not distributed well over the tape, only over a small part of the tape, where the pressure was higher than if the force would be neatly distributed over the tape. It seems that one side of the tape did not even make contact with glass, because no particles are collected by one side of the tape (in multiple trials).